

1

AD-A274 660

INVESTIGATION INTO MODEL-BASED FUZZY LOGIC CONTROL

THESIS

Presented to the Faculty of the Graduate School of Engineering
of the Air Force Institute of Technology

Air University

In Partial Fulfillment of the
Requirements for the Degree of
Master of Science in Electrical Engineering

SDTIC
ELECTE
DEC 23 1993
A

Michael W. Logan, B.S.
Captain, USAF

December, 1993

Approved for public release; distribution unlimited

93 12 22 1 07

93-30994
19308
02005

REPORT DOCUMENTATION PAGE

Form Approved
OMB No. 0704-0188

Public reporting burden for this collection of information is estimated to average 1 hour per response, including the time for reviewing instructions, searching existing data sources, gathering and maintaining the data needed, and completing and reviewing the collection of information. Send comments regarding this burden estimate or any other aspect of this collection of information, including suggestions for reducing this burden, to Washington Headquarters Services, Directorate for Information Operations and Reports, 1215 Jefferson Davis Highway, Suite 1204, Arlington, VA 22202-4302, and to the Office of Management and Budget, Paperwork Reduction Project (0704-0188), Washington, DC 20503.

1. AGENCY USE ONLY (Leave blank)	2. REPORT DATE December 1993	3. REPORT TYPE AND DATES COVERED Master's Thesis	
4. TITLE AND SUBTITLE INVESTIGATION INTO MODEL-BASED FUZZY LOGIC CONTROL			5. FUNDING NUMBERS
6. AUTHOR(S) Michael W. Logan, Captain, USAF			
7. PERFORMING ORGANIZATION NAME(S) AND ADDRESS(ES) Air Force Institute of Technology, WPAFB OH 45433-6583			8. PERFORMING ORGANIZATION REPORT NUMBER AFIT/GE/ENG/93D-25
9. SPONSORING/MONITORING AGENCY NAME(S) AND ADDRESS(ES) Capt. Stuart Sheldon Air Force Wright Laboratories, Flight Dynamics Directorate WL/FIGS Wright-Paterson AFB, OH 45433			10. SPONSORING/MONITORING AGENCY REPORT NUMBER
11. SUPPLEMENTARY NOTES			
12a. DISTRIBUTION/AVAILABILITY STATEMENT Approved for public release; distribution unlimited			12b. DISTRIBUTION CODE
13. ABSTRACT (Maximum 200 words) This thesis investigates the feasibility of a proposed hybrid linear/Fuzzy controller for nonlinear plants. The proposed controller concept is based on the use of multiple linearizations of a nonlinear plant, which describe the dynamics of perturbations about equilibrium points throughout the desired envelope of operation. A bank of linear compensators is developed, each corresponding to a linearized plant about a different equilibrium. The multiple control signals generated by the bank of compensators are then weighted and summed using Fuzzy Logic to produce a composite control perturbation signal, which is used to drive the nonlinear plant. Experiments were conducted to test and refine this control approach. Analysis shows that a linear/Fuzzy compensator based only on a bank of linear compensators is not feasible, largely due to the small regions for which the linearized models were valid and energy considerations within the plant/controller system. The analysis itself, however, suggests an alternate form for a hybrid Linear/Fuzzy approach, based on a bank of Fuzzy compensators smoothed by a linear controller. This concept is developed into the Model-Based Fuzzy Logic Controller (MBFLC). The concept of Fuzzy Logic Model Following Control is also addressed as a second hybrid approach.			
14. SUBJECT TERMS Fuzzy Logic control, Fuzzy Logic, model-based control, nonlinear control, robust nonlinear control			15. NUMBER OF PAGES 192
			16. PRICE CODE
17. SECURITY CLASSIFICATION OF REPORT Unclassified	18. SECURITY CLASSIFICATION OF THIS PAGE Unclassified	19. SECURITY CLASSIFICATION OF ABSTRACT Unclassified	20. LIMITATION OF ABSTRACT UL

Vita

Captain Michael W. Logan was born January 25, 1967 in St Louis, Missouri, to Bill and Pat Logan. He graduated from high school in Olathe, Kansas in 1985. He went on to graduate with a BS in Electrical Engineering from Northwestern University in June of 1989, where he graduated with departmental honors. After receiving his commission through the Reserve Officer Training Corps, he was assigned to the Plans and Advanced Programs Directorate of Electronic Systems Division at Hanscom AFB in Massachusetts. He served as project engineer and later project manager of the ESD Unmanned Air Vehicle Office, which supported the Joint DoD Unmanned Air vehicle Program. He was assigned to the Air Force Institute of Technology in May 92. He has a wife, Jana.

Permanent address: 8723 Mardi Gras
Huber Heights, OH 45424

AFIT/GE/ENG/93D-25

**INVESTIGATION INTO MODEL-BASED
FUZZY LOGIC CONTROL**

**THESIS
Michael W. Logan
Captain, USAF**

AFIT/GE/ENG/93D-25

Accession For	
NTIS CRA&I	<input checked="" type="checkbox"/>
DTIC TAB	<input type="checkbox"/>
Unannounced	<input type="checkbox"/>
Justification	
By _____	
Distribution/	
Availability Codes	
Dist	Availability or Special
A-1	

Approved for public release; distribution unlimited

DTIC QUALITY INSPECTED 3

Acknowledgements

I would like to thank all those in the AFIT community who helped me complete this research. First, my sincere thanks go to my fellow AFIT classmates for their help, advice and support. We formed an great team from the first day, and I wish them all the best in their future endeavors. Its been a pleasure working with Dr Meir Pachter, who has been a mentor and a source of boundless enthusiasm for this effort. Without his expertise in many technical fields, I never could have addressed such a unique research area. Above all, I would like to thank my wife, Jana, for her unwavering support and patience.

Michael W. Logan

Table of Contents

	Page
Acknowledgements	ii
List of Figures	vii
List of Tables	xiii
Abstract	xiv
I. Introduction	1-1
1.1 Background	1-3
1.1.1 Plant Uncertainty	1-4
1.1.2 Plant Nonlinearities	1-8
1.2 Proposed Approach	1-12
1.3 Scope and Assumptions	1-17
1.4 Summary	1-17
II. Plant Development and Current Approaches	2-1
2.1 Introduction	2-1
2.2 Reduced-Order Plant	2-2
2.3 Linearization of Nonlinear Plant	2-2
2.4 Control Performance Characteristics	2-7
2.5 Standard Control Approaches	2-9
2.5.1 Dynamic Inversion	2-9
2.5.2 Quantitative Feedback Theory	2-17
2.5.3 Fuzzy Logic Control	2-31
2.6 Summary	2-40

	Page
III. Model-Based Fuzzy Logic Control Linear Design Considerations	3-1
3.1 Introduction	3-1
3.2 Linear Compensation of Linearized Plant	3-2
3.3 Use of Multiple Compensators in Linear Systems	3-10
3.3.1 Positive Internal Compensator Energy/No Internal Plant En- ergy	3-10
3.3.2 No Internal Compensator Energy/Positive Internal Plant En- ergy	3-13
3.3.3 Positive Internal Compensator Energy/Positive Internal Plant Energy	3-16
3.4 Effect of Compensator Dissimilarities on System Response	3-18
3.5 Use of Multiple Compensators in Time-Varying Linear Systems	3-22
3.6 Controller Considerations Based on Linear Analysis	3-27
3.7 Summary	3-28
IV. Model-Based Fuzzy Logic Control Nonlinear Design Considerations	4-1
4.1 Introduction	4-1
4.2 Effectiveness of Linearized Plants in Nonlinear Control	4-1
4.3 Time-Varying Compensation of the Linear Time-Varying Plant	4-6
4.4 Nulling Compensation of the Nonlinear Plant	4-9
4.5 Banked Compensator Approximation of Time-Varying Compensation	4-19
4.6 Summary	4-27
V. Development of Model-Based Fuzzy Logic Controller	5-1
5.1 Introduction	5-1
5.2 Structure of Banked Model-Based Fuzzy Logic Controller	5-2
5.2.1 Limited Effectiveness of Intermediate Linear Compensators	5-3
5.2.2 Full Error Signal Input to Linearized Plants	5-8
5.2.3 System is Not at Equilibrium when Output Reaches Final State	5-14

	Page
5.3 Full-Envelope Banked MBFLC	5-20
5.4 Contribution of Linear Compensators to Banked MBFLC Design . . .	5-25
5.4.1 Effect of Linearized Plants on MBFLC	5-25
5.4.2 Effect of Robust Linear Compensators on MBFLC	5-33
5.4.3 Effect of Mismatching on Compensator Tuning	5-37
5.5 Model-Following Hybrid Compensators	5-39
5.6 Summary	5-42
VI. Conclusions and Recommendations	6-1
6.1 Introduction	6-1
6.2 Controller Summary	6-2
6.2.1 Formation of $U_{lin}(t)$	6-3
6.2.2 Formation of $C(t)$	6-3
6.3 Thesis Conclusions	6-5
6.3.1 Force a nonlinear plant to to exhibit linear-like performance and obey linear design specifications	6-5
6.3.2 Incorporate available models into controller structure	6-8
6.3.3 Enhance robustness of controller in the face of uncertainties	6-8
6.3.4 Eliminate the need for gain scheduling	6-9
6.3.5 Introduce some a priori synthesis and analysis capability	6-9
6.4 Recommendations for Future Research	6-9
6.4.1 Analysis of MBFLC error sources	6-10
6.4.2 Self-Tuning of Fuzzy Sets	6-10
6.4.3 Development of equivalent $G_2(s)$	6-10
6.4.4 Compensation of plants at non-zero initial conditions	6-11
6.4.5 Polynomial approximations to look-up table data	6-11
6.4.6 Model-Following Fuzzy Logic Controllers	6-11
6.4.7 Nonlinear Mathematical Analysis	6-12

	Page
6.4.8 Test controller in realistic environment	6-12
6.4.9 Implement Fuzzy Supervisor Between $U_{lin}(t)$ and $C(t)$	6-12
6.4.10 Apply MBFLC Approach to Uncertain Linear Systems	6-13
6.5 Summary	6-13
Bibliography	BIB-1
Vita	VITA-1

List of Figures

Figure	Page
1.1. Evaluation of the input variable $Y(in) = 0.75$ for membership in the Fuzzy Sets $YisNegative$, $YisZero$, and $YisPositive$	1-5
1.2. Activation of Implicate Fuzzy Sets based on membership values of premise statements	1-6
1.3. Block diagram showing closed-loop compensation of plant from Equation 1.1 using Fuzzy Logic to provide an "estimate" of τ	1-7
1.4. State space paradigm for nonlinear control	1-13
1.5. Weighting of a bank of linear compensators using Fuzzy Sets	1-14
1.6. Final structure of Model-Based Fuzzy Logic Controller	1-16
2.1. SIMULINK Model of Nonlinear Plant with Externally Defined a Parameter. . .	2-3
2.2. SIMULINK model of linearized plant with externally defined τ parameter	2-6
2.3. Response of Model Plant to Unit Step Input	2-8
2.4. Root Locus for $G(s)P(s)$, Dynamic Inversion Synthesis	2-10
2.5. SIMULINK Model of $G(s)$ Using Dynamic Inversion	2-11
2.6. Interpreter Block Which Converts V to U	2-12
2.7. Simulation of closed-loop tracking controller developed using dynamic inversion	2-13
2.8. Response of dynamic inversion simulation to unit step input. Model response is also plotted but is almost perfectly covered by system response.	2-14
2.9. State-space trajectory representation of dynamic inversion system response to a unit step input, $a=1.0$	2-15
2.10. Response of dynamic inversion simulation when the nonlinear plant takes on different values of the parameter a . $a = 1$ in the compensator for all simulations. .	2-16
2.11. QFT compensation scheme	2-18
2.12. The frequency responses of $T_{RU}(s)$ and $T_{RL}(s)$, comprising the QFT response thumbprint	2-19
2.13. Nichols Chart showing QFT boundaries and frequency response of worst-case plant	2-22

Figure	Page
2.14. Nichols Chart of worst-case plant in series with $G(s)$	2-23
2.15. Frequency response plot showing the variation of the family of plants is inside the maximum variation allowed by $T_{RU}(s)$ and $T_{RL}(s)$	2-24
2.16. Closed-loop time responses of all five linear plants to unit step at the reference input	2-25
2.17. Closed-loop time responses of all five linear plants to unit step at the plant input	2-26
2.18. Nichols chart showing the open-loop frequency response of $G(s)P(s)$ based on a modified family of plants	2-27
2.19. Closed-loop time responses of all five alternate linear plants to unit step at the reference input	2-28
2.20. Closed-loop time responses of all five alternate linear plants to unit step at the plant input	2-29
2.21. Response of nonlinear plant to unit step reference input for $a=0.5, 1.0,$ and 1.5	2-30
2.22. Closed-loop control of nonlinear plant with Fuzzy Logic Control	2-35
2.23. Fuzzy Logic Compensator for Nonlinear Plant	2-36
2.24. Closed-loop response of FLC to step inputs of strength $Ref = 1u-1(t)$ and $1.5u-1(t)$	2-37
2.25. Time response of FLC/nonlinear plant to step input assuming modeling errors.	2-38
2.26. Time response of FLC and DI controllers to time-varying a	2-39
3.1. Locus of poles of the linearized plant as a function of τ	3-3
3.2. Model of Compensator $G(s)$ with τ externally defined	3-4
3.3. Model of Compensator $G(s)$ with τ externally defined which meets disturbance rejection specifications	3-5
3.4. TOP: Closed-loop simulation given linear plant with time-varying plant parameter τ . BOTTOM: Closed-loop simulation given full nonlinear plant. Both simulations are run with each compensator.	3-6
3.5. Closed-loop system responses for the time-varying linear plant under both robust and non-robust compensation.	3-7

Figure	Page
3.6. Closed-loop disturbance rejection for nonlinear plant under both robust and non-robust compensation.	3-8
3.7. Closed-loop system responses for nonlinear plant under both robust and non-robust compensation.	3-9
3.8. Simulation to determine the effect of charged states in compensator applied to linear system	3-11
3.9. Closed-loop response of linear plant given varying "charging" times for the linear plant	3-12
3.10. SIMULINK simulation to test the effect of a quiescent compensator inheriting a non-quiescent plant	3-14
3.11. Closed-loop response of quiescent compensator/non-quiescent plant	3-15
3.12. Simulation of banked compensation technique for a linear plant	3-17
3.13. Response of Identical Compensators in a banked configuration	3-18
3.14. Output of compensator bank, shown in terms of each compensator contribution	3-19
3.15. Simulation applying a bank of identical linear compensators to a linear plant	3-20
3.16. Simulation of banked compensation technique for unlike compensators	3-21
3.17. Simulation testing the validity of linear compensators on time-varying linear plant	3-23
3.18. Closed-loop response of time-varying plant, linear compensator, for step inputs of .05,1.1, and 1.2. Starting from $Y(t_0) = 1$	3-24
3.19. Prototype MBFLC for Time-Varying Linear Plant	3-25
3.20. Closed-Loop Response of Prototype MBFLC	3-26
4.1. Determination of region of attraction for $Y = 4.0$	4-5
4.2. Control of Time-Varying Linear Plant Using Time-Varying Linear Compensator	4-7
4.3. Closed-loop response of LTV plant and Time-Varying Linear Compensator	4-8
4.4. Closed-loop response of nonlinear plant and Time-Varying Linear Compensator for various step inputs	4-10
4.5. Full-envelope nonlinear control scheme using trajectory following	4-13
4.6. Determination of the desired x_2 based on compensator outputs	4-14

Figure	Page
4.7. determination of U based on desired \dot{x}_2	4-15
4.8. Closed-Loop simulations of nonlinear controller using time-varying linear compensation, starting from $Y = 0$	4-15
4.9. Closed-Loop simulations of nonlinear controller using time-varying linear compensation, starting from $Y = 1$	4-16
4.10. SIMULINK simulation to test the disturbance rejection capabilities of nonlinear control scheme	4-17
4.11. Disturbance rejection capabilities of nonlinear controller for unit step injected at plant input	4-18
4.12. Simple compensator bank for MBFLC	4-20
4.13. Internal Structure of Fuzzy Supervisor	4-21
4.14. Activation of Fuzzy Membership functions for Fuzzy Supervisor	4-22
4.15. Time history of u outputs for time-varying compensator (TVC), Fuzzy Compensated Bank, and single linear compensator. The TVC and single linear compensator plots and nearly identical.	4-24
4.16. Responses of closed-loop system to a step input from $Y = 3$ to $Y = 4$ for both time-varying and Fuzzy Weight compensators.	4-25
4.17. State space trajectory of Nonlinear Plant driven by hybrid nonlinear/Fuzzy Controller	4-26
5.1. Banked Model-Based Fuzzy Logic Control paradigm	5-3
5.2. Compensator bank for MBFLC with universe of discourse from $Y = 0.6$ to $Y = 0.7$	5-6
5.3. closed-loop response of nonlinear plant when driven by Fuzzy Weighted Compensator Bank from $Y = 0.6$ to $Y = 0.7$	5-7
5.4. Fuzzy Weighted Compensator Bank with associated Fuzzy Limiter. This configuration is referred to henceforth as a Fuzzy Bank	5-11
5.5. Structure of SIMULINK block Fuzzy Limiter	5-12
5.6. Membership functions for Fuzzy Sets in Fuzzy Limiter	5-13
5.7. Closed-loop response of nonlinear system compensated by Fuzzy Bank	5-13
5.8. Desired form for $C(t)$ based on linear analysis of pre-weighted compensator bank	5-15

Figure	Page
5.9. $C(t)$ function formed by ANDing of Fuzzy Sets <i>Eis0</i> and <i>EdotisPositive</i>	5-16
5.10. SIMULINK implementation of Banked MBFLC	5-18
5.11. LEFT: Membership function for <i>E is Zero</i> . RIGHT: Membership function for <i>EisPositive</i>	5-19
5.12. Response of nonlinear plant in closed-loop simulation with Banked MBFLC . . .	5-19
5.13. SIMULINK simulation of Full Envelope Banked MBFLC	5-21
5.14. Top-level SIMULINK simulation of nonlinear plant in Full-Envelope Banked MBFLC	5-22
5.15. Closed-loop response of Full-Envelope MBFLC to step inputs of various magnitudes	5-24
5.16. Closed-loop response of Full-Envelope MBFLC for $a= 0.5, 1.0,$ and 1.5	5-24
5.17. SIMULINK simulation of MBFLC using only a single linear controller	5-26
5.18. Closed-loop response of single-compensator MBFLC to step inputs of various magnitudes	5-27
5.19. Closed-loop response of single-compensator MBFLC to step inputs starting from various initial equilibria	5-28
5.20. Closed-loop response of single-compensator MBFLC to step inputs starting from equilibria both above and below the equilibrium of the linear compensator . . .	5-29
5.21. Single-compensator MBFLC with a simplified 2-set Fuzzy Limiter	5-31
5.22. SIMULINK simulation of MBFLC with a two-set Fuzzy Limiter and a single linear compensator	5-32
5.23. SIMULINK simulation of single compensator MBFLC using robust compensator	5-34
5.24. Closed-loop tracking response of robust Single Compensator MBFLC to step inputs of various magnitudes	5-35
5.25. Disturbance rejection response of both robust and nonrobust MBFLC to a step disturbance of magnitude 0.1 injected at the plant input. Also shown is the response of the nonrobust compensator with the Fuzzy Limiter removed.	5-36
5.26. Hybrid linear/Fuzzy Controller using linear model-following and Linear/Fuzzy control input generation	5-40
5.27. Internal structure of SIMULINK block <i>Model</i>	5-41
5.28. Internal structure of SIMULINK block <i>FuzzyDriver</i>	5-42

Figure	Page
5.29. Membership functions for Fuzzy Sets within the Fuzzy Driver	5-43
5.30. Closed-loop responses of Model-Following hybrid controller for step inputs of various magnitudes and initial conditions.	5-44
5.31. Input signal to nonlinear plant generated by Fuzzy Driver and linear compensator	5-45
6.1. MBFLC Block Diagram	6-2
6.2. Closed-loop response of Nonlinear plant for step inputs of $Y_{ref} = 0.6+0.035u_{-1}(t)$, $0.6+0.05u_{-1}(t)$, $0.6 + 0.075u_{-1}(t)$, and $0.6 + 0.1u_{-1}(t)$	6-6
6.3. Closed-loop responses for QFT-based design and MBFLC design	6-7
6.4. Closed-loop responses for Dynamic Inversion-based design and MBFLC design .	6-7

List of Tables

Table	Page
2.1. Universe of Discourse for FLC	2-31
2.2. Membership Functions for FLC	2-32
2.3. Values for U suggested by Dynamic Inversion simulation	2-33
2.4. Values for U implicants based on tuning through simulation	2-34
4.1. Regions of attraction for linear compensators for originating, terminating, and traverse modes of operation	4-3
4.2. Regions of attraction for linear compensators in Banked MBFLC	4-4
5.1. Tuning Parameters for Fuzzy Supervisor Membership Function	5-5
5.2. Tuning Parameters for Fuzzy Limiter Membership Functions	5-8
5.3. Tuning Parameters for Fuzzy Sets E is Zero and \dot{E} is Positive	5-18
5.4. Look-up table data for full envelope MBFLC	5-23
5.5. Tuning parameters for Fuzzy Limiter driving robust linear compensator	5-33
5.6. Look-up table data for MBFLC incorporating the robust linear compensator . .	5-33
5.7. Tuning parameters for Fuzzy Limiter driving the mismodeled nonlinear plant ($a=1.5$)	5-38
5.8. Look-up table data for MBFLC incorporating the robust linear compensator . .	5-38

Abstract

This thesis investigates the feasibility of a proposed hybrid linear/Fuzzy controller for non-linear plants. The proposed controller concept is based on the use of multiple linearizations of a nonlinear plant, which describe the dynamics of perturbations about equilibrium points throughout the desired envelope of operation. A bank of linear compensators is developed, each corresponding to a linearized plant about a different equilibrium. The multiple control signals generated by the bank of compensators are then weighted and summed using Fuzzy Logic to produce a composite control perturbation signal, which is used to drive the nonlinear plant.

Experiments were conducted to test and refine this control approach. Analysis shows that a linear/Fuzzy compensator based only on a bank of linear compensators is not feasible, largely due to the small regions for which the linearized models were valid and energy considerations within the plant/controller system. The analysis itself, however, suggests an alternate form for a hybrid Linear/Fuzzy approach, based on linear waveforms tuned by Fuzzy Logic. This concept is developed into the Model-Based Fuzzy Logic Controller (MBFLC).

INVESTIGATION INTO MODEL-BASED FUZZY LOGIC CONTROL

I. Introduction

A wealth of information is available on the application of control theory to linear, time invariant (LTI) plants. Unfortunately, most processes of interest in nature are nonlinear. Though optimal control techniques such as dynamic programming can be used to derive optimal state feedback controllers for nonlinear systems, these algorithms are numerically intensive and, in general, don't lead to closed form solutions [1]. Approximations such as "linearization" and the "small perturbations hypothesis" must therefore be invoked to enable application of conventional LTI control methods to these problems. The control designs based on this linear hypothesis will then be valid for the nonlinear process to the extent that the linearity assumptions are not significantly violated.

The approximations required to obtain a linear problem formulation lead to dissimilarities between the plant dynamics and the dynamics of the model. The resulting modeling error is often neglected in engineering practice because the mathematical methods required to address this uncertainty are quite sophisticated [2]. In applications such as aircraft flight control, these neglected dynamics can become significant, resulting in system behavior not predicted by the linear model, as alluded to in [3:pages 17-26]. Consequently, a controller based on the linear model will become less effective as the flight condition of the aircraft moves away from the equilibrium condition about which the plant dynamics were linearized. Even when operating close to the linearization point, the actual system will seldom exhibit the performance predicted by linear analysis, especially over long periods of time relative to the natural frequency of the LTI model[4:18].

One possible means of addressing the inevitable disparity between the nonlinear physical plant and the linearized(LTI) plant model is through the use of Fuzzy Logic. Fuzzy Logic is a *partial* membership set theory developed by Lotfi Zadeh in the mid-1960's. Originally conceived for machine learning applications, Fuzzy Logic is now being used in many fields of academic and commercial endeavor, including control systems [5]. Fuzzy Logic is, in essence, a means of representing uncertainty about a given system or process without directly applying statistical methods [6].

Fuzzy Logic has been successfully applied to control system design, and represents one means of developing controllers for nonlinear plants [7]. reported applications of Fuzzy Logic Control (FLC) include automotive control (braking, automatic parking, automatic transmissions, exhaust emissions control) [8, 9], industrial automation [10], subway train braking [11], and flight control [12, 14]. Current FLC work focuses primarily on the automatic control of plants traditionally operated by humans. Though nonlinear, these plants exhibit simple, consistent dynamics with a sense of "directionality" associated with control actions. Therefore, the effect of a given control action is known, at least qualitatively, without the aid of a system model. Even in cases where models are available, they are largely overlooked in current FLC development, inhibiting the application of FLC to complex plants. It is reasonable to assume that a hybrid conventional-Fuzzy control technique, dubbed *model-based Fuzzy control* (MBFLC) for this thesis, may provide better overall control than either control approach alone. This thesis addresses the integration of FLC concepts and techniques into traditional model-based controller design methods.

This research is motivated by the desire to develop a full-envelope aircraft flight controller. Current flight controllers rely on gain scheduling to compensate for the nonlinear aircraft operating in different regions of the (u_A, α_{cg}) flight envelope. MBFLC represents one alternative approach to gain scheduling, especially in flight regimes such as high angle of attack flight where sensor inputs, and thus full knowledge of u and α , are often noise-corrupted. Though this work is intended to lay the groundwork for a full-envelope flight controller, the results are equally applicable to any system for which the agreement between physical plant and linearized model is uncertain.

In this thesis report, hybrid nonlinear/Fuzzy and linear/Fuzzy controllers will be developed based on linearizations of a highly nonlinear plant. The resulting hybrid controllers will then be applied to tracking and regulation of the nonlinear plant, rather than linearizations assumed to represent the nonlinear plant. Fuzzy Logic, in this context, will be used to bridge the gap between linear systems theory and nonlinear control application. Said another way, the language of Fuzzy Logic will be used to quantify the way in which linear controllers eventually fail when applied to the control of nonlinear plants. This will then be incorporated into an otherwise deterministic controller structure. Since even the simplest MBFLC controller will be more complex than a conventional linear controller, a commensurate increase in performance, robustness, and/or envelope of operation is to be expected.

This thesis is divided into six chapters:

- 1. Introduction - This chapter outlines the problem being addressed, the current state of Fuzzy Logic Control, any necessary assumptions, and the proposed solution. The introduction develops the justification and conceptual basis for Model-Based Fuzzy Logic Controllers.**
- 2. Problem Development and Current Approaches - In this section the criteria for a suitable nonlinear test plant and its performance specifications is given. The final form of the nonlinear plant will be developed as well as the linearized plant model. To gain control insights, compensators will be developed for the nonlinear plant using dynamic inversion, Quantitative Feedback Theory(QFT), and FLC concepts. These designs will serve as benchmarks to measure the true effectiveness of Model-Based Fuzzy Logic Control.**
- 3. Linear Design Considerations - In this chapter, a linear compensator is developed for the linearized version of the nonlinear plant. A linear time-varying version of the nonlinear plant is also developed and justified. The feasibility and desirability of using banks of linear compensators to control linear and linear time-varying plants is explored. Error sources inherent in banked compensator designs applied to linear and linear time-varying plants are identified.**
- 4. Nonlinear Design Considerations - The effectiveness of linear compensators when applied to the nonlinear plant is quantified. Time-varying linear compensation is developed to control the time-varying linear plant. A nonlinear compensator incorporating time-varying linear models is proposed and validated. The effect of the time-varying linear compensator is then approximated using Fuzzy Logic, thereby creating a hybrid nonlinear/Fuzzy controller.**
- 5. Model-Based Fuzzy Logic Controller Development - The effect of the nonlinear elements of the hybrid nonlinear/Fuzzy controller is analyzed in light of Fuzzy Logic approximation. A linear/Fuzzy structure is developed to eliminate the need for nonlinear processing. The hybrid linear/Fuzzy design is modified to encompass full-envelope operation. This is the final configuration of the Model-Based Fuzzy Logic Controller. The performance of the MBFLC will be compared with other design approaches.**
- 6. Conclusions and Recommendations - This chapter contains an overall assessment of the promise MBFLC shows based on the research conducted for this thesis. Unresolved issues and recommendations for future work are provided.**

1.1 Background

FLC has the potential to overcome two obstacles inevitably confronted when designing control systems for real-world plants: 1) Plant uncertainty, and 2) Plant nonlinearity. Each of these difficulties is addressed in detail below.

1.1.1 *Plant Uncertainty.* Consider a plant whose transfer function is:

$$\frac{Y(s)}{U(s)} = \frac{1}{\tau s + 1} \quad (1.1)$$

with the value of τ being dependent on the value of the output/state Y ($\tau = f(Y)$). This is a common situation where, for example, the dynamic pressure on an aircraft is a function of its altitude. Note that this plant is nonlinear, so expressing this plant model using a transfer function is an abuse of notation. However, by assuming τ is approximately constant, is time-varying independent of $Y(t)$, or is unknown, all allow for linear or linear stochastic descriptions of this nonlinear problem. An additional approach to linear analysis could be to assume that τ is *Fuzzy*.

If we wished to develop a controller for this plant based on a Fuzzy assumption, we could consider τ to be a Fuzzy variable. The information available on τ could be as rudimentary as:

- IF *Y is Negative* THEN *τ is Small*
- IF *Y is Zero* THEN *τ is Medium*
- IF *Y is Positive* THEN *τ is Large*

This would approximate the true knowledge that τ varies with Y . These rules make up a *Fuzzy Inference* system.

The terms in italics are to be considered linguistic labels for Fuzzy Sets. Hence, the Y input to the controller will first be *fuzzified*. That is, the antecedent Y will be converted from a *crisp* (single-valued) variable to a *Fuzzy* (multi-valued) variable. The fuzzification procedure involves the input value Y being evaluated for membership in each of the sets defined over the *universe of discourse* (total allowed variation) of Y – in this case *Negative, Zero, and Positive*. The degree to which a given Y will be considered a member of any Fuzzy Set is given by a *membership value*, μ , which ranges from 0 (complete exclusion) to 1 (complete membership). The value which μ takes on is determined by an appropriate *membership function* for the set in question, $\mu(Y)$, defined over the entire universe of discourse. Sample membership functions for the sets *Negative, Zero and*

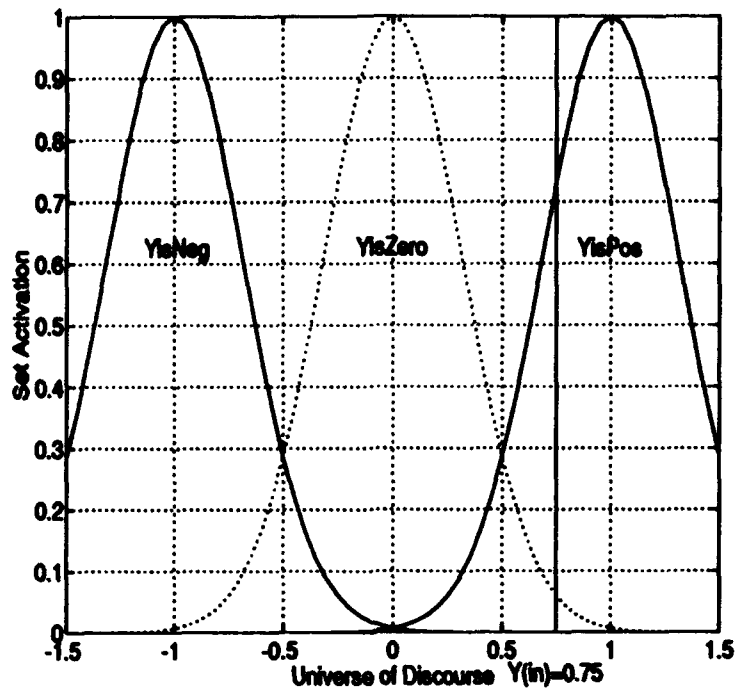


Figure 1.1 Evaluation of the input variable $Y(in) = 0.75$ for membership in the Fuzzy Sets $YisNegative$, $YisZero$, and $YisPositive$

Positive are shown in Figure 1.1. Note in the Figure that $Y(in) = 0.75$ is shown being evaluated for membership in each of the three defined Fuzzy Sets. $Y = 0.75$ is a member of Negative to $\mu_N = 0.0$, of Zero to $\mu_Z = 0.062$, and of Positive to $\mu_P = 0.745$. These three partial set memberships represent $Y = 0.75$ in the Fuzzy domain. Similarly, the output variable τ is also described by three Fuzzy Sets that span its universe of discourse— τ is *Small*, τ is *Medium*, and τ is *Large*, as shown in Figure 1.2. In this case, membership functions relate the Fuzzy Sets for τ to a range of possible crisp τ values. The membership functions defining the Fuzzy Sets for τ will not, in general, resemble the membership functions for the fuzzification of Y . The Fuzzy Implicate τ is related to the Fuzzy Variable Y through the Fuzzy Inference system given above. Because the Fuzzy Inference rules contain only a single premise (for this example, "IF Y is Negative"), the Fuzzy Set representing the resultant will be activated to the same degree as its premise. This is illustrated in the Figure. Therefore, $\mu_N = 0.0 \rightarrow \mu_S = 0.0$, $\mu_Z = 0.062 \rightarrow \mu_M = 0.062$, $\mu_P = 0.745 \rightarrow \mu_L = 0.745$.

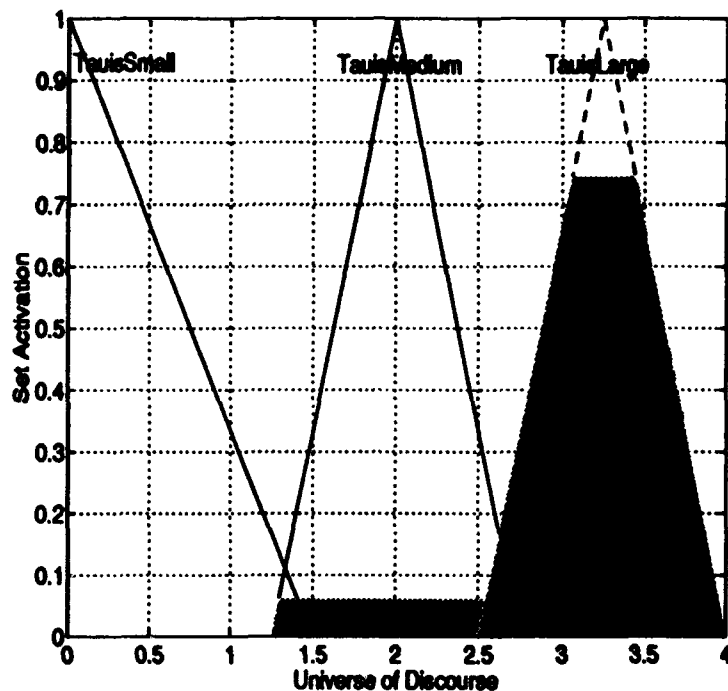


Figure 1.2 Activation of Implicate Fuzzy Sets based on membership values of premise statements

A "crisp" (single valued) estimate of τ can be produced by any of a number of *defuzzification* routines [13]. Generally, these algorithms involve taking some sort of centroid of the polygon formed by all of the activated regions of the implicate sets, as shown in the Figure. In this manner, for any crisp input Y , a crisp output τ will be produced. A compensator of the form $U = F(E, \tau)$ can then be developed for the plant in (1.1) based on estimates of τ supplied by the Fuzzy Logic. This represents the first MBFLC scheme for feedback control, and is shown in Figure 1.3. For an overview of Fuzzy Sets and Fuzzy Membership Functions, refer to [7] or [15].

Of course, the true utility of this Fuzzy approach is realized only when the relation between τ and Y is poorly understood or variable. In the case where $\tau = f(Y)$ is known or statistically modeled, other approaches will probably yield better performance, though at higher computational expense. The objective of this type of hybrid Fuzzy design would be, not to obtain optimum performance at a single τ trajectory, but to obtain "acceptable" performance over a broad range of τ trajectories.

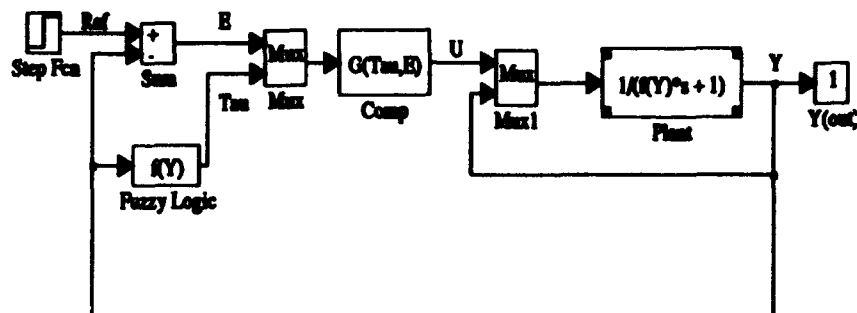


Figure 1.3 Block diagram showing closed-loop compensation of plant from Equation 1.1 using Fuzzy Logic to provide an "estimate" of τ

The Fuzzy Logic element in Figure 1.3 serves essentially as a nonlinear look-up table, with the qualities of the table alterable in real-time. If the Fuzzy Logic estimate of τ was perfectly accurate, then a system response very similar to the established linear specifications is possible. It should be noted, however, that even for a known τ history, stability is not guaranteed by using a linear compensator based on τ [16]. As the estimates are degraded, closed-loop system performance degrades as well. Simulation and on-line retuning would be required to maximize performance.

This MBFLC approach offers several benefits over conventional techniques (parameter estimation or robust control). The controller is conceptually simpler and quicker to synthesize than other control laws, as is the case with most Fuzzy Logic Controllers [18]. Lessons learned from testing can be directly included in the control law. The flexible structure of the MBFLC could make the system less susceptible to external disturbances, and some types of system noise will be filtered from the feedback channel [19]. Finally, Model-Based Fuzzy Logic Control, as with other

Fuzzy Logic control methodologies, is well suited to real-time adaptive control. The drawbacks to MBFLC include lack of stability guarantees, lack of a priori performance analysis techniques, tuning requirements, and the requirement for an on-line processor to perform the Fuzzy Logic operations.

It is reasonable to ask when it would be beneficial to consider MBFLC over statistically based techniques. The answer is that the benefit of using a MBFLC is directly related to the amount of *non-statistical* or unmodeled uncertainty present in the system. As will be shown in the next section, the non-statistical uncertainty present in the unknown parameter τ is directly related to the nonlinear model from which the linearized system was derived. The idea that both parameter uncertainty due to unmodeled nonlinearities and uncertainty due to linearization of nonlinear plants can be expressed as time-varying parameters in otherwise linear systems will serve as the justification for MBFLC.

1.1.2 Plant Nonlinearities. Consider the general control problem, as it applies to a nonlinear plant. Assume a model of the plant dynamics—however complicated—is available. It can be expressed in the form:

$$\dot{\underline{X}} = f(\underline{X}, \underline{U}) \quad (1.2)$$

where $\underline{X} \in \mathfrak{R}^n$ is a vector of system states, $\underline{U} \in \mathfrak{R}^m$ is a vector of system inputs (controls), and f is a smooth nonlinear function of \underline{X} and \underline{U} . It is desired to drive the system from some initial state, $\underline{X}_o, \underline{U}_o$, to some final state, $\underline{X}_f, \underline{U}_f$, within a given maximum settling time t , and with no state $X_i(t)$ overshooting its final desired value $X_{if}(t)$ by more than a ratio M_p .

This problem, as formulated, cannot be directly addressed using LTI control theory. However, a linearized model of the plant dynamics at certain points in state space can be derived by expressing the state and control vectors in terms of perturbations from a given nominal condition, $\bar{\underline{X}}, \bar{\underline{U}}$ [20:pages 83-97]. The state and control vectors become:

$$\underline{X} = \bar{\underline{X}}_i + \underline{x} \quad (1.3)$$

$$\underline{U} = \underline{\bar{U}}_i + \underline{u} \quad (1.4)$$

where $\underline{\bar{X}}_i$ and $\underline{\bar{U}}_i$ are determined by setting:

$$f(\underline{\bar{X}}_i, \underline{\bar{U}}_i) = 0. \quad (1.5)$$

That is, the i th nominal point $\underline{\bar{X}}_i, \underline{\bar{U}}_i$ is an equilibrium or trim point. The subscript $i, i = 1, 2, \dots, N$, indicates that there could be many such nominal points. The plot of these equilibria points in an $n \times m$ -dimensional space defined by the ranges of \underline{X} and \underline{U} is referred to in this thesis as a *nominal locus*.

Inserting the expressions (1.3) and (1.4) into (2.36) and expanding the nonlinear f function by a Taylor series about $(\underline{\bar{X}}_i, \underline{\bar{U}}_i)$ yields:

$$\dot{\underline{X}} + \underline{\dot{x}} = f(\underline{\bar{X}}_i, \underline{\bar{U}}_i) + \frac{\delta f(\underline{\bar{X}}_i, \underline{\bar{U}}_i)}{\delta \underline{X}} \underline{x} + \frac{\delta f(\underline{\bar{X}}_i, \underline{\bar{U}}_i)}{\delta \underline{Y}} \underline{u} + H.O.T. \quad (1.6)$$

The partial derivatives are Jacobian matrices and "H.O.T." represents higher-order terms in the Taylor series. Two assumptions must be made at this point in order to obtain a linear model of plant dynamics about the i th equilibrium point:

1. Only small perturbations about the equilibrium condition will occur ("H.O.T" terms are then negligible).
2. The equilibrium point is static ($\dot{\underline{X}} = 0$).

By applying these two assumptions and noting that f evaluated at the equilibrium point is zero (by definition), (1.6) becomes a linear equation in the perturbation variables:

$$\underline{\dot{x}} = \underline{A}_i \underline{x} + \underline{B}_i \underline{u}. \quad (1.7)$$

This is the familiar derivation of an LTI plant by linearization. Note the explicit dependence of the (A, B) plant model on the i th equilibrium point. This linearization is only valid at or near

this equilibrium point. This model says that, though the behavior of the system is nonlinear, the movement of the states relative to an equilibrium point can be modeled as linear, provided the actual states and controls are "close enough" to equilibrium. At what distance from the nominal the linear model no longer holds depends on the extent of the original nonlinearities.

When designing a control system for a nonlinear plant such as an aircraft, it is customary to consider the performance of the plant at many equilibrium points. In fact, *gain scheduling* in flight control systems is required because aircraft exhibit such varied dynamics about different equilibria within their flight envelope [21]. However, by observing that the dynamics change in a smooth, continuous manner throughout the flight envelope, it becomes clear that the aircraft transfer function may be considered linear but containing parameters varying as a function of the current state, as in the case of parameter uncertainty discussed in Section 1.1.1. The linearization process introduces significant non-statistical uncertainty into the unknown parameters [22].

Other sources also contribute to the non-statistical uncertainty associated with the analysis of a nonlinear plant such as an aircraft. First, all higher order dynamics are assumed negligible. These terms are only negligible in actuality when the system is exactly at the nominal condition. Second, though the model is now expressed in terms of perturbations from the nominal, all incoming measurements will be of the full state \underline{X} and the full control \underline{U} . The nominal conditions will have to be subtracted from each measurement, and any error in the nominal condition will directly manifest itself as a disturbance driving the linearized system model [14]. These errors will be compounded by any actual parameter variation exhibited by the physical plant itself, as well as by noise present in the signal paths [2].

As developed in the previous two sections and elsewhere [4:688-690], most error sources can be accounted for by assuming parameter and signal uncertainty in a linear system model. The current practice is to ignore these uncertainties or to include them by assuming a linear system driven by statistically modeled process and measurement noises [4, 2]. In both cases the controller is then derived in a linear fashion. However, by defining a "Fuzzy linear system," where parameters are assumed to have a certain non-statistical uncertainty, the effects of linearization can be explicitly

included in the model. Though the idea of a time-varying linear system represented by a Laplace Transform is an abuse of notation, it nonetheless provides valuable insight into the operation of the proposed Model-Based Fuzzy Logic Compensator.

1.2 Proposed Approach

Control systems based on Fuzzy Logic have been developed and implemented for many plants in science and industry [5]. Current Fuzzy controllers are based on a mapping of the input/output relations for a given plant. These relations are formulated as a series of IF...THEN-type rules which comprise the Fuzzy Inference system within the Fuzzy Controller. Fuzzy Controller development is therefore contingent on the availability of a system control knowledge base, obtained either from interviews with human operators or from tests on the actual hardware. The concept of a Fuzzy Controller based on a model of the system behavior rather than expert "rules of thumb" has not been addressed in the literature.

To better understand the potential benefits of model-based Fuzzy compensation, consider the control design problem in graphical form, shown in Figure 1.4. This figure shows the parameter space for a scalar version of the nonlinear system discussed in Section 1.1.2. In this diagram, the x and u axes of the graph represent the allowable range of variation of the state and the input respectively. The objective, as stated above, is to drive the plant from an initial equilibrium state, assumed $X = 0, U = 0$ in the Figure, to a final value which is shown at the end of the $X(t), U(t)$ -Optimal trajectory curve. If a system were to traverse the optimal trajectory, it would be assured of reaching the final state within desired specifications. Unfortunately, this trajectory is a mathematical abstraction and is not known prior to simulation. Only the nonlinear equations describing the plant are available, as well as N linearized plants describing the dynamics about N "evenly" spaced operating points on the locus of equilibrium points. The objective of the controller is to remain approximately on the optimal trajectory by using the dynamics information available in the form of the linearized plants.

Given that the system is at the point labeled "Current Position" in the Figure, the question is: which linearized model yields the best approximation of the dynamics at the current point? Plant 3 yields a better model of the U dynamics while Plant 2 yields a better model of the X dynamics at the point in question. Therefore, without resorting to a nonlinear compensator, the best controller is based on a weighted combination of these two plant models. An implementation of this approach

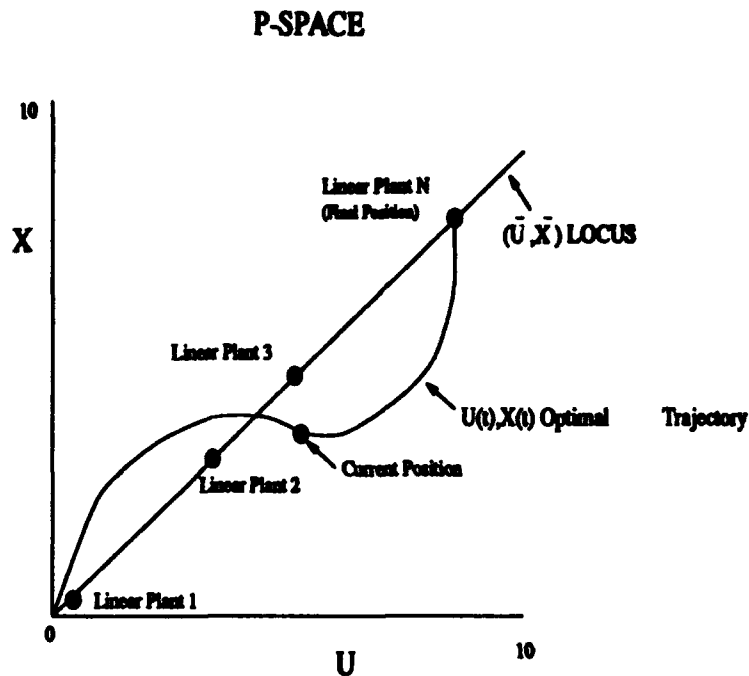


Figure 1.4 State space paradigm for nonlinear control

is shown in Figure 1.5. Here, a linear controller is developed for each of the N linearized plants. Each compensator provides adequate closed-loop performance for state trajectories originating and terminating "sufficiently close" to the equilibrium about which the compensator is based. The value corresponding to "sufficiently close" depends on the extent of the nonlinearities exhibited by the plant and will be referred to in this report as the *region of attraction* of that compensator. The N compensators are all implemented in the forward path of the closed-loop system, and all receive the error signal E . Which compensator(s) will actually drive the plant, however, is determined by the *Fuzzy Supervisor*. The Fuzzy Supervisor will appropriately weight each compensator based on a Fuzzy assessment of system's position in the state space of Figure 1.4. The Fuzzy Supervisor will base its decision on a measurement of the current system state Y , as shown in the Figure.

Each linearized plant is represented by a Fuzzy Set within the Fuzzy Supervisor. When a measurement of the current state is input, the Supervisor will assign a membership value μ_i for that input to each Fuzzy Set. The values of μ are based on membership functions $\mu_i(Y)$ which represent

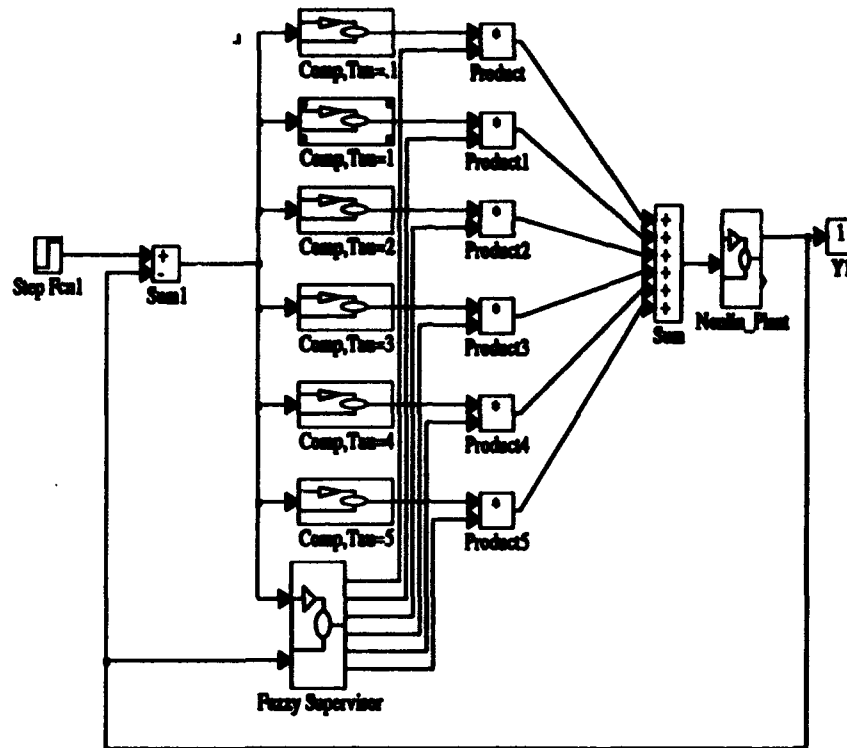


Figure 1.5 Weighting of a bank of linear compensators using Fuzzy Sets

the "rules of thumb" for properly weighting the compensators. In this research, the membership functions are Gaussian-like and are based on the regions of attraction of the compensators.

This simple control approach leaves many questions unanswered, particularly for multi-state problems. First, there are the linear questions associated with the use of multiple compensators in the forward path of the simulation. For example, the fact that each compensator is valid within its region of attraction does not necessarily imply proper dynamic control of a plant traversing multiple regions of attraction. Even the location of the weighting blocks (whether before or after the compensator) will determine the distribution of energy throughout the system. This will have a bearing on the transition from one compensator to another.

Second, there are also nonlinear considerations to be addressed. The most pressing of these is that some appropriate control action must be taken even when none of the compensators are considered valid. This will be a common occurrence, especially for multi-state plants, so how this situation is handled will greatly impact the complexity and performance of the final solution. The designer would like the controller to respond with *caution*. When the the Fuzzy Supervisor finds no close correspondence between the estimated system state and the Fuzzy sets corresponding to the universe of discourse, the compensator should decrease the input to the plant (Caution and other characteristics exhibited by optimal controllers are discussed in Maybeck [1:229]).

The above considerations and others will be used to determine the feasibility of a hybrid linear/Fuzzy Logic controller based only on linear compensators and Fuzzy Sets. Analysis in the chapters to follow show that this configuration is *not* adequate to control a nonlinear plant. The analysis itself, however, suggests an alternate controller configuration based on linear-like waveforms generated using Fuzzy Logic. This alternative design for the Model-Based Fuzzy Logic Controller is shown in Figure 1.6.

Note that this design has only a single linear compensator, which corresponds to the highest gain required for any linearization under consideration. It was found that the linear compensators intermediate to the initial state and final state of the system contributed nothing to the successful control of the nonlinear plant. Therefore, only starting and terminating compensators are necessary. Between the two regions of compensator validity, a Fuzzy "squashing function" is required to avoid overdriving the nonlinear plant.

Of the two "compensators," only one is implemented as a linear transfer function (shown at the top in the Figure). The second is a Fuzzy Logic emulation of the $u(t)$ output which would have been produced by a second linear compensator corresponding to the final desired state of the system. This "compensator" is implemented as shown in the lower portion of Figure 1.6. This Fuzzy Logic approximation is necessary because the required form of the second compensator does not correspond to the linear compensator based on the final equilibrium state of the system. The required controller output, then, must be determined through simulation.

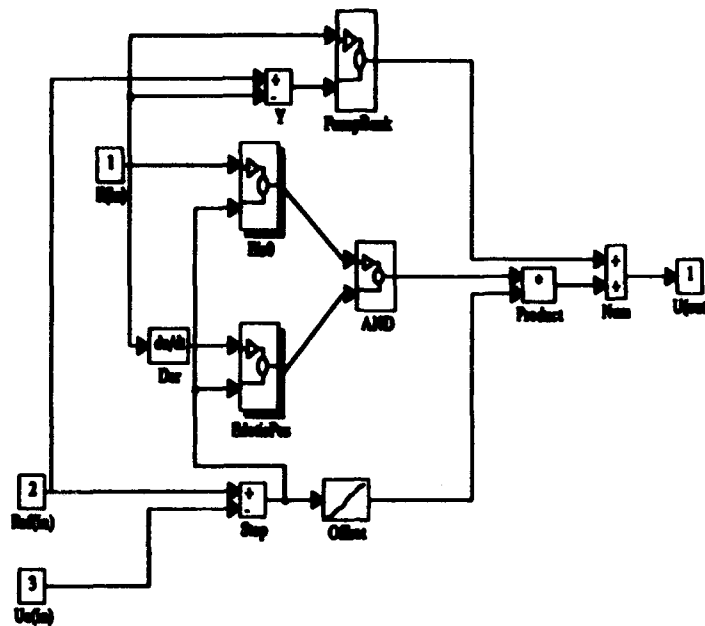


Figure 1.6 Final structure of Model-Based Fuzzy Logic Controller

This alternate Model-Based Fuzzy Logic Controller induces linear-like closed-loop performance from a nonlinear plant over a specified envelope of operation, but at the expense of most linear components in the originally proposed controller. The internal operation of this concept controller is developed further in the chapters to follow.

1.3 Scope and Assumptions

As this study involves both non-linear plants and non-linear compensators, the issues of stability, performance, and steady-state error will only be addressed through experimentation via simulation. Rigorous exploration of these topics is beyond the scope of this study and, in some cases, beyond the state of current nonlinear mathematics [21, 27].

This study is exploratory in nature so it cannot be exhaustive in its inclusion of all possible nonlinear plants. The objective is to address plants pertinent to aerospace science. The stipulation that f be smooth is necessary to the description of nonlinear systems as linear perturbation models with varying parameters. f need not be smooth in general, though the applicability of MBFLC to plants with discontinuities within the range of operation is beyond the scope of this study.

The design approach developed here is germane to both uncertainty due to nonlinearity and uncertainty due to parameter variation or mismodeling. The controller developed herein is based only on the former, though the performance is also measured against an uncertain modeling parameter. Encompassing both non-statistical error sources simultaneously is left for later research.

Broadly stated, the objective of this research is to develop a full-envelope controller for a nonlinear plant using only linear control techniques and Fuzzy Logic. The expected benefits of the Model-Based Fuzzy Logic Control approach are:

1. Force a nonlinear plant to exhibit linear-like performance and conform to linear design specifications.
2. Incorporate available models into controller structure.
3. Enhance robustness of controller in the face of unmodeled uncertainties (system damage, noise).
4. Obtain full envelope operation without the need for gain scheduling.
5. Introduce some a priori synthesis and analysis capability into Fuzzy Controller Design.

1.4 Summary

Engineering models of real-world systems are inevitably abstractions of reality. By modeling the extent of this abstraction, a more accurate representation of the physical system can be obtained.

Fuzzy Logic is one means by which this non-statistical uncertainty can be taken into account in a mathematically tractable way.

Flight controllers based on Fuzzy Logic have been developed and presented in the open literature [19, 12]. These designs, however, are based on the assumption that no adequate plant models exist for aircraft. This is not the case, though the models are nonlinear and exhibit complex dynamics. The objective of this thesis is to explore the application of Fuzzy Set theory in an environment where the systems of interest are described as essentially linear with non-statistical parameter variation.

The result of this research is a hybrid linear/Fuzzy controller which forces a nonlinear plant to exhibit linear-like closed-loop behavior.

II. Plant Development and Current Approaches

2.1 Introduction

The goal of this research area is to explore *intelligent flight control*, where controllers utilize concepts from both the control and artificial intelligence fields. It is hoped that these hybrid controllers will demonstrate some advantages over current controllers, if not in performance then in areas of robustness, noise rejection, and ease of design. The objective of this thesis effort is to demonstrate the value of applying both Fuzzy Set theory and linear systems theory to the control of nonlinear plants. It is conjectured that the resulting controller will be more successful than either Fuzzy Logic Control or Linear Control alone.

Because the final envisioned application is automatic flight control, it would be reasonable to develop controllers based on the nonlinear aircraft equations of motion. However, this thesis effort was conducted using a reduced-order plant which is subject to parameter variation. The reasons for this are three-fold:

1. ***Availability of Nonlinear Models*** - The use of linearized aircraft models about a given equilibrium condition is so pervasive that few simulations are available to adequately solve the nonlinear equations of motion in real-time. Developing the hardware and software interfaces required for this type of simulation is prohibitive.
2. ***Complexity of Linear Controllers*** - The linearized models resulting from the nonlinear aircraft equations of motion would have, as a worst case, eighth-order characteristic equations. The linear controller required to adequately compensate this plant would be very complex, and simulations would be ponderous.
3. ***Difficulty in Fuzzy Tuning*** - The number of Fuzzy parameters present in the Fuzzy controller for a full-envelope flight control system would be large. Without some predetermined rules for tuning, and perhaps even pre-tuned components, the challenge of holistic tuning could be insurmountable.

Because of these three considerations, this research was conducted using a two-state nonlinear plant. The chosen plant is developed in this chapter. Conventional "benchmark" approaches to the control of this nonlinear plant will also be discussed. All designs are validated using the SIMULINK®simulation environment for MATLAB®.

2.2 Reduced-Order Plant

The following criteria were used in deciding upon the form of the nonlinear model used in this effort:

- The plant should exhibit significant nonlinearities over the expected ranges of the state and input vectors.
- The plant should exhibit parameter uncertainty.
- The plant should have an infinite number of equilibrium conditions.
- The locus of points associated with equilibria should be smooth and monotonic.
- The system nonlinearities should be odd-symmetric to ensure tracking of system inputs for both positive and negative input values and preserve some features of a linear plant.
- The form of the linearized plant model should resemble the plants used in other studies of linear systems theory, to the extent possible.
- The plant should be as simple as possible to clearly demonstrate the the developed controller.

The nonlinear plant chosen to fit these requirements is:

$$\dot{X}_1 = -X_1 + aX_2 \quad (2.1)$$

$$\dot{X}_2 = -X_1^3 + U^3 \quad (2.2)$$

$$Y = X_1 \quad (2.3)$$

$$0.5 \leq a \leq 1.5. \quad (2.4)$$

When addressing only uncertainty due to linearization, a is set to 1. The SIMULINK model of this plant is shown in Figure 2.1. In subsequent simulations, the nonlinear plant is represented as a single block called *Nonlin_Plant*, with a externally defined.

2.3 Linearization of Nonlinear Plant

In order to apply linear system theory to this plant, a linearized model of this plant must be considered, as discussed in Section 1.1.2. First, the states and inputs are described in terms of an equilibrium value, plus a perturbation:

$$X_1 = X_{1o} + x_1 \quad (2.5)$$

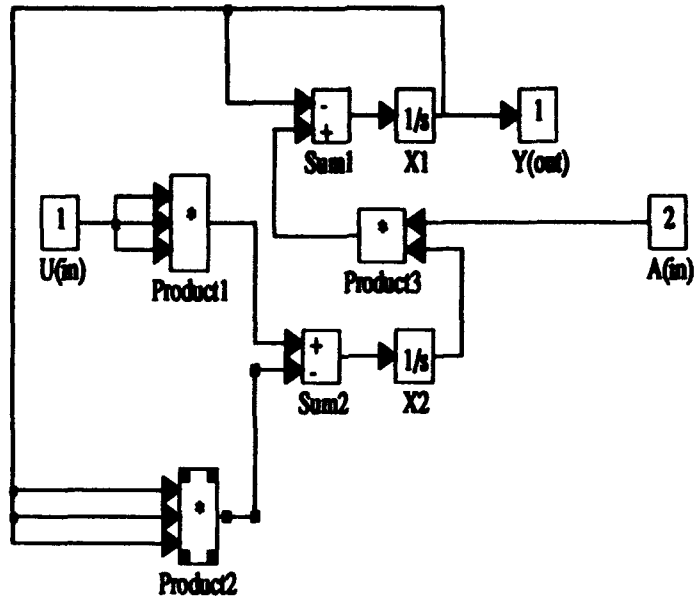


Figure 2.1 SIMULINK Model of Nonlinear Plant with Externally Defined α Parameter.

$$X_2 = X_{2o} + x_2 \quad (2.6)$$

$$U = U_o + u. \quad (2.7)$$

The relationship between the equilibrium values X_{1o}, X_{2o} , and U_o can be found by setting the right-hand sides of (2.1) and (2.2) equal to 0:

$$0 = -X_1 + X_2 \quad (2.8)$$

$$0 = -X_1^3 + U^3 \quad (2.9)$$

or,

$$X_1 = X_2 \quad (2.10)$$

$$X_1^3 = U^3. \quad (2.11)$$

This implies that $X_{1o} = X_{2o} = U_o$. Note that this plant has perfect tracking even without the benefit of feedback compensation.

To determine the linearized model, substitute (2.5), (2.6), and (2.7) into (2.1) and (2.2). This yields:

$$\frac{d}{dt}(X_{1o} + x_1) = -X_{1o} - x_1 + X_{2o} + x_2 \quad (2.12)$$

$$\frac{d}{dt}(X_{2o} + x_2) = -(X_{1o} + x_1)^3 + (\bar{U}_o + u)^3. \quad (2.13)$$

Expanding the cubic terms and rearranging:

$$\dot{X}_{1o} + \dot{x}_1 = -\bar{X}_{1o} + \bar{X}_{2o} - x_1 + x_2 \quad (2.14)$$

$$\dot{X}_{2o} + \dot{x}_2 = -\bar{X}_{1o}^3 - 3\bar{X}_{1o}^2 x_1 - 3\bar{X}_{1o} x_1^2 - x_1^3 + \bar{U}_o^3 + 3\bar{U}_o^2 u + 3\bar{U}_o u^2 + u^3. \quad (2.15)$$

Applying the small perturbation assumption yields:

$$\dot{X}_{1o} + \dot{x}_1 = -\bar{X}_{1o} + \bar{X}_{2o} - x_1 + x_2 \quad (2.16)$$

$$\dot{X}_{2o} + \dot{x}_2 = -\bar{X}_{1o}^3 - 3\bar{X}_{1o}^2 x_1 + \bar{U}_o^3 + 3\bar{U}_o^2 u. \quad (2.17)$$

Finally, by assuming the plant is operating about a static equilibrium point, then $\dot{X}_{1o} = \dot{X}_{2o} = 0$ and noting that the terms which involve only equilibrium quantities cancel out, the linearized model for (2.1) and (2.2) is:

$$\dot{x}_1 = -x_1 + x_2 \quad (2.18)$$

$$\dot{x}_2 = -3\bar{X}_{1o}^2 x_1 + 3\bar{U}_o^2 u \quad (2.19)$$

$$y = x_1. \quad (2.20)$$

Because $X_{1o} = X_{2o} = \bar{U}_o$, a new quantity τ can be defined as $\tau = 3X_{1o} = 3\bar{U}_o$. Therefore, the linearized model becomes:

$$\dot{x}_1 = -x_1 + x_2 \quad (2.21)$$

$$\dot{x}_2 = -\tau x_1 + \tau u \quad (2.22)$$

$$y = x_1. \quad (2.23)$$

As mentioned in Chapter 1, the linear model is based on two assumptions: 1) Small perturbations from the equilibrium condition, and 2) Static equilibrium condition. As long as a single equilibrium point is chosen, as was the case in developing the Banked Compensators, τ is a constant and the Laplace domain transfer function for this state space description can be derived via $G(s) = C(sI - A)^{-1}B + D$ as:

$$P(s) = \frac{\tau}{s^2 + s + \tau}. \quad (2.24)$$

Two points should be mentioned about this plant selection which will bear on the design of a successful controller:

1. τ changes rapidly relative to the eigenvalues of the linearized model. The eigenvalues of the linearized model are given by:

$$\lambda_{1,2} = \frac{-1 \pm \sqrt{1 - 12Y^2}}{2}. \quad (2.25)$$

Comparison with the expression for τ shows that the A matrix will vary rapidly with time for large step inputs. Much of the linear controller analysis will assume that the plant can be considered piecewise LTI, but research has shown that this is precisely the type of plant which frequently violates these assumptions [16]. Linear analysis must be viewed with caution, as stability and performance are not guaranteed. This is, indeed, a difficult nonlinear control problem.

2. Plant is unstable for $Y < 0$. As $Y \rightarrow 0+$ the system will become less and less stable. This will adversely impact control around the origin.

The SIMULINK model of this plant is shown in Figure 2.2. Note that it is represented in the state space form of (2.21) and (2.22). In subsequent simulations, this model will be represented as a single block called *Lin_Plant* with the parameter τ externally defined.

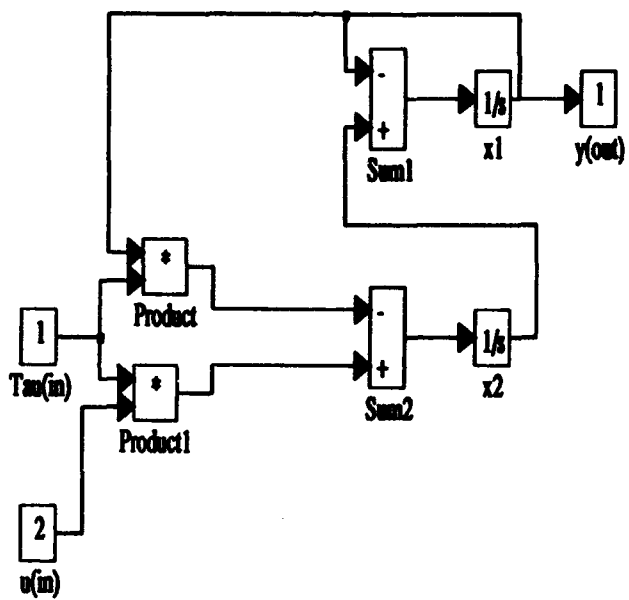


Figure 2.2 SIMULINK model of linearized plant with externally defined τ parameter

2.4 Control Performance Characteristics

It is desired to develop a control system for the nonlinear plant of interest. The following performance characteristics were arbitrarily chosen as a basis for controller design:

- Peak Overshoot (M_p): 1.12 ($\zeta = 0.5594$)
- Maximum Settling Time (t_s): 1.62 seconds
- Disturbance Rejection: $|Y(t)_{\text{disturbance}}| \leq 0.1$

The desired response is produced by the following model:

$$M(s) = \frac{19.5}{s^2 + 4.9405s + 19.5} = \frac{19.5}{(s + 2.47 + j3.66)(s + 2.47 - j3.66)} \quad (2.26)$$

This response is shown in Figure 2.3.

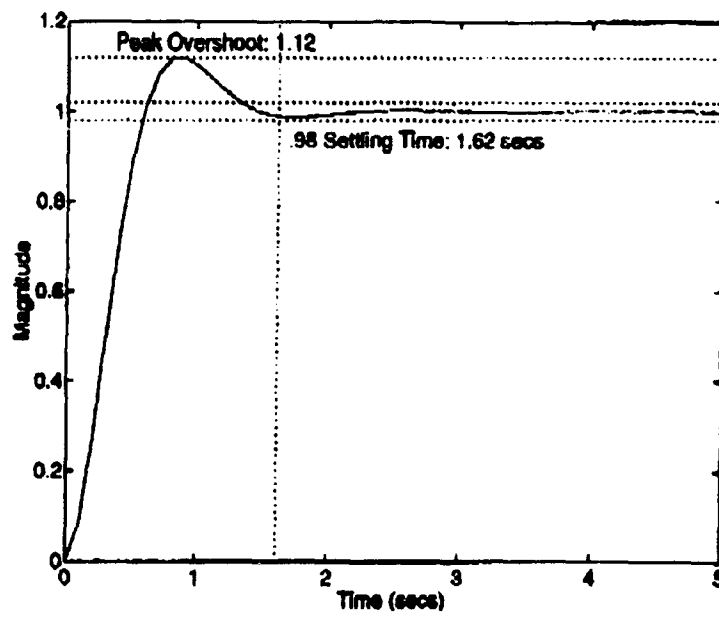


Figure 2.3 Response of Model Plant to Unit Step Input

2.5 Standard Control Approaches

Before considering the synthesis of two control approaches, it is important to assess the potential of each technique alone. This analysis will not only provide valuable benchmarks for performance, but will also provide insight into how a MBFLC compensator should operate.

Three techniques were considered in this research: Dynamic Inversion, Quantitative Feedback Theory, and Fuzzy Logic Control. The performance of these techniques was measured using the SIMULINK® simulation environment for MATLAB®.

2.5.1 Dynamic Inversion. *Dynamic Inversion (DI)* is a straightforward technique which leads to nonlinear controllers for many types of nonlinear plants. Though the objective of this thesis is not to address nonlinear control techniques explicitly, Fuzzy Logic Controllers are themselves nonlinear and the operation of the DI-based controller will serve as the starting point for Fuzzy tuning.

The objective of DI is to reformulate the problem into a linear system through the use of intermediate quantities. Linear systems theory can then be used to synthesize a controller for the "linear" plant. In implementation, the intermediate quantities required to obtain a linear system model can be solved for in an ad hoc fashion and fed into the nonlinear plant. For more on Dynamic Inversion, see Reference [27].

The nonlinear plant of (2.1) and (2.2) can be viewed as linear by defining an intermediate control variable $V = -\dot{X}_1^3 + U^3$. This leads to:

$$\dot{X}_1 = -X_1 + aX_2 \quad (2.27)$$

$$\dot{X}_2 = V \quad (2.28)$$

$$Y = X_1, \quad (2.29)$$

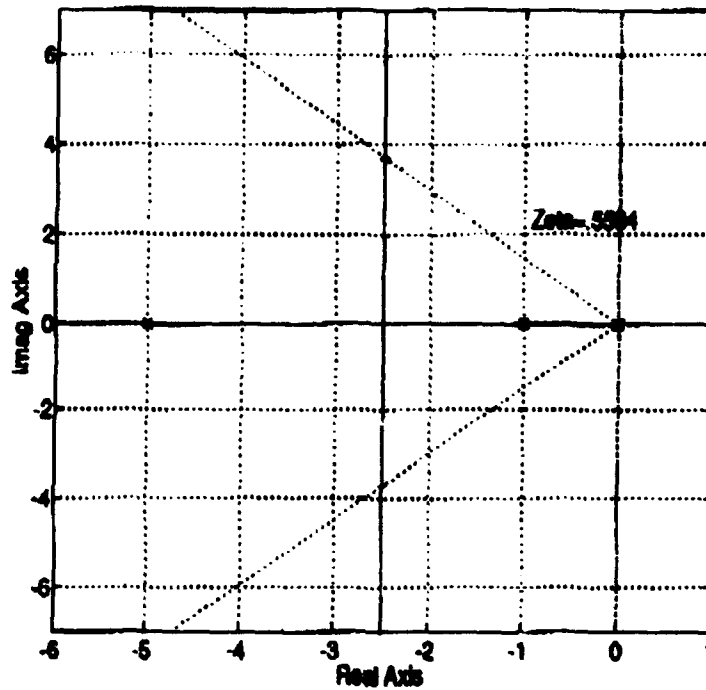


Figure 2.4 Root Locus for $G(s)P(s)$, Dynamic Inversion Synthesis

which is a linear system. The transfer function is:

$$P(s) = \frac{a}{s(s+1)} \quad (2.30)$$

It is clear from root locus analysis that the desired poles of $s = -2.47 + j3.66, -2.47 - j3.66$ cannot be obtained by gain adjustment alone. It is necessary to cancel out the plant pole and $s = -1$ and add a compensator pole further to the left in the s -plane. The proposed linear compensator is therefore:

$$G(s) = \frac{k(s+1)}{(s+5)}. \quad (2.31)$$

The root locus associated with this $G(s)P(s)$ is shown in Figure 2.4. The desired $\zeta = .5594$ is shown on the plot and can be used to determine the value for k . From this analysis, $k = \frac{12.8}{\phi}$.

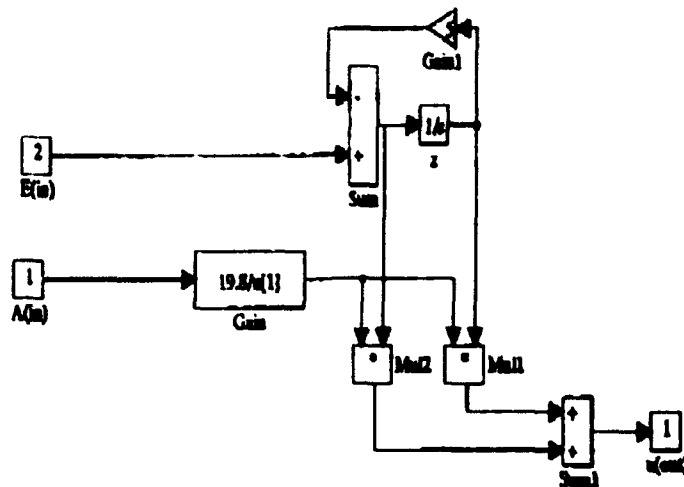


Figure 2.5 SIMULINK Model of $G(s)$ Using Dynamic Inversion

This transfer function can be represented in state space form using the technique in [4] as shown in Figure 2.5. This model is referred to with a single block called *DIComp* in subsequent simulations.

The controller described by (2.31) will accept the error signal E as input and will output V , the intermediate control quantity. In order to determine the correct input into the plant, the control U must be solved for via:

$$U = \sqrt[3]{V + Y^2}. \quad (2.32)$$

This equation will be solved in a simulation block called an *interpreter*, thus yielding a nonlinear control law. Though the interpreter should only consist of a single function block, MATLAB is unable to perform the cubed root operation when the argument is negative. Therefore, the more complex structure shown in Figure 2.6 was required.

The simulation of this control system is shown in Figure 2.7. The response of the system to a unit step input are shown in Figure 2.8. Also plotted in the Figure is the response of the model

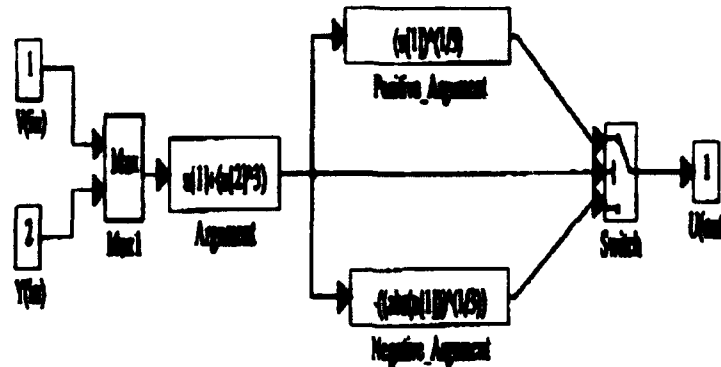


Figure 2.6 Interpreter Block Which Converts V to U

plant. The model response and closed-loop response based on DI are almost identical. The state-space representation (similar to Figure 1.4) of the plant transfer from $X_1 = 0, X_2 = 0, U = 0$ to $X_1 = 1, X_2 = 1, U = 1$ is shown in Figure 2.9. The nominal locus is also plotted on this figure as a dashed line. Note that the locus takes a step up along the U axis immediately upon onset of the step input. This moves the system state away from the nominal locus, where linearized approximations are valid. In three dimensions, the state trajectory never again approaches the equilibrium locus, where all compensator regions of attraction are centered. This is a source of problems in the banked compensator approach, which hinges on proximity to the equilibrium points for the compensators to be valid.

The response of the system when the nonlinear plant takes on various values of a is shown in Figure 2.10. The compensator is designed in all cases for $a = 1$. This Figure shows that this simulation is affected significantly though not catastrophically by errors in modeling the nonlinear plant.

Though dynamic inversion is a simple technique in nonlinear control, it will not work in many situations [27]. A more sophisticated technique called *progressive linearization* provides a more general solution to the nonlinear control problem. Both of these synthesis techniques produce

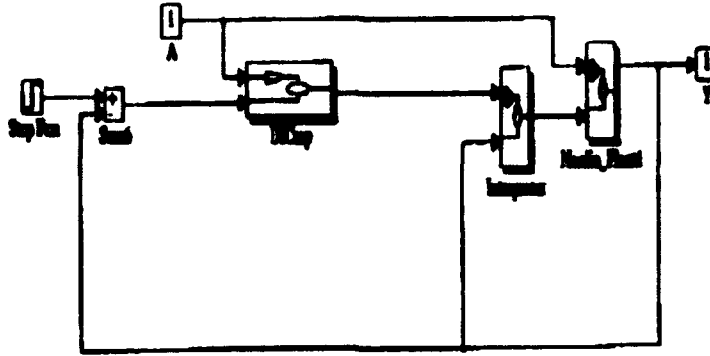


Figure 2.7 Simulation of closed-loop tracking controller developed using dynamic inversion nonlinear controllers and neither explicitly address disturbance rejection or parameter robustness. Disturbance rejection can be accounted for to some degree, however, in the the linear compensator design. A dynamic inversion-like approach will serve as the model for initial MBFLC designs.

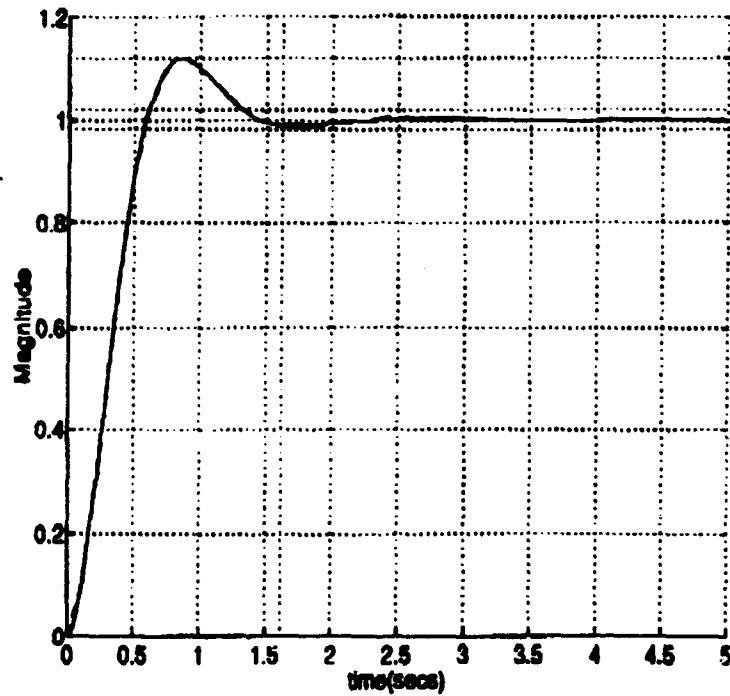


Figure 2.8 Response of dynamic inversion simulation to unit step input. Model response is also plotted but is almost perfectly covered by system response.

State Space Representation of System Dynamics, DI Compensator, $a=1$

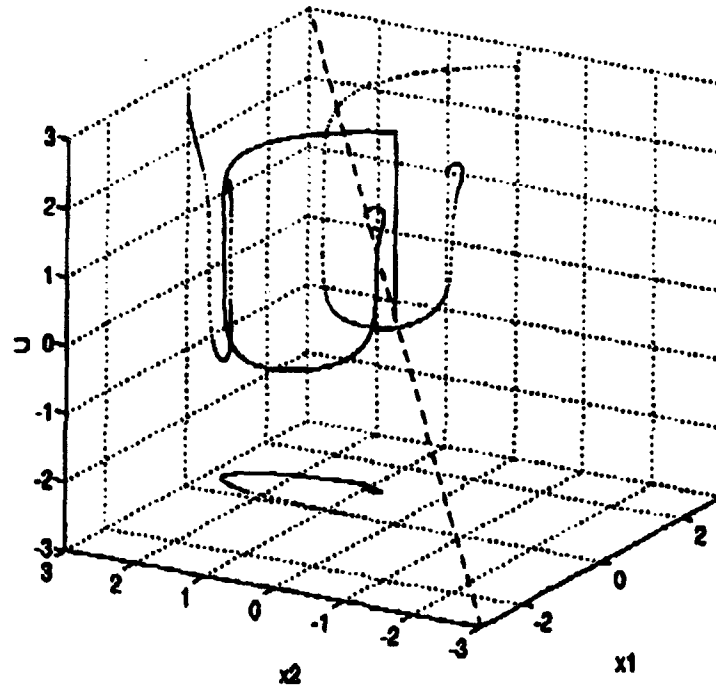


Figure 2.9 State-space trajectory representation of dynamic inversion system response to a unit step input, $a=1.0$

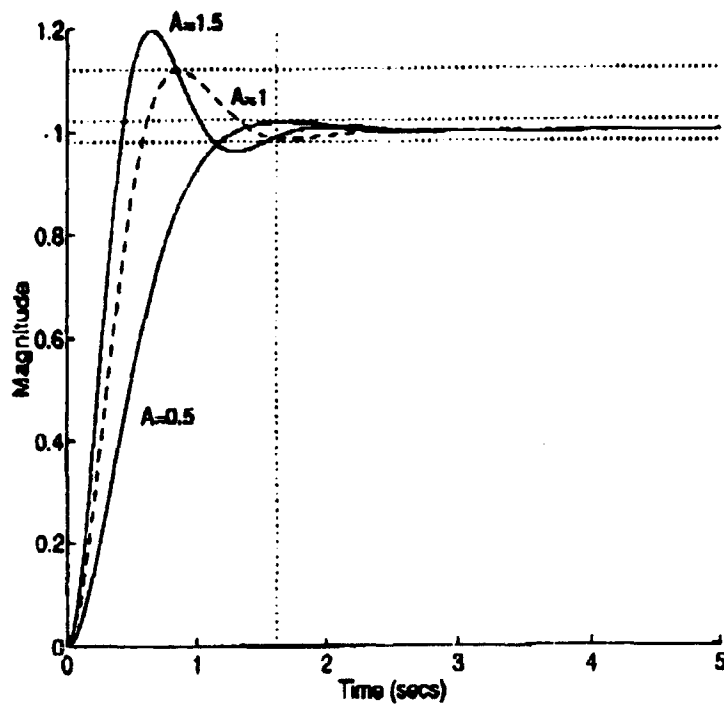


Figure 2.10 Response of dynamic inversion simulation when the nonlinear plant takes on different values of the parameter a . $a = 1$ in the compensator for all simulations.

2.5.2 Quantitative Feedback Theory. The previous two sections addressed nonlinear compensation for nonlinear plants. Since the objective of this thesis is to apply linear and Fuzzy control theory to nonlinear plants, it is important to consider a purely linear technique as well. Though linear system theory is generally applicable only as long as the linearization assumptions hold, some techniques lead to linear controllers with some applicability to nonlinear plants over a given operating range. One such technique is Quantitative Feedback Theory (QFT).

QFT was developed by Dr Isaac M. Horowitz in the 1970s to address parameter uncertainty in linear plants [29]. As discussed previously, the variation could be due to mismodeling, parameter uncertainty, or underlying nonlinear dynamics. QFT synthesis yields a linear compensator and prefilter which ensures adequate performance for any one of a family of linear plants. A top-level view of QFT-derived compensation is illustrated in Figure 2.11. Though the resulting closed-loop performance is only guaranteed for linear time-invariant plants, the QFT compensator is often capable of controlling even a nonlinear plant over a limited operating range.

The QFT design process is initiated by first defining both a family of plants to be controlled and an "acceptable" region of performance. Each of the plants should represent an extreme of the anticipated parameter variation. In the case of the nonlinear plant under consideration, the parameter variation of the linearized models depends directly on the desired operating range and the parameter a . An initial QFT design was developed for the region between $Y = 0$ and $Y = 0.5$. Five plants were used to define this operating range: $Y = 0.1, 0.2, 0.3, 0.4,$ and 0.5 , with a assumed fixed. All of these plants are of the form $P(s) = \frac{\tau}{s^2 + s + \tau}$.

The region of acceptable performance is defined by upper and lower transfer function specifications, $T_{RU}(s)$ and $T_{RL}(s)$. The magnitude versus frequency plots of these transfer functions exhibit the range of acceptable closed-loop responses. For this case, $T_{RU}(s)$ is an underdamped response with $M_p = 1.12$, and $t_r = 1.62$ secs. $T_{RL}(s)$ is an overdamped function with $t_r = 1.62$ secs. They are given as:

$$T_{RU}(s) = \frac{.8116(s + 14.814)}{(s + 1.96 \pm j2.86)} \quad (2.33)$$

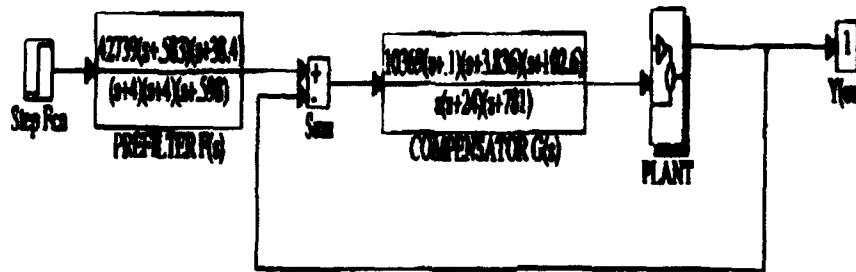


Figure 2.11 QFT compensation scheme

and,

$$T_{RL}(s) = \frac{39.99}{(s + 3.45)(s + 2.7 \pm j2.074)} \quad (2.34)$$

The resulting "thumbprint" of acceptable responses is determined by the *frequency responses* of (2.33) and (2.34). This is shown graphically in Figure 2.12. As a general rule, the larger the thumbprint of acceptable responses, the simpler the design will be. The thumbprint can also be made so small, or the range of plant variation so large, that successful design is impossible. The additional poles and zeros in (2.33) and (2.34) are to ensure that the upper and lower thumbprint boundaries are always diverging for lower frequencies, as shown in Figure 2.12. For any given frequency, the maximum allowable change in the frequency response due to parameter variation is the difference between the magnitude of the upper and lower bounds. This value is designated $\delta_R(j\omega_i)$.

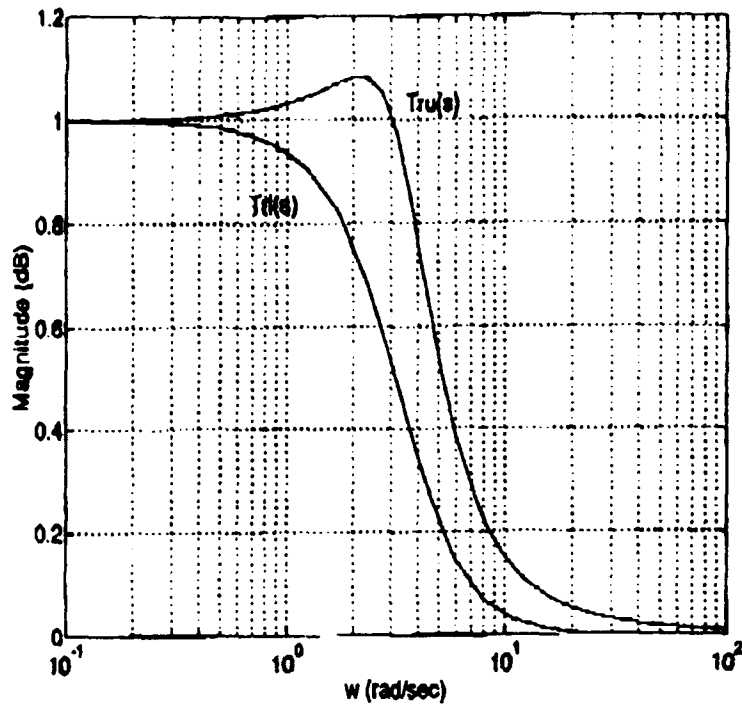


Figure 2.12 The frequency responses of $T_{RU}(s)$ and $T_{RD}(s)$, comprising the QFT response thumbprint

The development of the compensator $G(s)$ is accomplished on a Nichols Chart similar to that shown in Figure 2.13 for the current design example. The open-loop magnitude and phase data for the *least* stable (closest to the $-180^\circ/0$ dB point) plant is plotted on the Nichols Chart. In this case, the response for the $Y = 0.1$ plant is plotted. The other lines on the chart represent boundaries for certain frequencies of interest. These boundaries correspond to the points on the Nichols Chart, for any value of phase shift, at which the maximum uncertainty in M_m (caused by parameter variation) is equal to the maximum variation allowed by $\delta_R(j\omega_i)$. If the plot of the least stable plant falls below or to the left of these performance bounds for the frequency of interest, then the thumbprint of responses cannot be obtained.

Boundary lines can be determined for both tracking response (input at the reference point) and for disturbance rejection (input directly into the plant). The boundary which imposes the most severe restriction (highest in magnitude on the Nichols chart) for a particular frequency of

interest is plotted on the Nichols Chart. It can be shown that QFT control of a nonlinear plant will always involve rejection of an unwanted input at the plant [21]. Therefore, a good signal rejection capability should be designed into the compensator $G(s)$. The boundaries plotted in Figure 2.13 are almost all due to signal rejection requirements. The cylindrical boundary around the $-180^\circ/0$ dB point represents the desired stability margins of the system. The Nichols plot of the compensated system should pass to the right of or below this encircling boundary.

Clearly, the frequency response in Figure 2.13 does not meet the established boundaries. The plot of the least stable plant falls considerably below the composite bounds and violates the stability margin boundary. Therefore, a cascade compensator is required. With the addition of a compensator $G(s)$ the response shown in Figure 2.14 is obtained. Figure 2.14 shows that all of the tracking and disturbance rejection bounds are being met. The compensator used to obtain this response is given by:

$$G(s) = \frac{477900(s + 0.1)(s + 0.3)(s + 7.92)}{s(s + 1.44)(s + 51.13 \pm 74.551j)} \quad (2.35)$$

Successful compensator design ensures that the variation in frequency response due to parameter uncertainty is less than or equal to $\delta_R(j\omega_i)$. The next step is to ensure that this variation occurs within the absolute limits set by $T_{RU}(s)$ and $T_{RL}(s)$ in Figure 2.12. Figure 2.15 shows the frequency response of a successful design. The outer lines are the boundaries established by the upper and lower tracking bounds. The inner lines represent the frequency response variation of $G(s)P(s)$ in closed-loop. The $F(s)$ required to obtain this response is given by:

$$F(s) = \frac{13.063(s + .41)}{(s + .425)(s + 3.54)(s + 3.56)} \quad (2.36)$$

Notice that the steady-state gain of $F(s)$ is 1.

The performance of the final closed-loop system is shown in Figures 2.16 and 2.17. For each individual plant, the resulting tracking and disturbance rejection responses are within design specifications. This illustrates the power of the QFT synthesis technique.

Unfortunately, this $G(s)$ (2.35) and $F(s)$ (2.36) developed through QFT synthesis do not produce a stable response for the *nonlinear plant* from which the linearizations were derived. The response quickly shoots to $Y = +\infty$. This illustrates the challenge associated with using linear design techniques to control a time-varying linear plant with parameters changing faster than the plant dynamics (eigenvalues). A redesign of the QFT controller is required.

This redesign is accomplished simply by allowing the a parameter to vary between 0.5 and 1.5 over the intended region of operation from 0 to 0.5. The effect of this parameter variation is to add linear plant cases that are farther away from the origin (farther from the singularity at $Y = 0.0$). For this alternate design, the plants chosen correspond to $Y = 0.2, 0.5, 0.7, 1.0$, and 2.5 . The compensator based on this new extended family of plants is:

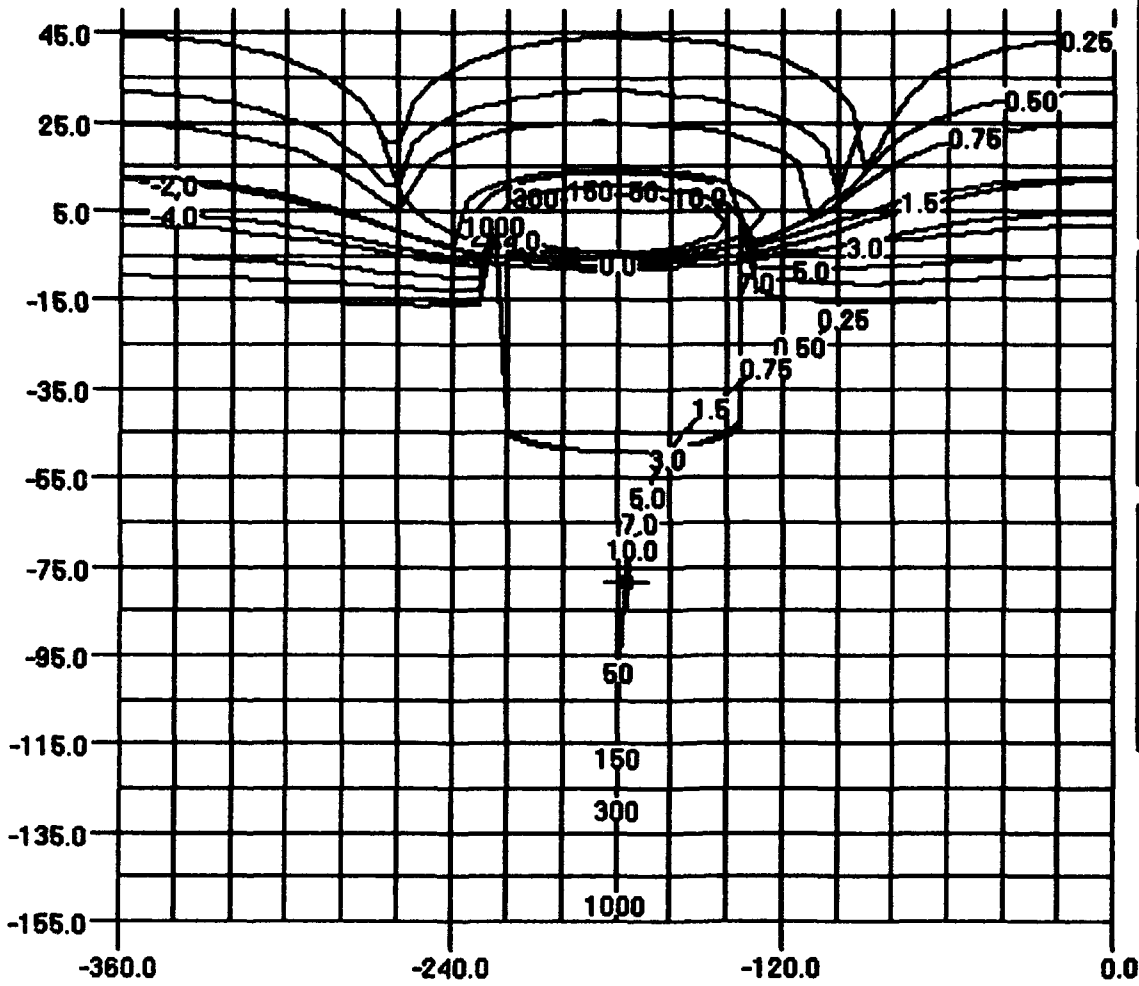
$$G(s) = \frac{1228(s + 0.1)(s + 0.3)(s + 7.92)}{s(s + 1.44)(s + 210)} \quad (2.37)$$

This $G(s)$ yields the frequency response shown in Figure 2.18. The prefilter given by (2.36) is sufficient for this design as well, so no $F(s)$ synthesis is necessary. Figures 2.19 and 2.20 show the responses of each linearized plant to reference and disturbance unit step inputs. Note that the linear performance for both QFT designs is very similar. Indeed, they both even share the same precompensator.

The new design is also effective when applied to control of the *nonlinear plant*. Figure 2.21 shows the response of the nonlinear plant with QFT-based compensation to a 0.5 step input at the reference, for various values of a . Notice that the a variation has almost no perceptible effect on the response of the system. The plots fall almost exactly on top of one another, showing the insensitivity of the QFT design to parameter uncertainty.

All plots used in this section were obtained using the QFT CAD package developed by Oded Yaniv at the University of Tel Aviv, Israel. For additional information on QFT the reader is referred to references [4] and [29].

Element Val Temp Bnd Scale Fast slow -> <- s-> s<- home end up s-up dn s-dn esc



M = 15.81
 Open Loop
 dB = -78.42
 PH = -176.38
 Closed Loop
 dB = -78.42
 PH = -176.38

Cursor speed:
 1
 Cursor index:
 149

Parameter:
 NONE
 Value :
 Step :

Figure 2.13 Nichols Chart showing QFT boundaries and frequency response of worst-case plant

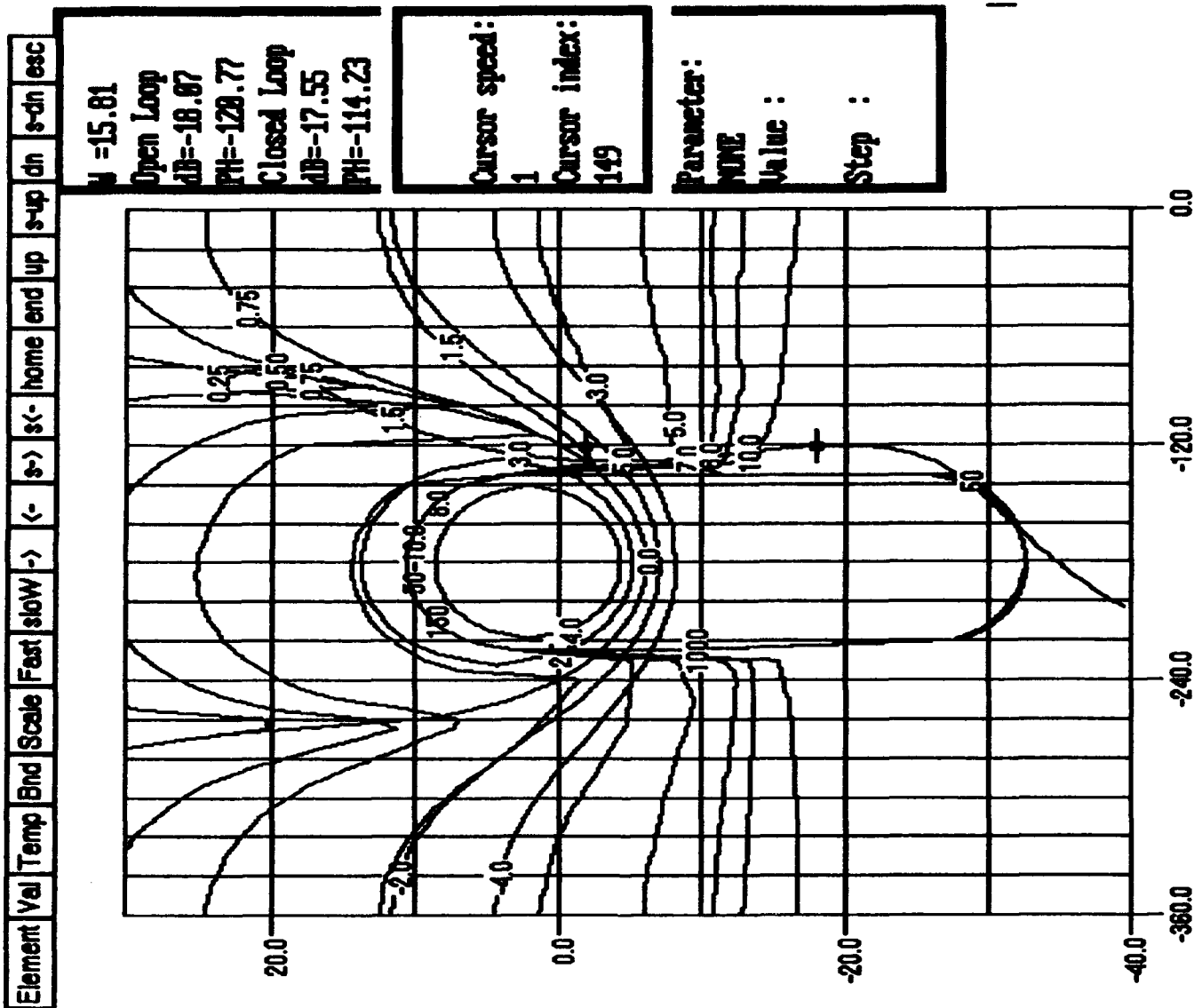


Figure 2.14 Nichols Chart of worst-case plant in series with $G(s)$

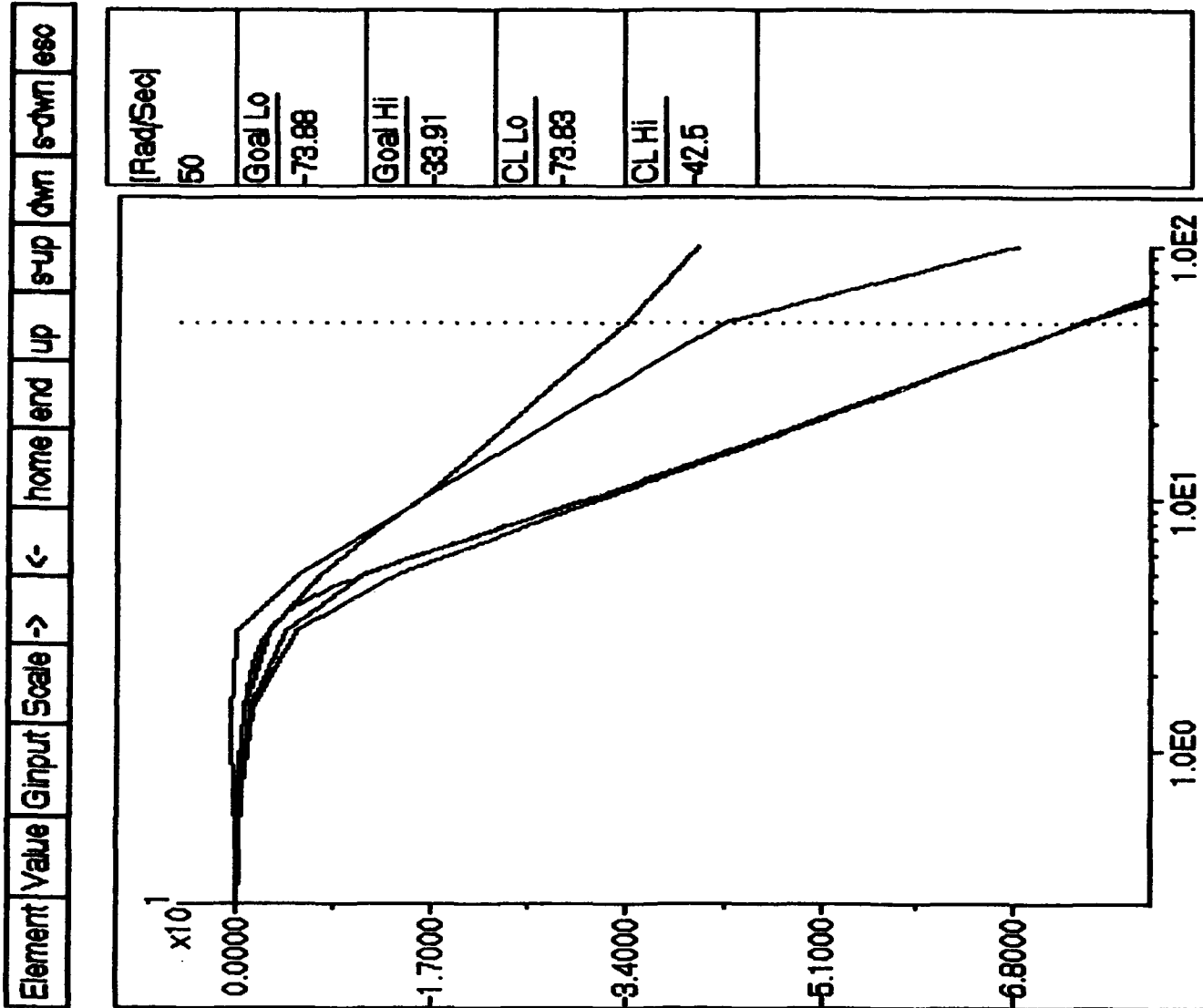


Figure 2.15 Frequency response plot showing the variation of the family of plants is inside the maximum variation allowed by $T_{RU}(s)$ and $T_{RL}(s)$

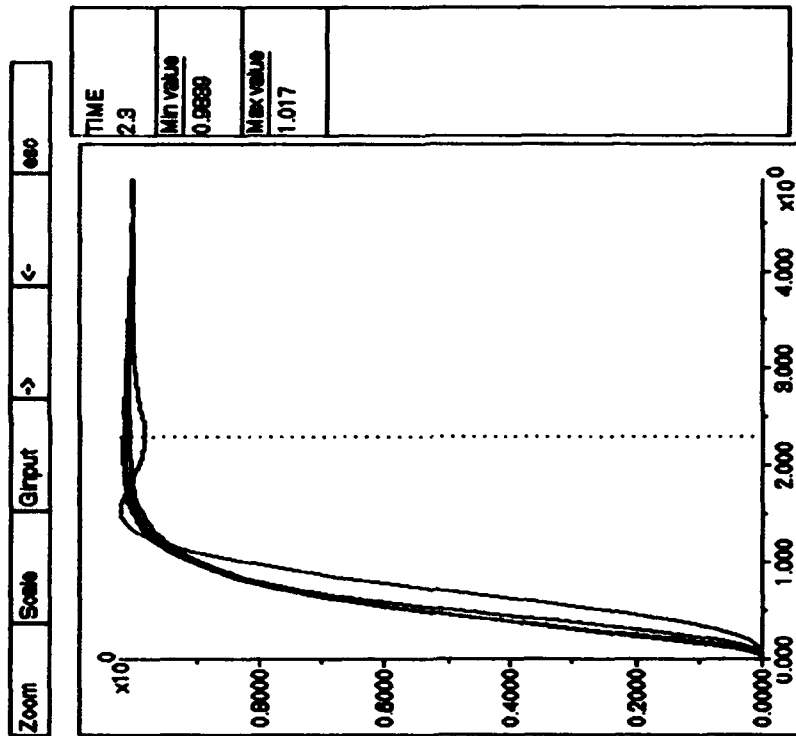


Figure 2.16 Closed-loop time responses of all five linear plants to unit step at the reference input

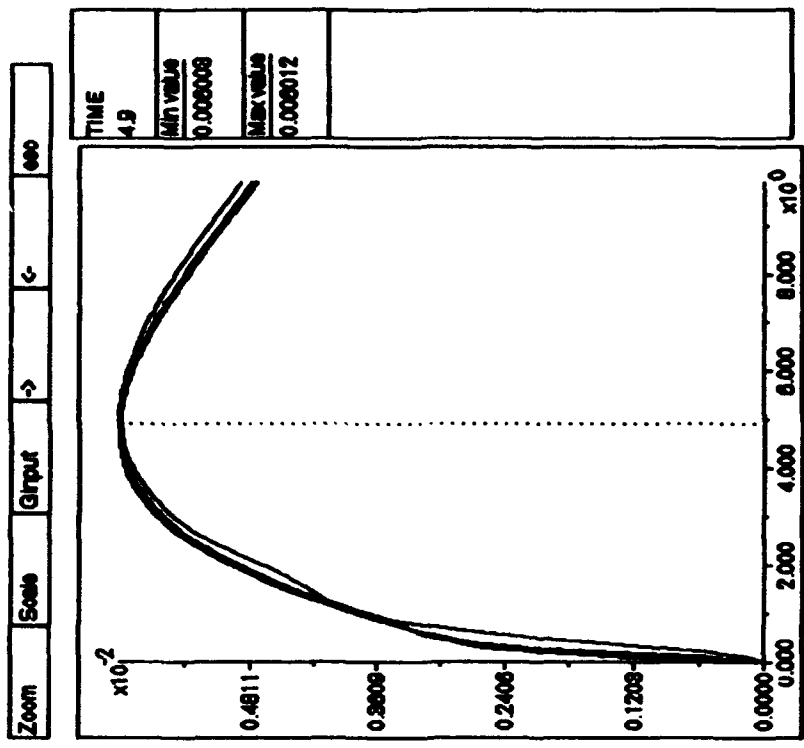
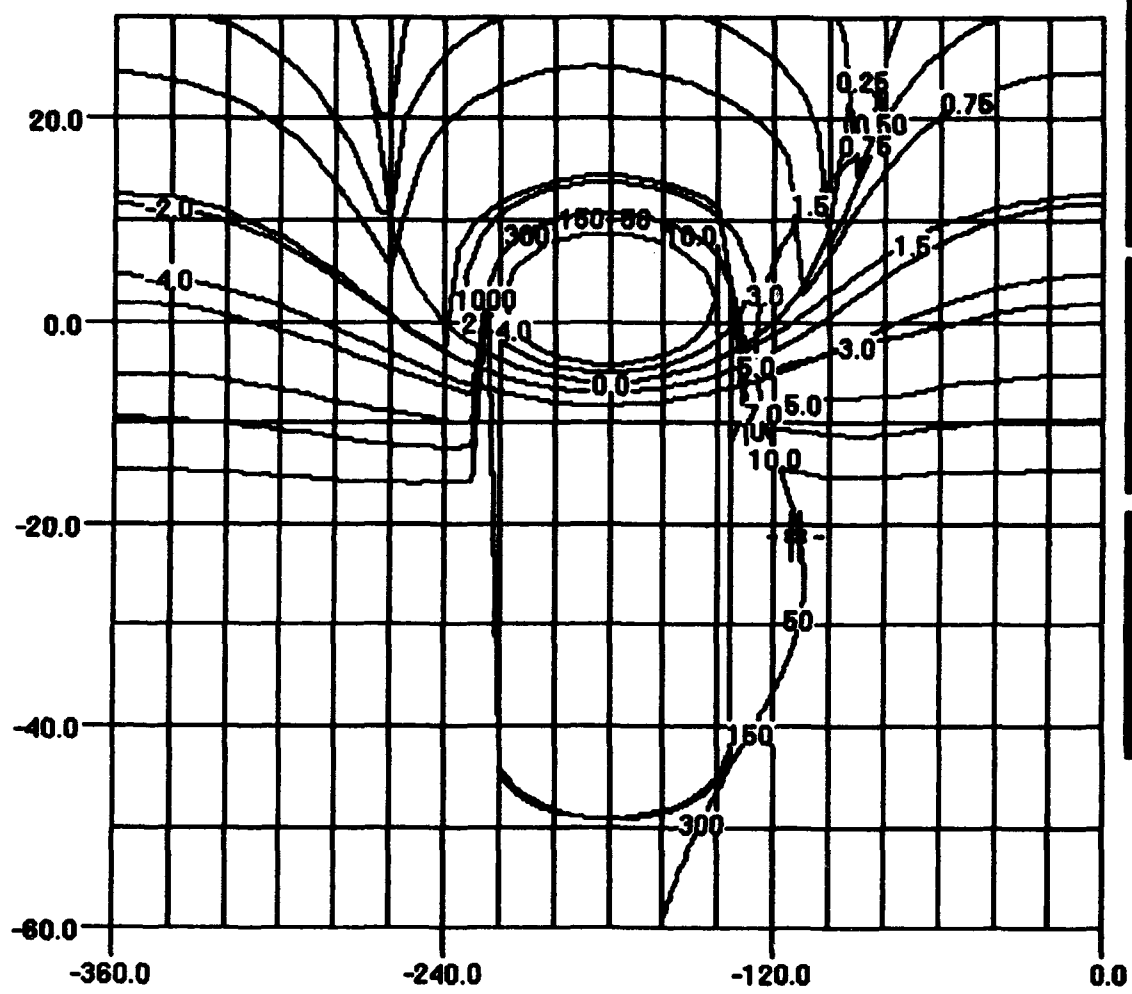


Figure 2.17 Closed-loop time responses of all five linear plants to unit step at the plant input

Element	Val	Temp	Bnd	Scale	Fast	slow	->	<-	s->	s<-	home	end	up	s-up	dn	s-dn	esc
---------	-----	------	-----	-------	------	------	----	----	-----	-----	------	-----	----	------	----	------	-----



M =-21.47
Open Loop
dB=-21.26
PH=-110.65
Closed Loop
dB=-21.02
PH=-105.08

Cursor speed:
 1
Cursor index:
 160

Parameter:
 NONE
Value :

Step :

Figure 2.18 Nichols chart showing the open-loop frequency response of $G(s)P(s)$ based on a modified family of plants

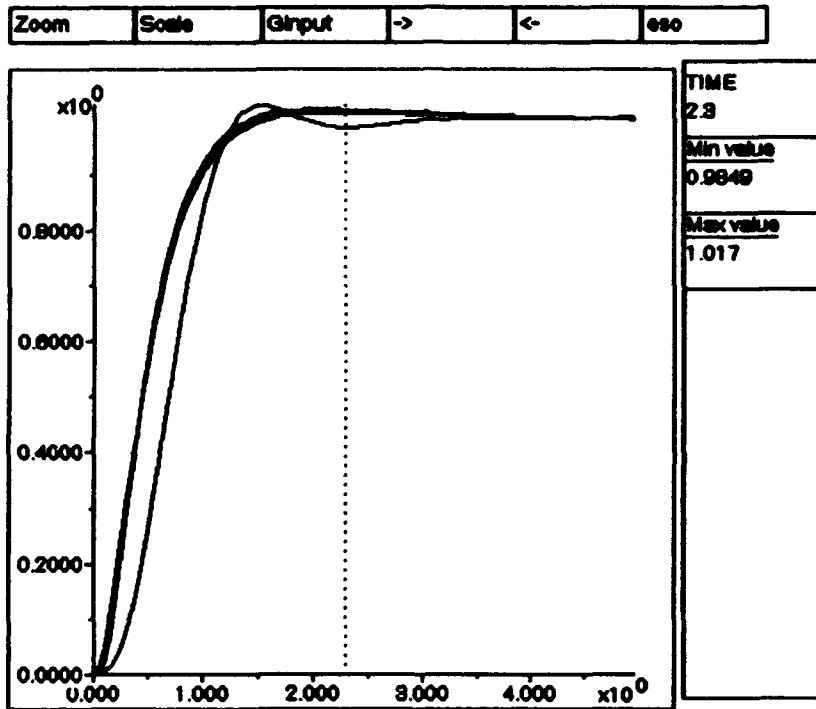


Figure 2.19 Closed-loop time responses of all five alternate linear plants to unit step at the reference input

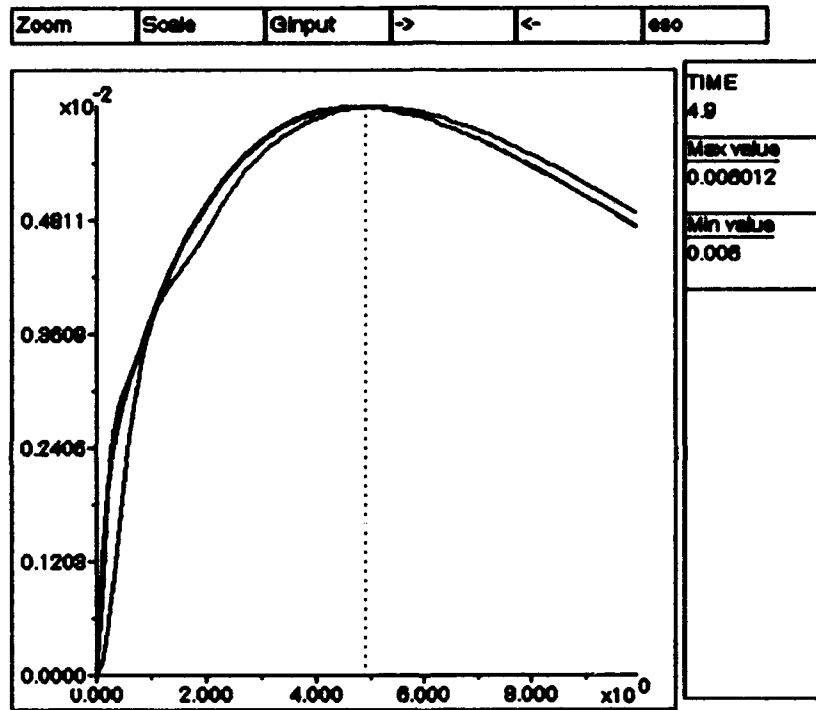


Figure 2.20 Closed-loop time responses of all five alternate linear plants to unit step at the plant input

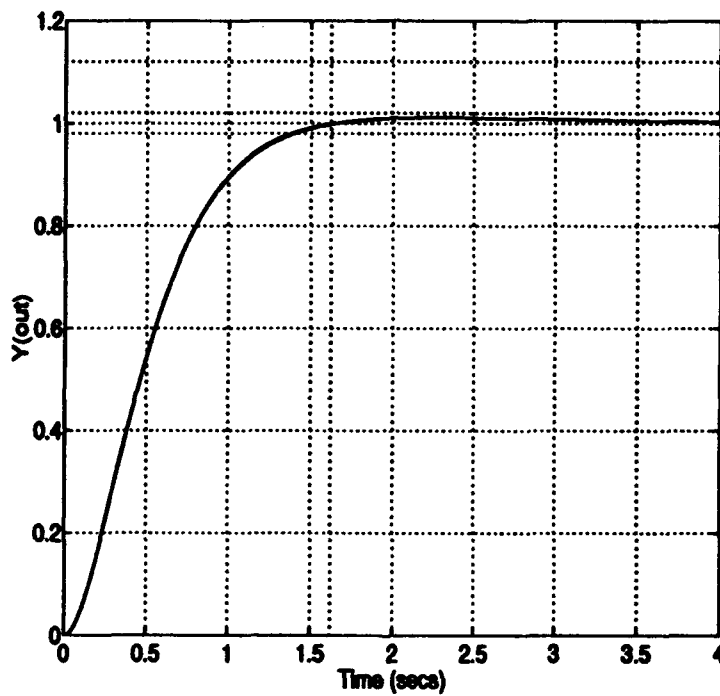


Figure 2.21 Response of nonlinear plant to unit step reference input for $a=0.5, 1.0,$ and 1.5

Variable	Min	Max
E	-.12	1
\dot{E}	-2.77	.28

Table 2.1 Universe of Discourse for FLC

2.5.3 Fuzzy Logic Control. A Fuzzy Logic Controller can be developed using the performance of the Dynamic Inversion controller as a basis for Fuzzy tuning. The first step in constructing this controller is to determine the inputs required to provide adequate information on the state of the plant. In this case, the linearized plant is second order, so it is reasonable to assume that E and \dot{E} will be adequate to control the nonlinear plant. This assumption proves correct.

E and \dot{E} will be input into the Fuzzy controller and then fuzzified as discussed in Chapter 1. All Fuzzy membership functions in this controller are of the form:

$$\mu(x) = e^{-\frac{(x-\bar{x})^2}{\sigma^2}}, \quad (2.38)$$

where \bar{x} represents the mean of the function and σ^2 is a variance-like term expressing the spread of the function. The equation (2.38) produces membership functions similar to those shown in Figure 1.1. The Gaussian form for the membership functions simplifies implementation of the FLC on SIMULINK and allows for simple tuning of the Fuzzy sets by altering \bar{x} and σ^2 . Note that the membership function is completely specified by these two quantities.

The universe of discourse for E and \dot{E} suggested by the DI simulation is shown in Table 2.1. This data, however, assumes that the plants remain on a ideal trajectory between 0 and 1. Because this may not always be the case, the universe of discourse for the FLC will be expanded slightly. Note also that by choosing this range for E and \dot{E} , the controller will only be effective for $R_{r_ej}(t) \leq 1$. The FLC will not necessarily break down for $R_{r_ej}(t) > 1$, but the results will be unpredictable.

Next, the *granularity* of each input must be determined. Granularity is simply the number of Fuzzy Sets which will be used to quantify the universes of discourse of the input variables. The objective is to use the fewest sets possible to adequately represent the data contained in the

	E		\dot{E}	
	χ	σ^2	χ	σ^2
Positive	0.5	0.0417	2	0.4343
Zero	0	.00678	0	0.4343
Negative	-0.2	0.00558	-2	0.4343

Table 2.2 Membership Functions for FLC

input. In this case, that number is 3 for each variable: "positive", "zero", and "negative." So once fuzzified, each input will be considered to be some combination of positive, zero, and negative. As mentioned above, each membership function for the linguistic variables will be completely defined by an appropriate \bar{x} and σ^2 . These values, chosen using "engineering insight," are shown in Table 2.2.

By modifying the DI simulation, a time history of E, \dot{E} , and U . can be generated for "successful" plant control. This data can be used to generate a first-cut at the Fuzzy inference system which links the compensator inputs E and \dot{E} to the output U . The following rules can be generated by inspection of the DIC simulation data:

1. IF E is P AND \dot{E} is N THEN U is PS.
2. IF E is P AND \dot{E} is Z THEN U is PL.
3. IF E is P AND \dot{E} is P THEN U is PL.
4. IF E is Z AND \dot{E} is N THEN U is NS.
5. IF E is Z AND \dot{E} is Z THEN U is O.
6. IF E is Z AND \dot{E} is P THEN U is PS.
7. IF E is N AND \dot{E} is N THEN U is NL.
8. IF E is N AND \dot{E} is Z THEN U is NS.
9. IF E is N AND \dot{E} is Z THEN U is PS.

In the above rules, P is "Positive," Z is "Zero," N is "Negative," PS is "Positive Small," PL is "Positive Large," NS is "Negative Small," NL is "Negative Large," and O is One. This Fuzzy inference system addresses all possible combinations of the two compensator inputs E and \dot{E} .

	<i>E+</i>	<i>E0</i>	<i>E-</i>
<i>E-</i>	1.5	-1.5	-2.7
<i>E0</i>	2.7	1.0	-1.0
<i>E+</i>	2.7	1.15	1.5

Table 2.3 Values for *U* suggested by Dynamic Inversion simulation

In many FLC applications, the next step would be to define the universe of discourse and membership functions for the output *U*. In this case, however, a value of *U* from the DI simulation can be associated with each combination of input arguments. The values of *U* can still be viewed as Fuzzy Sets, but in the limiting case where each premise maps to a delta function corresponding to a single point in the output universe of discourse. The values for *U* are shown in Table 2.3.

The Fuzzy Inference system above is the heart of the FLC, linking the fuzzified controller inputs to the appropriate outputs. What remains to be resolved is the exact numerical procedure that will be used to implement these rules and how multiple control conclusions will be resolved to produce a single "crisp" output. This is accomplished in several steps. First, the AND statement in the argument of each rule must be resolved. The standard solution to the Fuzzy AND statement, proposed by Zadeh and others is [28]:

$$C(x) = A(x) \text{ AND } B(x) \rightarrow \mu_C(x) = \text{Min}(\mu_A(x), \mu_B(x)). \quad (2.39)$$

Therefore, whichever term in the premise is activated the *least* will determine the level of activation of the implicated control action. In this way, every possible control action will receive a membership value which indicates the degree of confidence the controller has that each course of action is the "correct" one.

Before being output to the nonlinear plant, *U* must be defuzzified. To accomplish this, the defuzzification routine of [13] will be used:

$$U(t) = \frac{\sum_{i=1}^9 x_{Ui} \mu_{Ui}}{\sum_{i=1}^9 \mu_{Ui}}. \quad (2.40)$$

	<i>E+</i>	<i>E0</i>	<i>E-</i>
<i>E-</i>	1.9	-9.3	-2.7
<i>E0</i>	2.7	1.0	-1.0
<i>E+</i>	2.7	8	4

Table 2.4 Values for *U* implicants based on tuning through simulation

The numerator of this expression is simply the sum of all possible courses of action times the degree of confidence the controller has that the given course of action is correct. The denominator is a normalization term to ensure that the sum of all the membership functions is 1. Note also that because the membership functions are Gaussian, every resultant control action will be activated to some degree at all times. Then the state of the actual plant is far away from the mean of the membership function, however, the activation will be very small.

This FLC was implemented and tuned using SIMULINK. Not surprisingly, the values for *U* suggested by the DI simulation did not produce an acceptable response. The compensator is unable to produce the required dynamic range of *U* outputs. Many possible changes could have been undertaken to correct the system response. However, rather than change the structure of the Fuzzy Sets or resort to a finer granularity, it was simpler to change the values of the implicate *U* values. The new values are given in Table 2.4.

The simulation set-up is shown in Figure 2.22, with the FLC shown as a single block, *Fuzzy Controller*. The FLC as implemented in SIMULINK is shown in Figure 2.23. Fuzzification of inputs, ANDing of the premises and defuzzification of resultants is all carried out in this simulation. The closed-loop responses of the system to step inputs of $Ref = 1u-1(t)$ and $1.5u-1(t)$ are shown in Figure 2.24.

The purpose of showing the response of the FLC simulation to the 1.5 unit step is to show the effect of reference inputs beyond the range of the universe of discourse for which the compensator was designed. In this case the response does not exhibit a 0 steady-state error. As is to be expected, the performance degrades further for larger and larger step inputs.

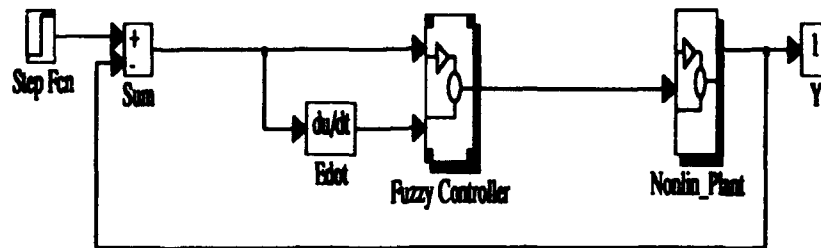


Figure 2.22 Closed-loop control of nonlinear plant with Fuzzy Logic Control

Consider, however, variations in the plant parameter A , indicating mismodeling or non-statistical uncertainty. Figure 2.25 shows the system response to a unit step given three different values for A . The response corresponding to mismodeling A ($A = 0.5$ and $A = 1.5$) are much closer to the correct response than are the responses for the DI compensator. This demonstrates that FLC offers advantages in robustness over other approaches.

As a final example, Figure 2.26 shows the response of both compensators to a step input in the face of a *time-varying* A parameter. In this case $a = 0.5 + .2t$. The FLC is more able to maintain the shape of the desired response in the face of this type of plant variation.

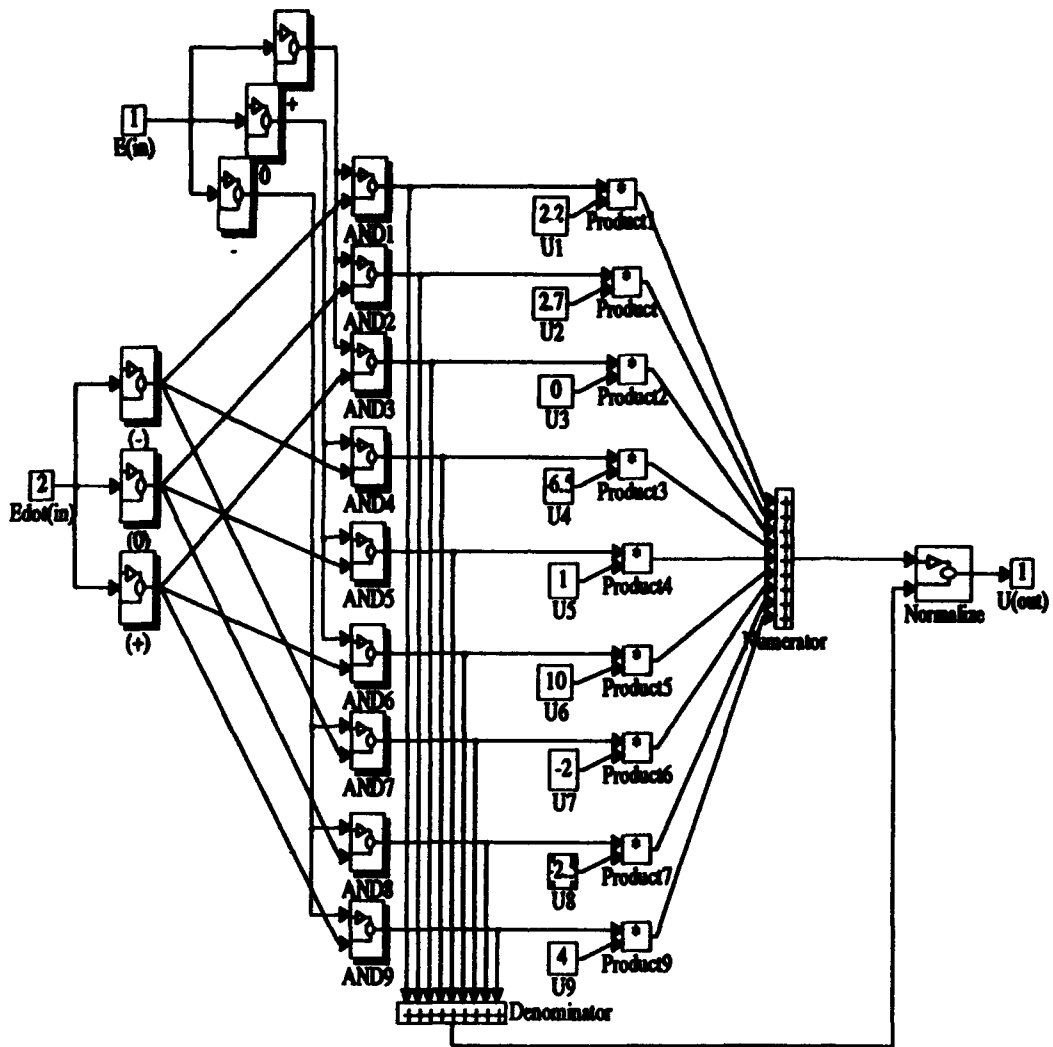


Figure 2.23 Fuzzy Logic Compensator for Nonlinear Plant

**THIS
PAGE
IS
MISSING
IN
ORIGINAL
DOCUMENT**

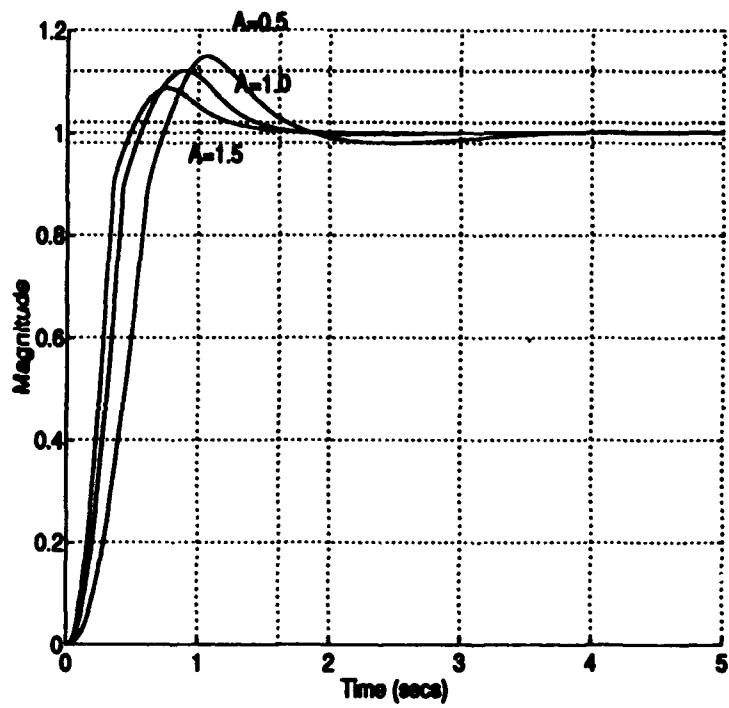


Figure 2.25 Time response of FLC/nonlinear plant to step input assuming modeling errors.

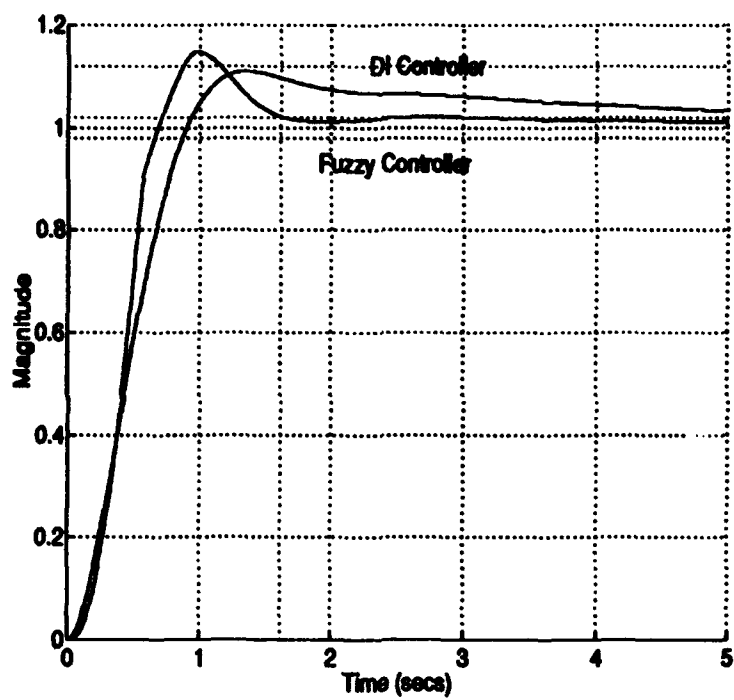


Figure 2.26 Time response of FLC and DI controllers to time-varying α

2.6 Summary

In this chapter, a nonlinear plant was developed to explore hybrid linear/Fuzzy control concepts. Desired performance characteristics were established, and a closed-loop model was presented. The desired characteristics are such that compensation is required to properly control the plant.

In order to establish a control baseline and to develop insights into the nonlinear control problem, three conventional designs were presented. A purely nonlinear technique was demonstrated using dynamic inversion. This will serve as the paradigm for a nonlinear/Fuzzy controller in Chapter 4. Second, a conventional Fuzzy Logic Controller was developed to show the structure and demonstrate the insensitivity to modeling errors. Finally, a linear design was developed based on Quantitative Feedback Theory. This serves as a benchmark for performance of other linear designs.

III. Model-Based Fuzzy Logic Control Linear Design Considerations

3.1 Introduction

The previous chapter demonstrated the potential of FLC controllers to adequately control a nonlinear plant for a single prespecified unit step input. The resulting FLC actually had advantages in robustness over more conventional designs. The FLC was not based on a plant model, and the relationship between inputs and the desired outputs was determined in an ad hoc manner through simulation. The remainder of this report addresses the use of linear compensators to control nonlinear plants with Fuzzy Logic serving as an "interpreter." Because there are quantifiable relationships between the linear compensators and the nonlinear plant, the extent of the non-statistical uncertainty is reduced to some extent compared to the Fuzzy Logic Controller, and enhanced performance is to be expected.

One possible means of applying linear systems theory to nonlinear control is through the use of a bank of linear compensators. As discussed in Chapter 1, a nonlinear plant can be linearized about a given trim condition with system dynamics described in terms of perturbations from the equilibrium point. Nonlinear plants such as aircraft have many such equilibria, corresponding to straight and level flight at a given airspeed and altitude. As the nonlinear plant changes equilibria, the linear perturbation model can be expressed as a time-varying linear function. This function can serve as the basis for multiple linear compensators which can then be used to compensate the original nonlinear plant.

In the Banked Compensation MBFLC approach, the compensators themselves would all be present in the forward control path and their outputs would be weighted according to an estimation of which compensator most accurately reflects the current state of the system. When none of the models are considered valid, combinations of outputs or Fuzzy Logic-induced *caution* would drive the system to a region where the controllers are again effective. Figure 1.5 gives a conceptual view of a Banked Model-Based Fuzzy Logic Controller.

This chapter addresses the linear considerations associated with the proposed MBFLC architecture. Because it is not clear if the compensator bank will, in fact, achieve the desired goal,

several areas will be explored in this chapter to resolve this question. The following issues will be explored:

1. Linear Compensation of Linearized Plant
2. Use of Multiple Compensators in Linear Systems
3. Effect of Compensator Dissimilarities on Closed-Loop Linear System Response
4. Use of Multiple Compensators in Time-Varying Linear Systems

Based on these design considerations, a prototype Model-Based Fuzzy Logic Controller will be proposed in the next chapter.

3.2 Linear Compensation of Linearized Plant

At any given equilibrium condition, the dynamics of the plant about that equilibrium can be described through a linear perturbation model. A linear compensator based upon this model can be used to control the plant, provided the plant remains sufficiently close to the equilibrium. A succession of linear compensators based on this concept will be used to produce the Banked Controller.

As stated in the previous chapter, the form of the linearized plant from the last chapter, given a fixed equilibrium point is:

$$P(s) = \frac{\tau}{s^2 + s + \tau}. \quad (3.1)$$

This is the transfer function form of the state-space linear model of (2.21) and (2.22) shown in Figure 2.2. The plant consists of two poles, both real for small values of τ , and as a complex pair for large values of τ . Figure 3.1 shows the locus of poles as τ increases from 0. The break-away point on the real axis occurs at $x = -0.5$. The compensation approach taken is to cancel the poles of the linearized plant with zeros in the compensator. The demoninator of the compensator will contain one pole at the origin and one pole at $x = -5$. As the compensator gain is increased, the poles at 0 and -5 will come together at $x=-2.5$ and break away at 90° . To obtain poles similar to the model (2.26), a gain of $K = \frac{19.5}{\tau}$ is required. Note that this approach breaks down as $\tau \rightarrow 0$, so

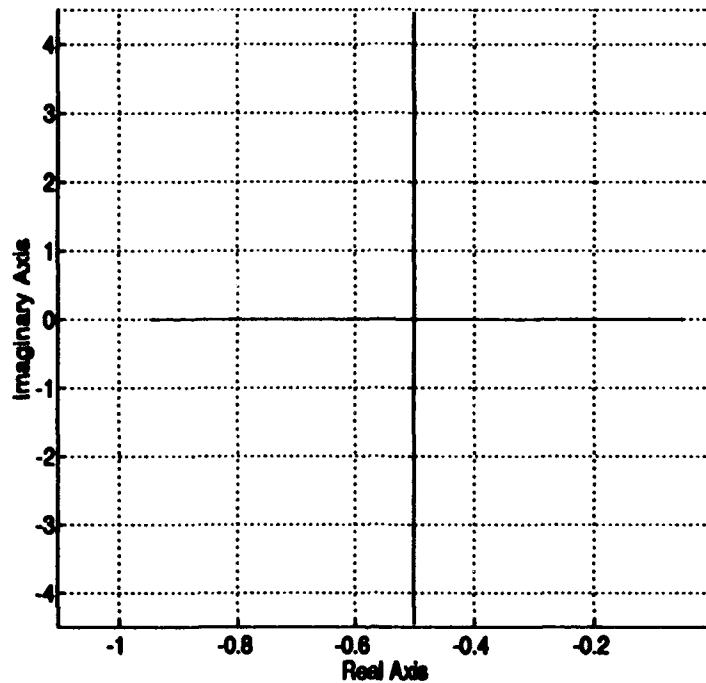


Figure 3.1 Locus of poles of the linearized plant as a function of τ

a perturbation in K will be required as $Y \rightarrow 0$. This will yield the desired pair of dominant poles, as given in the model(2.26).

For a given value of τ , the form of the compensator is:

$$G(s) = \frac{19.5(s^2 + s + \tau)}{s^2 + 5s}. \quad (3.2)$$

This compensator is shown as implemented in SIMULINK in Figure 3.2. This model is represented in subsequent simulations as a single block, *TVComp*. The compensator was converted to state space form to accommodate an externally defined τ . As expected, for any constant value of τ this compensator will yield the correct closed-loop response.

This compensator, however, does not meet the specifications for disturbance rejection ($|C_{\text{disturbance}}(t)| \leq 0.1$), so a second design must be considered. In order to add robustness in the face of noise injected at the input to the linearized plant, three poles and three zeros will be added to the compensator.

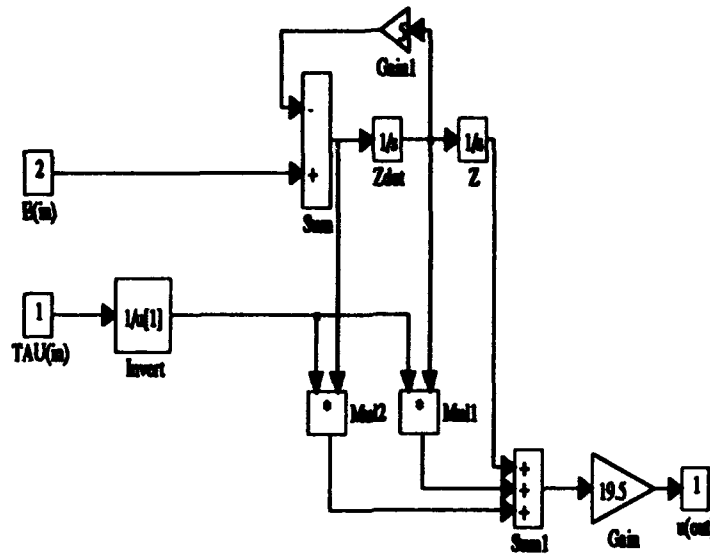


Figure 3.2 Model of Compensator $G(s)$ with τ externally defined

The form of the compensator with disturbance rejection is:

$$G(s) = \frac{2305(s^2 + s + \tau)(s + 45)^3}{s(s + 4.5)(s + 200)^3}. \quad (3.3)$$

Notice that in order to achieve disturbance rejection yet maintain acceptable tracking performance the other poles in the denominator also had to be moved. While the performance of the compensator given by (3.2) produces a response precisely as given in the model, the response of (3.3) will be slightly faster. The implementation is also considerably more complex. The SIMULINK model of (3.3) is shown in Figure 3.3.

Because the benefit of linear robustness to the control of *nonlinear* plants is not clear, two simulations were run specifically to explore this issue. Both simulations are shown in Figure 3.4. The first tests the ability of each compensator (given by (3.2) and (3.3)) to control the linearized plant when τ was allowed to vary with the output ($\tau = 3Y^2$). Because τ is a function of Y , this

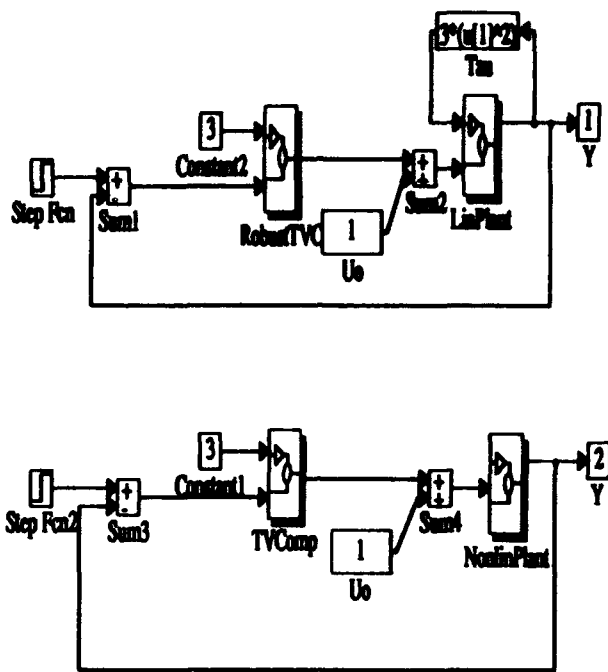


Figure 3.4 TOP: Closed-loop simulation given linear plant with time-varying plant parameter τ . BOTTOM: Closed-loop simulation given full nonlinear plant. Both simulations are run with each compensator.

Consider, however, the response of the full nonlinear plant, shown in Figure 3.7. This Figure shows the response of the closed-loop system to a step input of $Ref = 0.1u_{-1}(t)$, and it is clear that the non-robust controller yields significantly better results than the robust controller. The difference in performance is rooted in the fact that the robust compensator has a significantly higher gain than the nonrobust controller and thus a smaller region of attraction. As the step input becomes smaller, the closed-loop responses of the compensators converge. This is clearly a nonlinear phenomenon.

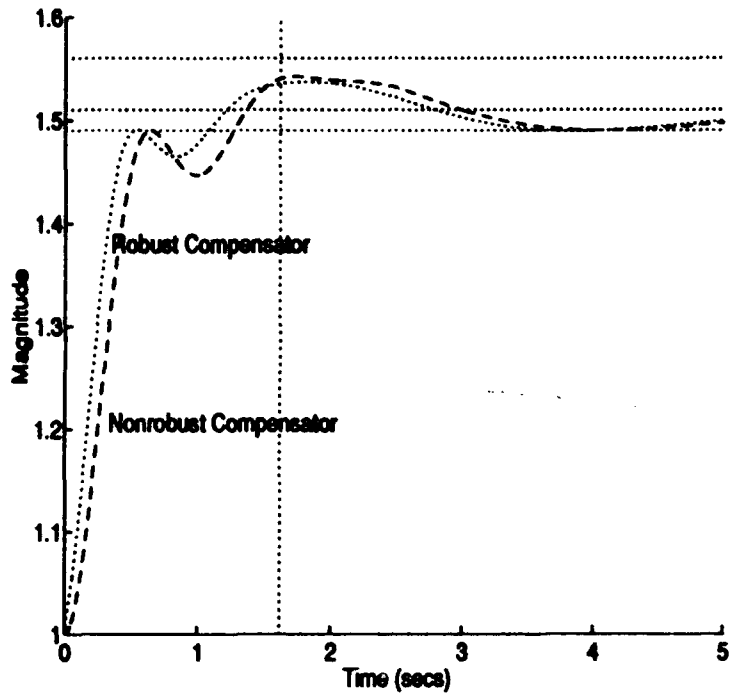


Figure 3.5 Closed-loop system responses for the time-varying linear plant under both robust and non-robust compensation.

Based on this analysis, most simulations to follow will be conducted using the nonrobust compensator design. Which compensator is actually superior depends on the the desired application. The robust controller is superior for disturbance rejection. The nonrobust controller contributes much less overshoot for tracking. Use of the robust compensator is revisited in Chapter 5.

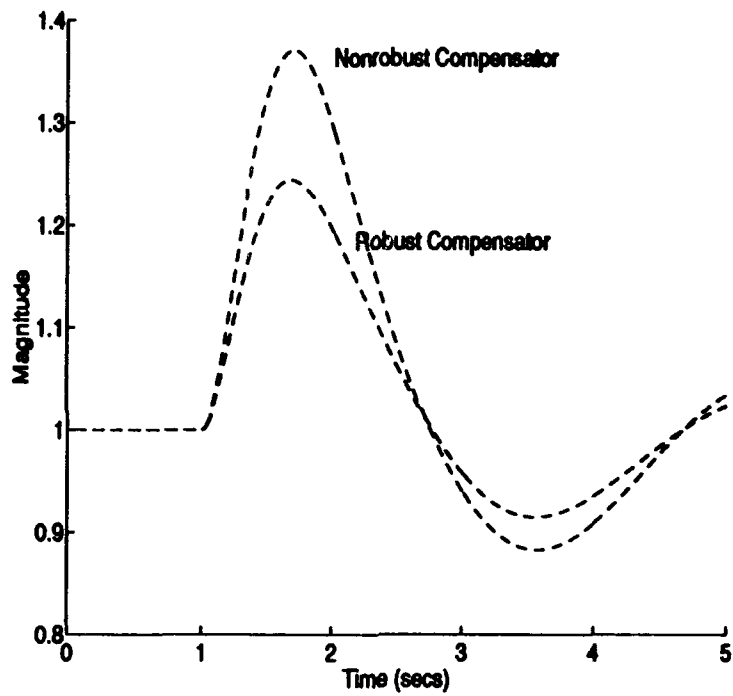


Figure 3.6 Closed-loop disturbance rejection for nonlinear plant under both robust and non-robust compensation.

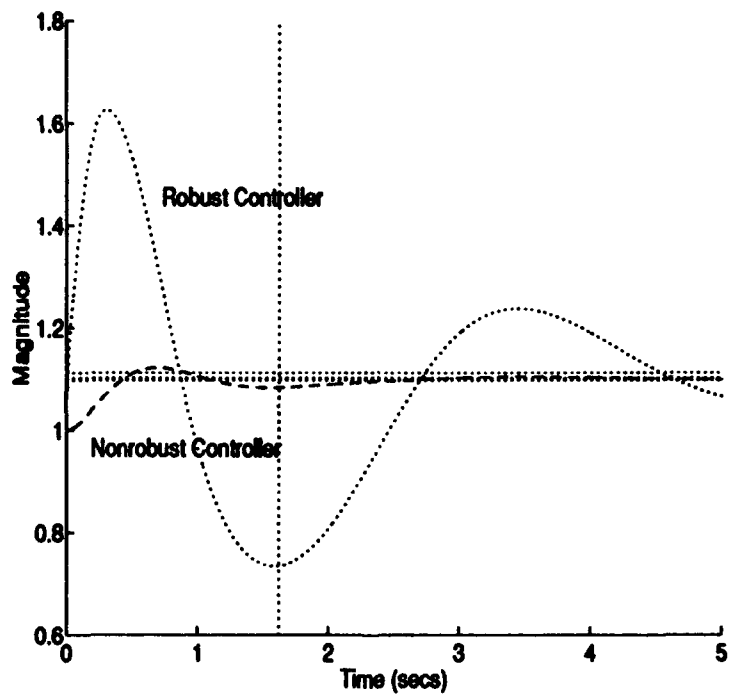


Figure 3.7 Closed-loop system responses for nonlinear plant under both robust and non-robust compensation.

3.3 Use of Multiple Compensators in Linear Systems

The next question to be addressed is how exactly to apply multiple linear compensators to a single linear plant. Of special interest is the compensation of a plant which is not at a quiescent condition at the starting time t_0 . This situation would arise repeatedly as each new compensator in the bank were activated due to a change in the equilibrium point of the plant. If the act of changing compensators disturbs the nonlinear plant, then the banked configuration may not be desirable.

A proper treatment of linear control systems operating from non-zero initial conditions was not found in the literature search for this thesis. Therefore, several simulations were necessary to determine the appropriate structure for the MBFLC. Because both the compensator bank and the plant have the ability to store energy, both of these cases must be considered separately, and in terms of their interaction.

3.3.1 Positive Internal Compensator Energy/No Internal Plant Energy. Figure 3.8 shows a simple simulation used to determine the effect of "charging" the compensator before applying it to the quiescent plant. In this Figure the compensator will be receiving the error signal E at all times. A switch just beyond the compensator prevents the output of the compensator from reaching the linear plant for a prespecified length of time t_d . From time 0 to time t_d the states of the compensator will be receiving energy from the error signal, while the plant is forced to remain at 0. At $t = t_d +$ the plant will begin receiving inputs.

Figure 3.9 shows the effect on the system response as t_d increases. Clearly, as t_d gets larger, the response of the plant system gets less and less desirable. This shows that the effect of energy in the compensator is to underdamp the system in direct proportion to the energy in the compensator at $t_d +$. This demonstrates that compensator charging is undesirable, at least when applied to a quiescent plant.

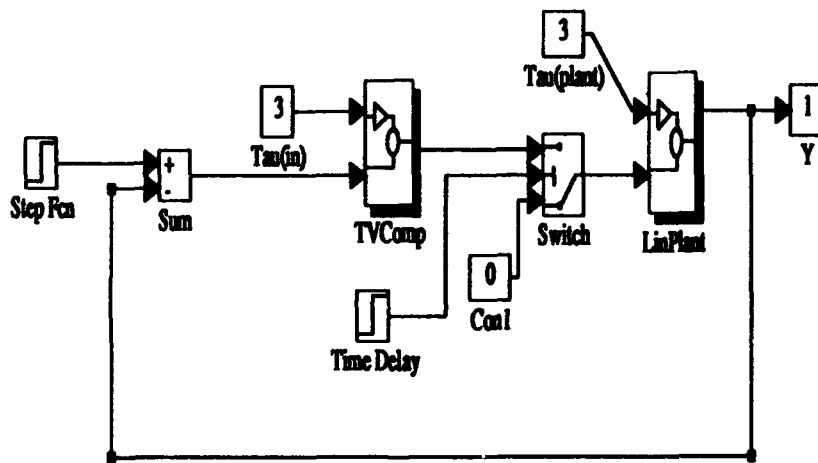


Figure 3.8 Simulation to determine the effect of charged states in compensator applied to linear system

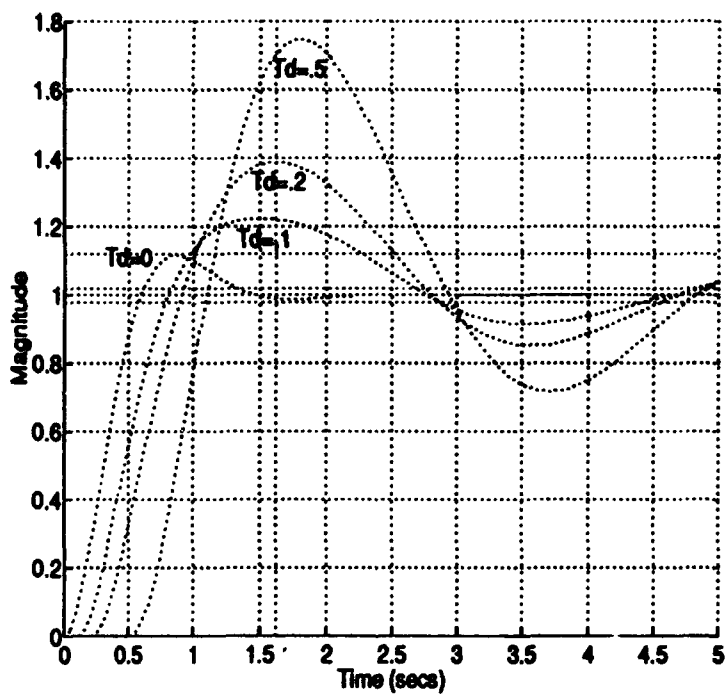


Figure 3.9 Closed-loop response of linear plant given varying "charging" times for the linear plant

3.3.2 No Internal Compensator Energy/Positive Internal Plant Energy. The previous result assumed the plant was at 0 initial conditions at the time of compensator activation. A similar simulation can be run but with the plant itself starting from a nonzero initial condition, and the compensator starting from 0 internal energy. There are two possible situations which could arise: 1) A plant starting from a nonzero quiescent position and 2) A plant starting with non-quiescent initial conditions.

In both cases, linear systems theory can be used to predict the outcome [31]. For the first situation, the desired output form will only be obtained if an additional constant input is added to the input from the compensator. The value of this input is equal to the steady-state input which would have induced the existing quiescent condition. The linearized plant plant in this research effort, for example, is in equilibrium at $x_1 = x_2 = U$. Therefore, if the plant states here have initial conditions $x_1 = x_2 = 0.2$, the required control input to the plant would be 0.2 plus the control determined by the linear compensator. The effect is simply to move the starting point of the simulation, and this has no consequences for LTI systems.

The second case is much more difficult to predict in general. The complete response of a linear system is always equal to the response of the system due to initial conditions (homogeneous solution) plus the response of the system to driving terms (particular solution) [17]. When the system is not at equilibrium there will be a homogeneous solution intermingled with the particular solution. All that can be said with certainty is that the response will deviate from the desired trajectory to some degree proportional to the strength of the homogeneous response.

This is illustrated using the simulation shown in Figure 3.10. Here, two identical compensators, $G_1(s)$ and $G_2(s)$, are included in the forward path, with the input to the plant being determined by a switch. The position of the switch is determined by the current output of the system. The switch will toggle from the top compensator to the bottom compensator at $Y = 0.5$, halfway to the reference input of $Y = 1.0$. A second switch prevents $G_2(s)$ from receiving the error signal until $Y = 0.5$. The effect is that $G_2(s)$ will "inherit" the plant when the plant is in a

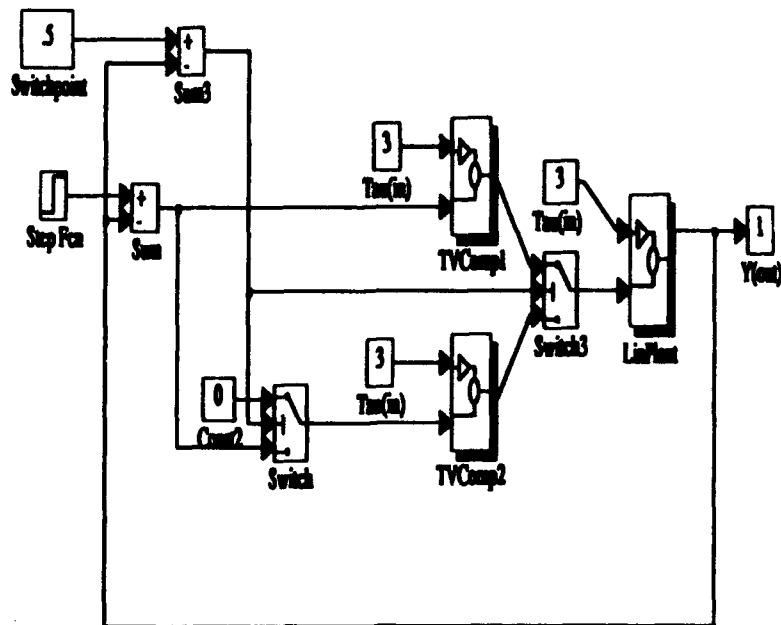


Figure 3.10 SIMULINK simulation to test the effect of a quiescent compensator inheriting a non-quiescent plant

non-equilibrium state. The state of the plant, however, is not arbitrary: it is precisely the state that $G_2(s)$ would have driven the plant through had it been utilized from t_0 .

The result of this simulation is shown in Figure 3.11. The optimal closed-loop trajectory is also shown in the Figure (optimal being the closed-loop response using a single compensator for all time). The compensator with zero initial conditions is unable to correctly drive the system when the plant has internal energy at the time the switch is thrown. An identical compensator, then cannot simply "pick up where the first compensator left off." A mechanism in the control strategy must be devised to account for the existing plant energy.

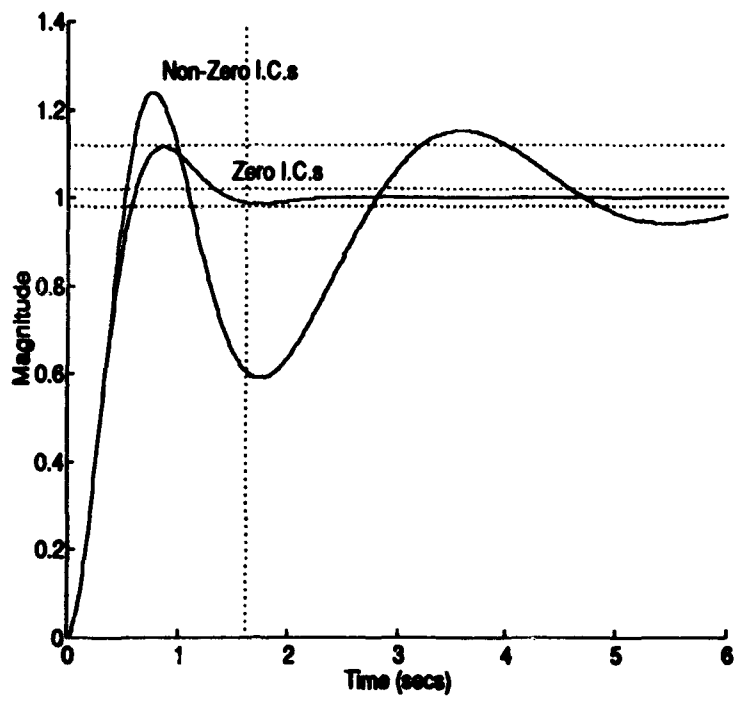


Figure 3.11 Closed-loop response of quiescent compensator/non-quiescent plant

3.3.3 Positive Internal Compensator Energy/Positive Internal Plant Energy. To account for the energy internal to the plant, consider the simulation shown in Figure 3.12. In this Figure, the plant is linear and corresponds to the equilibrium condition $\tau = 3$ or $Y = 1$. A bank of two compensators— τ set to 3 for both— feed into the plant, and they are weighted at their error signal inputs. In this case, the only two inputs into either compensator are possible: 1) $R = 0$ or 2) the actual error signal, $R = E$. The difference between this simulation and the simulation in Figure 3.10 is that now $G_1(s)$ has the ability to effect the plant for all time.

The closed-loop response of this system for various switching times is shown in Figure 3.13. Regardless of the time when the compensators are switched, the closed-loop response will be unaffected and equivalent to the response of a single compensator in series with the plant. By driving the error signal into the $G_1(s)$ to 0 at the time of compensator switch, but allowing the output of $G_1(s)$ to continue to drive the plant, the energy currently in the plant is accounted for.

In this situation, the bank can be thought of as a single compensator. When $G_2(s)$ inherits the system, it has no "knowledge" of the internal plant energy. It simply receives an error signal and produces an output "assuming" the plant is starting at a quiescent condition. This is far from being the case, and $G_2(s)$ supplies a much larger control input than is actually required. This overzealous output from $G_2(s)$ is apparent from the response of Figure 3.11. In this latest simulation, however, $G_1(s)$ actually corrects for this error by introducing a *negative* control at the summing junction to the plant. This ensures that the \dot{X}_1 and \dot{X}_2 already present in the system at the time of control transfer are accounted for from the switch time forward.

It is important to see just what $G_1(s)$ is doing to make this simulation successful. The input to $G_1(s)$ is forced to 0 at $t = 0.25$ secs, but the integrators in the compensator will continue to produce an output, which will eventually reach steady-state. In this case, $G_1(t_\infty) = 0.5622$. Figure 3.14 shows the input signal to the plant (sum of control signals for both compensators) and breaks it down in terms of the contribution by each compensator alone. Either forcing the output of $G_1(s)$ to zero or replacing the compensator with a constant signal equal to $G_1(t_\infty)$ have destabilizing effects on the system output. Therefore, the *dynamics* of $G_1(t)$ are important.

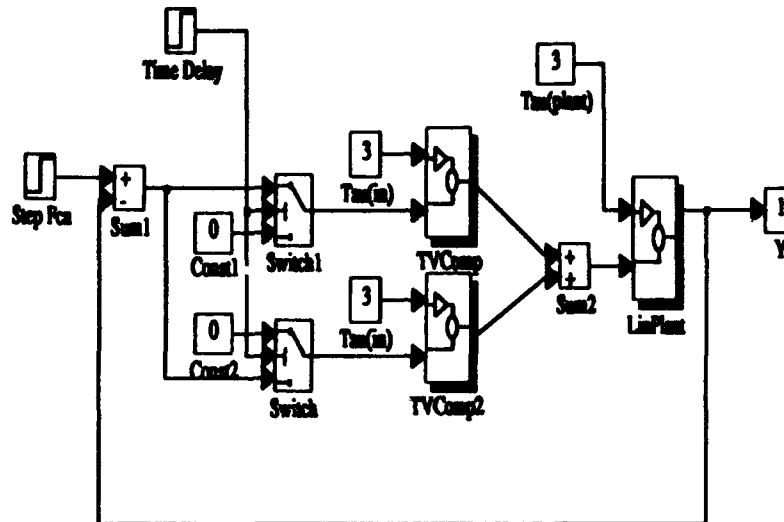


Figure 3.12 Simulation of banked compensation technique for a linear plant

A bank of linear compensators can be implemented in an alternate, but more straightforward way by simply postweighting the compensators, as shown in Figure 3.15. In this case, both compensators receive the error signal, though only one influences the plant at any time. One drives the plant from t_0 to t_d , while the second from t_d+ on. In this case, the switching process once again has *no effect* on the response, regardless of the switching time. This result is not surprising. The compensators are identical, receiving identical error signal histories, and so they produce the same input signal u to the plant. Regardless of which is actually driving the plant, the response will be the same. This also serves to illustrate that only when plant and compensator states are adequately charged will the response be unaffected by the switching operation.

An important conclusion can be drawn from this analysis. There must be internal energy in the compensator to account for internal energy in the plant. Whether the internal compensator energy is provided by the previous compensator (pre-weighted case) or built up in the compensator about to inherit the system (post-weighted case) is a question of implementation. When a linear

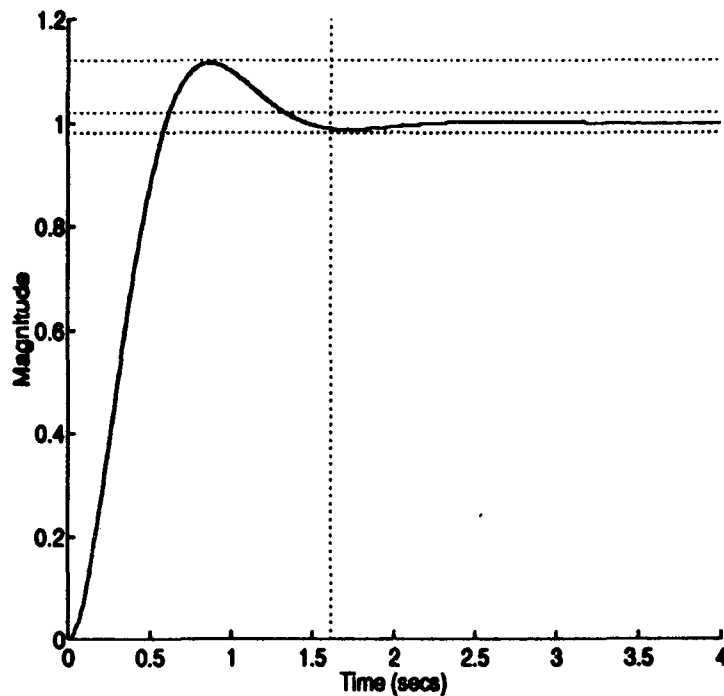


Figure 3.13 Response of Identical Compensators in a banked configuration

compensator inherits a system that is not at equilibrium, undesired oscillations will occur unless an added signal is included account for the non-equilibrium condition. Further, the form of this compensation signal is approximated by the linear response of $G_1(s)$ in Figure 3.14 for $t > 0.5$ secs. This general conclusion will be the basis for Model-Based Fuzzy Logic Controller design in Chapter 5.

3.4 Effect of Compensator Dissimilarities on System Response

In the above simulations, the two compensators in the bank were identical. By using dissimilar compensators, the question of compensator autonomy can be addressed. The ideal scenario would be to have each hand-over point be equivalent to a quiescent condition. In this case, each new compensator could start "fresh," without regard to the past history of the system. Unfortunately, the effects of unanticipated internal energy are once again introduced into the system.

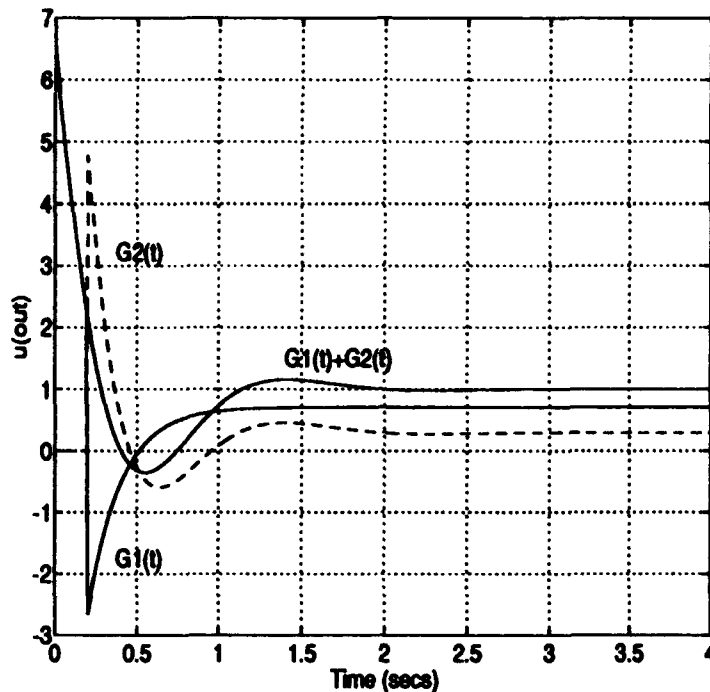


Figure 3.14 Output of compensator bank, shown in terms of each compensator contribution

To test compensator autonomy, one of the compensators in Figure 3.12 was changed. A second compensator was developed, based on the same linear plant, but with a settling time $t_s = 2.5$ seconds rather than 1.62 seconds. The transfer function for this new compensator is:

$$G_{ALT}(s) = \frac{2.44(s^2 + s + 3)}{s(s + 3)} \quad (3.4)$$

$G_1(s)$ was replaced by this new compensator. The results of this simulation for various switching times are shown in Figure 3.16. The responses at the far right and far left correspond to $t_d = \infty$ secs (only $G_{ALT}(s)$ drives the plant) and $t_d = 0$ (only $G_2(s)$) respectively. In the intermediate simulations the effect of the two different settling times is apparent, but the correct waveform is preserved. Notice, however, that none of the responses influenced by both compensators have the correct overshoot, even though both are designed to the same ζ specifications. This is the effect of

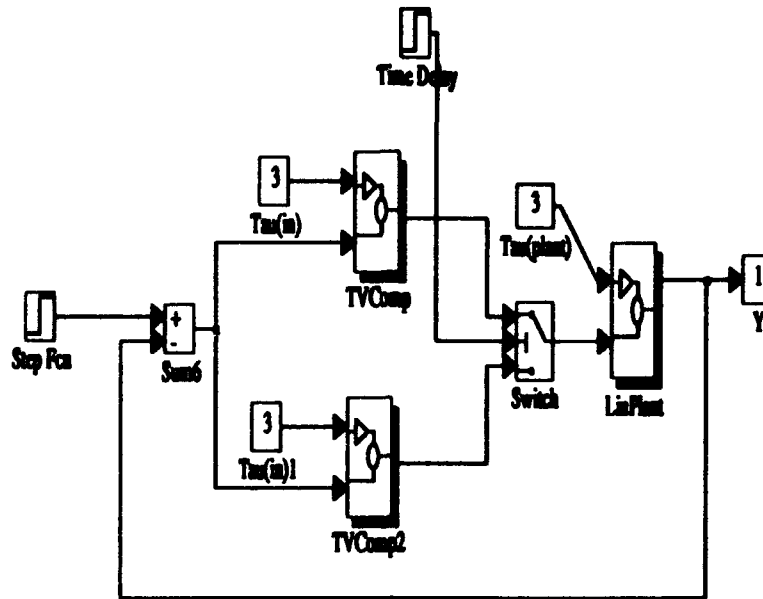


Figure 3.15 Simulation applying a bank of identical linear compensators to a linear plant

the second compensator inheriting a plant which is in an unanticipated state: the states are not along the trajectory which the compensator would have induced had it been in control since $t = 0$.

This effect is inverted when $G_{ALT}(s)$ is substituted for $G_2(s)$. In this case the response starts out much faster due to $G_1(s)$, then slows down due to $G_{ALT}(s)$. This leads to an overshoot smaller than is desired when both compensators are involved in controlling the plant.

If the control transfer point behaved like an equilibrium point, then the overshoot could be calculated by $M = Y_{AtTransfer} + 1.12 * (1 - Y_{AtTransfer})$. Because the actual overshoot does not follow this relation, the conclusion is that the switch point must not imply an equilibrium point. Therefore, error in overshoot must be due to a mismatch between the internal energy in the plant and the internal energy of the compensator. Since $G_1(s)$ is the only compensator element with internal energy at the switching time, it must be unable to account for the energy it induced in the plant when $G_2(s)$ attempts to drive the plant along a different state trajectory. The output of

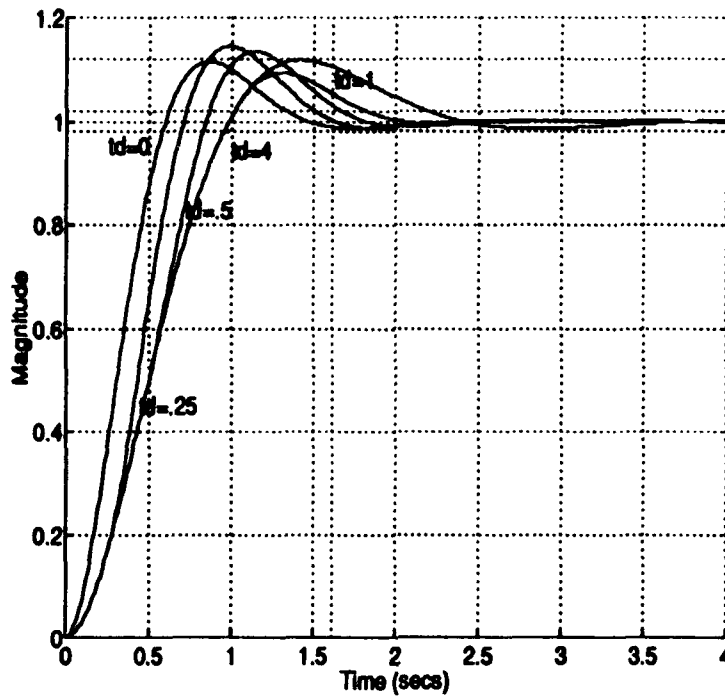


Figure 3.16 Simulation of banked compensation technique for unlike compensators

$G_1(s)$ for all time after the error signal is driven to zero must, therefore, be adequate only when the compensator continues along the same trajectory $G_1(s)$ would have induced had it been in control for all time.

A similar analysis was carried out using the post-weighting approach of Figure 3.15. Inserting mismatched compensators into this configuration, led to large, lightly-damped oscillations in the closed-loop response. This suggests that the final Model-Based Fuzzy Logic Controller should incorporate pre-weighted compensators to minimize the effect of modeling errors.

3.5 Use of Multiple Compensators in Time-Varying Linear Systems

As was mentioned in the introduction, the nonlinear plant can be approximated by a time-varying linear model by relaxing the fixed equilibrium assumption of the linearization process. The resulting transfer function is time-varying and, in fact, nonlinear as the value of τ . However, by conveniently neglecting the fact that τ is a function of Y , the plant can (and will) be considered linear, time-varying. The plant will be referred to in this report as the *linear time-varying linear plant (LTV)*. Simulation shows that a compensator which adequately controls the LTV plant will also control the nonlinear plant to the extent that the small perturbation assumption is not violated.

Figure 3.17 shows a simulation to test the effectiveness of a single linearized compensator against the LTV plant. The plant is operating from a nominal value of $C(t) = 1$. Figure 3.18 shows the response of the system for step inputs of various magnitudes. Notice that the response steadily decays as the system moves away from the nominal value. The largest step input for which the compensator will produce an acceptable closed-loop output, will be referred to as the *region of attraction* for that compensator. That is, as long as the plant is operating within a compensator's region of attraction, that compensator will be capable of inducing an acceptable closed-loop response.

Based solely on the use of compensators within their regions of attraction, a non-fuzzy Banked Compensator for the LTV plant can be postulated, as shown in Figure 3.19. Unlike the Banked Compensator for the linear system, shown in Figure 3.12, Figure 3.19 is designed to switch at a particular output value rather than a particular time. In this case, the objective of the system is to drive the LTV plant from $Y(t) = 1$ to $Y(t) = 1.2$. The bank consists of two controllers, one about $Y(t) = 1$ and one for $Y(t) = 1.2$. The switch will change from one compensator to the other at $Y(t) = 1.1$, halfway between compensators. Even at $Y(t) = 1.1$, both compensators demonstrate a reasonable capability to control the plant. Therefore, these compensators have overlapping regions of attraction.

The closed-loop response of this system is shown in Figure 3.20. The banked compensator has had the *opposite* effect than was intended. The response is actually worse than the response

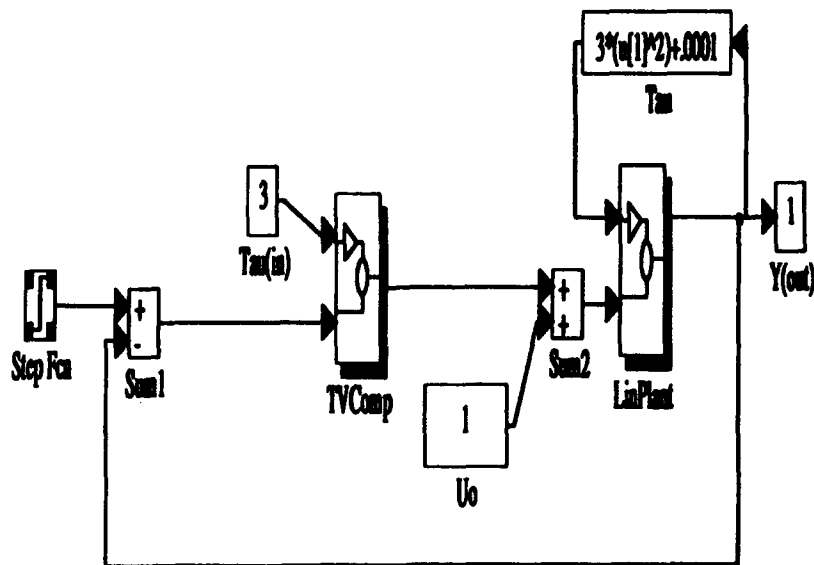


Figure 3.17 Simulation testing the validity of linear compensators on time-varying linear plant of the single compensators alone, shown in Figure 3.18. Clearly, an analog to the error source identified last section is also at work here. Though the compensators are all designed to the same specifications, they are both customized for a single equilibrium point. Once the LTV plant moves away from the equilibrium a modeling error is introduced between the plant and the compensator. This results in unmodeled control effects. Auxiliary processing is required to produce successful non-Fuzzy Banked Compensation for the LTV plant.

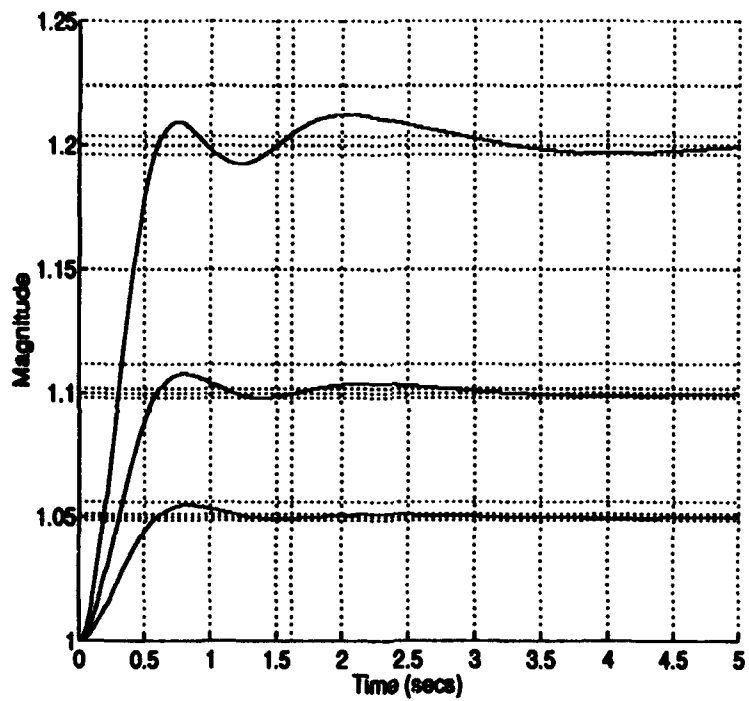


Figure 3.18 Closed-loop response of time-varying plant, linear compensator, for step inputs of .05, 1.1, and 1.2. Starting from $Y(t_0) = 1$.

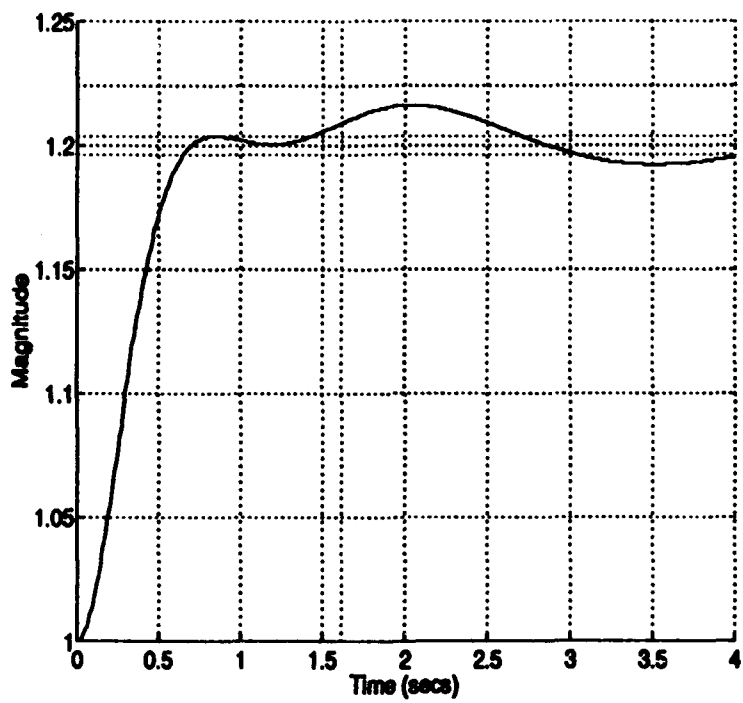


Figure 3.20 Closed-Loop Response of Prototype MBFLC

3.6 Controller Considerations Based on Linear Analysis

There are at least three possible causes for the failure of the banked compensator above, for:

1. Each compensator is not valid over its entire region of operation. Even though the compensators provide reasonable performance, the time of hand-over the plant is off the trajectory which the inheriting compensator would have induced had it been driving an equivalent linear plant the entire time. This introduces a non-statistical error.
2. Each compensator is unable to properly account for the dynamics induced while driving the nonlinear plant. Because the plant is changing with time, none of the compensators will be valid for all time. The compensator will be accounting for the dynamics it had induced, assuming the plant is precisely the linear plant for which the compensator is designed. This is another source of non-statistical error.
3. The region of attraction is a limitation that applies, not just to the equilibrium condition of the plant, but to the magnitude of the error signal into the compensator as well. The error signal received by the first compensator will be telling the compensator to drive the plant to a point outside of its region of attraction. Therefore, the compensator output will not be valid, as it will be based on the assumption that the LTV plant does not change between $Y = 1$ and $Y = 1.2$.

These considerations account for the poor performance shown in Figure 3.20.

These limitations cannot be completely overcome using linear control theory. Therefore, some degree of uncertainty will be inevitable in a banked controller. It will be the function of Fuzzy Logic within this controller to account for these shortfalls in linear theory. An interesting extension to the above simulations is to allow the τ upon which the *compensator* is based vary as a function of the plant output. This approach leads to time-varying linear compensators and is explored in more detail in the next chapter

3.7 Summary

This chapter demonstrates that banked compensation is possible in the linear sense if each compensator in the bank is able to account in some way for the energy it injects into the plant while in control. This can be accomplished either by preweighting the compensators and allowing each compensator to affect the plant for all time, or by post-weighting the compensators and allowing energy to build up in inheriting compensators. For pre-weighting, the compensator input must be driven to zero in order to counter the tendency of later compensators to overdrive the system. For post-weighting, each compensator is receiving an identical error signal, so every compensator will have built up internal state energy at the time of transfer.

Banked compensation only proves successful for the simple case of a linear plant and identical linear compensators. Under these conditions the resulting performance will be the same as that of a single compensator in series with the plant. Undesired dynamics are induced by dissimilar compensators, time-varying plants, and modeling errors. A prototype non-Fuzzy banked compensator using dissimilar compensators to drive a time-varying plant was unsuccessful due to these unmodeled effects.

IV. Model-Based Fuzzy Logic Control Nonlinear Design Considerations

4.1 Introduction

The last chapter developed a linear, non-Fuzzy Banked Compensator which performed well for linear, time-invariant plants. However, the compensator was inadequate when applied to the LTV plant, a simplified version of the nonlinear plant. It is clear that a more sophisticated structure is required, involving the analysis of both the nonlinearities exhibited by the plant, and the effectiveness of linear control approaches at addressing these nonlinearities.

This chapter will address the following areas of concern:

1. Effectiveness of Linearized Plants for Nonlinear Control
2. Time-Varying Compensation of the Linear Time-Varying Plant
3. Time-Varying Compensation of Nonlinear Plant
4. Banked Compensator Approximation of Time-Varying Compensation
5. Fuzzy Weighted Bank Control of Nonlinear Plant
6. Summary

4.2 Effectiveness of Linearized Plants in Nonlinear Control

Linear perturbation models are routinely used by control engineers to develop controllers for nonlinear systems [17]. However, it is reasonable to question just how effective controllers based on perturbation models actually are. Linear analysis will certainly be valid for operating conditions very close to the equilibrium condition upon which the linearization is based, but the actual region of linear behavior will be heavily dependent on the extent of the underlying nonlinearity.

To address this question, the concept of *region of attraction* has been introduced for this thesis. The region of attraction is a sphere in state space within which the dynamics demonstrated by the linearized model represent a reasonable approximation of the behavior of the nonlinear plant. The regions of attraction for the linearized model and for the compensator based on that model are considered one and the same. For example, consider the nonlinear state equation $\dot{y} = \sin x$. In this case, y may be assumed linear for $|x| < \pi/6$ ($\dot{y} \approx x$). Therefore the region of attraction for the

linearized model and for the compensator based on that model would be $|x|, |y| < \pi/6$. Of course, this nonlinearity is much more benign than that considered in this thesis. The regions of attraction for the nonlinear plant under consideration will, in general, be much smaller.

The boundaries of the regions of attraction will be based on the controller being capable of delivering good performance, with "good" defined as:

- Within 5% of correct overshoot ($1.064 \leq M_p \leq 1.176$).
- Within 4% of final value within specified settling time ($t_s = 1.62$ secs).

By analyzing Equations (4.11) and (4.12) it is reasonable to assume that linearized plants would become more effective as the equilibrium values become larger. As X_{1o}, X_{2o}, U_o get larger, the perturbations contribute a smaller percentage of the overall state energy. As $X_{1o} = X_{2o} = U_o \rightarrow 0$ the linearized model should become essentially worthless at estimating the response of the nonlinear plant. This is borne out in simulation.

As the objective is to drive the nonlinear plant from 0 to 1, linearized plants in this region should be examined first. In each case the effectiveness of the compensator at a given equilibrium condition is determined as follows:

1. A linear compensator is developed using Equation (3.2) for the appropriate linearized plant.
2. The compensator is simulated in closed-loop with the nonlinear plant.
3. The simulation is set up to begin from rest conditions on or near the equilibrium point for the plant on which the compensator is based.
4. Successively larger steps away from the equilibrium are attempted.
5. The largest step input with good performance is recorded as the region of attraction for that compensator.

Table 4.1 shows the results these tests. For each equilibrium point, three values are given: originating, terminating, and traversing. These labels refer to starting point of the simulation versus the equilibrium point of the compensator. For originating simulations, the simulation starts from the equilibrium point and steps up. For terminating simulations, the simulation starts from an equilibrium below the compensator and attempts to step up the equilibrium for which the compensator is designed. For traversing, the simulation attempts to drive the system from an

Equilibrium	Originating Region of Attraction	Terminating	Traversing
0.1	0.000025	0.000027	0.000025
0.2	0.00022	0.00024	0.00023
0.3	0.0008	0.00084	0.00082
0.4	0.002	0.0022	0.0024
0.5	0.004	0.0043	0.0042
0.6	0.0075	0.0078	0.0076
0.7	0.0097	0.0097	0.0097
0.8	0.01	0.012	0.01
0.9	0.013	0.014	0.013
1.0	0.018	0.02	0.018
1.1	0.02	0.03	0.022
1.2	0.03	0.05	0.038

Table 4.1 Regions of attraction for linear compensators for originating, terminating, and traverse modes of operation

equilibrium below the compensator to a final steady-state value above the equilibrium point for the compensator. In all traversing simulations, the originating and terminating equilibria are symmetrically distributed about the compensator equilibrium.

Prior to the 0.7 equilibrium point, overshoot is the limiting factor. After 0.7, settling time determines region of attraction. Beyond approximately $Y = 1.4$, system response will always be good by the established criteria. However, the response will be highly nonlinear for large step inputs. Appearance of the closed-loop response will be the determining factor for regions of attraction above 1.4.

Notice in the table that in all cases originating, terminating and traversing values are very similar. This indicates that the model is good within the region of attraction, regardless of where you start and finish within the region. Because the "originating" column is generally the most restrictive, this value will be used when referring to region of attraction in the future.

The number of compensators required for a Banked MBFLC is not clear. For initial designs, the number will be established by requiring that at least one compensator be considered valid at any point between the origin and reference value. Table 4.1 shows that the number of compensators

Equilibrium	Region of Attraction
3.0	0.08
3.1	0.12
3.2	0.19
3.3	0.22
3.4	0.3
3.5	0.33
3.6	0.37
3.7	0.44
3.8	0.5
3.9	0.52
4.0	0.55

Table 4.2 Regions of attraction for linear compensators in Banked MBFLC

required to ensure this can be very large, especially near the origin where the strong nonlinearity forces the regions of attraction to zero. Perhaps more importantly, the regions of attraction impose severe limits on the magnitude of the *error signal* for which the compensator will respond properly. Linear compensators near the origin will provide very little information as to the dynamics of the nonlinear system.

Because of these factors, initial Banked MBFLC development will take place away from the nonlinear distortions near the origin. The system will be driven from $Y = 3$ to $Y = 4$, rather than from $Y = 0$ to $Y = 1$. This provides for more effective and homogeneous linearized models. The results obtained within this range will then be reproduced over a smaller range closer to the origin. The regions of attraction for the region between $Y = 3$ and $Y = 4$ are shown in Table 4.2.

As mentioned above, establishing the region of attraction becomes more objective as Y gets larger. As the system moves further and further from the origin, the compensators require less gain and so fail less dramatically. For large step inputs the system response gets very distorted but never actually violates the boundaries established for a "good" system response in the last section. Figure 4.1 shows steps of varying magnitudes away from the equilibrium point at $Y = 4.0$. At no time does the response violate any of the good performance boundaries (shown in the Figure), but the quality of the response drops off significantly. In order to minimize unwanted dynamics, the

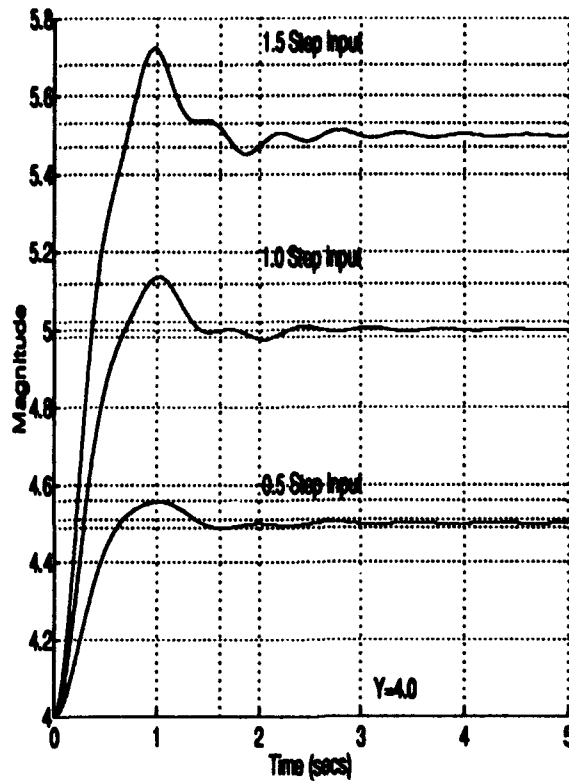


Figure 4.1 Determination of region of attraction for $Y = 4.0$

region of attraction for $Y = 4.0$ was set at 0.55, as given in the Table. Similar trade-offs were made for all other equilibrium points.

The compensators can only be considered "good" as long as they do not receive error signals larger than their regions of attraction. Error signals larger than the region of attraction will induce unmodeled dynamics and oscillations in the system caused by mismodeling of the plant, as discussed in Sections 3.6 and 3.7. Fortunately, the undesirable dynamics in the region between $Y = 3$ and $Y = 4$ will be much slower and contain less energy than those induced by higher-gain compensators near the origin. An effective banked MBFLC compensator should be capable of quelling these dynamics and inducing a smooth response within the established parameters. An effective design at higher outputs could then be "slid down" to encompass lower regions of the system output.

4.3 Time-Varying Compensation of the Linear Time-Varying Plant

As was mentioned in the last chapter, the Linear Time-Varying Plant (LTV plant) is a simplified, but still nonlinear representation of the full nonlinear plant. The LTV plant is analogous to relaxing the static equilibrium point assumption of the linearization procedure. Control of the LTV plant is equivalent to control of the nonlinear plant to the extent that the small perturbation assumption holds.

The non-Fuzzy Banked Compensator proved unable to adequately drive the LTV plant to a given reference value. An adequate controller can be formulated, however, by considering a single time-varying compensator in the context of *nonlinear* control theory. The resulting controller can then be approximated using only linear control theory and Fuzzy Logic.

This controller can be developed by considering a compensator containing an inverse of the linearized plant dynamics, as was developed in Chapter 3 (3.2). In this approach, the compensator will attempt to null out the dynamics generated by the LTV plant and replace these dynamics with the response of an ideal system model resident in the compensator. The nulling portion of the compensator is based on canceling the poles of the *linearized* plant. Because the linearized plant model varies according to the equilibrium point, the compensator should be made time-varying as well. This approach depends heavily on an accurate model of the plant, and is generally not used in linear designs. The *TVcomp* block with τ provided in real time based on Y will be referred to as the Time-Varying Compensator (TVC).

Figure 4.2 shows a SIMULINK simulation in which a single Nulling Compensator is used in the forward path. Internally, this compensator is the same as the linear banked compensators considered last chapter, but with the value of τ determined in real-time based on the output. Therefore, at any instant t_i ($t_i \geq 0$), the appropriate value of τ ($\tau = 3Y(t_i)^2$) will be fed into the compensator. This ensures a proper control input to the LTV plant for all time [30].

Figure 4.3 shows the response of this plant to a step reference signal $Ref = 3 + u_{-1}(t)$. In this case, the response is equivalent to that of the model closed-loop response $M(s)$, shown in

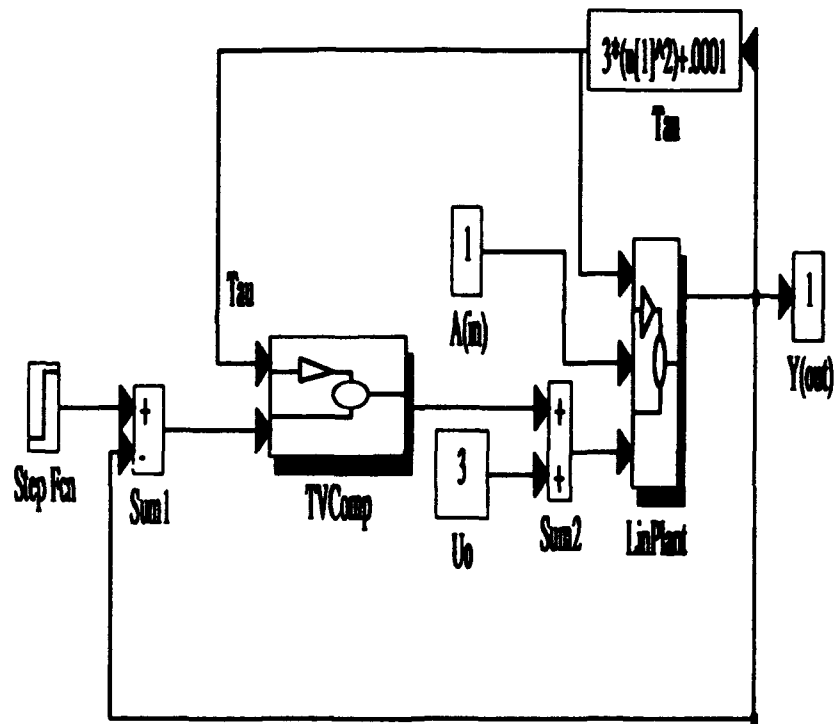


Figure 4.2 Control of Time-Varying Linear Plant Using Time-Varying Linear Compensator

Figure 2.3. The time-varying compensator is capable of controlling the LTV plant throughout its envelope of operation ($Y \geq 0$).

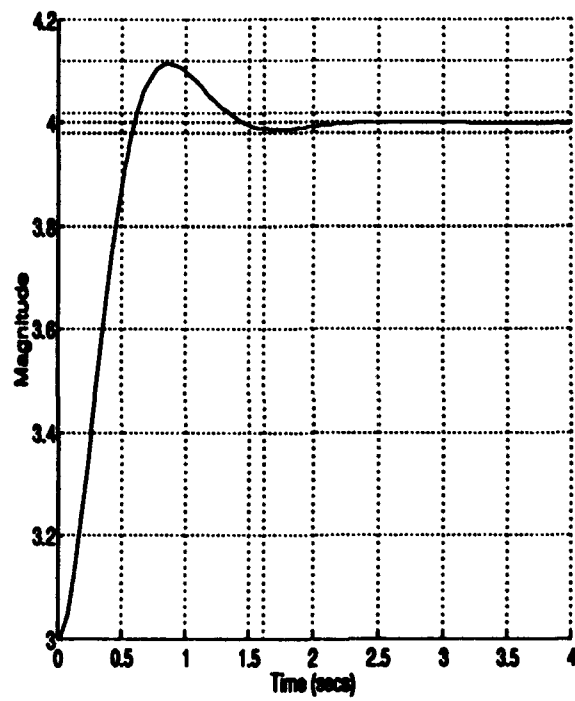


Figure 4.3 Closed-loop response of LTV plant and Time-Varying Linear Compensator

4.4 Nulling Compensation of the Nonlinear Plant

It has been claimed that the LTV plant is the equivalent of relaxing the static equilibrium point assumption of the linearization process. If this is true, then a controller applicable to the LTV plant should also be acceptable for the full nonlinear plant, as long the small perturbation assumption holds.

Figure 4.4 verifies that this is, indeed, the case. The Figure shows the response of the *nonlinear plant* about $Y = 3$ for various step reference inputs. For small inputs, where the small perturbation assumption holds, the response of the nonlinear plant resembles that of the LTV plant. As the step reference input becomes larger, the system response decays. The next step is to develop a mathematical approach to overcome the limitations imposed by the small perturbation assumption.

In order to develop an overall control approach, the original linearization of the nonlinear plant must be revisited. The nonlinear plant, once again, is described by:

$$\dot{X}_1 = -X_1 + X_2 \quad (4.1)$$

$$\dot{X}_2 = -X_1^3 + U^3 \quad (4.2)$$

$$Y = X_1 \quad (4.3)$$

and the linearized plant is described by:

$$\dot{x}_1 = -x_1 + x_2 \quad (4.4)$$

$$\dot{x}_2 = -\tau x_1 + \tau u \quad (4.5)$$

$$y = x_1 \quad (4.6)$$

$$\tau = 3y^2. \quad (4.7)$$

As mentioned several times, the linear model is based on two assumptions: 1) Small perturbations from the equilibrium condition, and 2) Static equilibrium condition. As long as a single equilibrium point is chosen, as was the case in developing the banked compensation approach, τ is

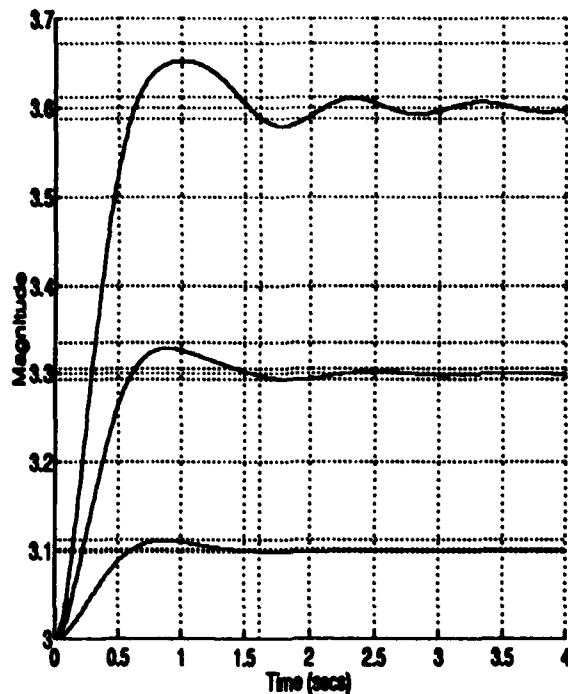


Figure 4.4 Closed-loop response of nonlinear plant and Time-Varying Linear Compensator for various step inputs

a constant and the Laplace domain transfer function is:

$$P(s) = \frac{\tau}{s^2 + s + \tau}. \quad (4.8)$$

This plant model can be used as the basis for a time-varying compensator by simply allowing τ to vary with the desired change in equilibrium. However, this violates one of the assumptions upon which (4.8) is based, so the linearization process should be reexamined with the static equilibrium assumption relaxed. This is easily accomplished by expressing (2.1) and (2.2) in terms of the equilibrium conditions plus a perturbation, as was done in the initial derivation.

$$\dot{\bar{X}}_{1o} + x_1 = -\bar{X}_{1o} - x_1 + \bar{X}_{2o} + x_2 \quad (4.9)$$

$$\dot{\bar{X}}_{2o} + x_2 = -(\bar{X}_{1o} + x_1)^3 + (\bar{U}_o + u)^3. \quad (4.10)$$

Expanding the cubic terms and rearranging yields:

$$\dot{X}_{1e} + \dot{x}_1 = -\bar{X}_{1e} + \bar{X}_{2e} - x_1 + x_2 \quad (4.11)$$

$$\dot{X}_{2e} + \dot{x}_2 = -\bar{X}_{1e}^3 - 3\bar{X}_{1e}^2 x_1 - 3\bar{X}_{1e} x_1^2 - x_1^3 + \bar{U}_e^3 + 3\bar{U}_e^2 u + 3\bar{U}_e u^2 + u^3. \quad (4.12)$$

Applying the small perturbation assumption yields:

$$\dot{X}_{1e} + \dot{x}_1 = -\bar{X}_{1e} + \bar{X}_{2e} - x_1 + x_2 \quad (4.13)$$

$$\dot{X}_{2e} + \dot{x}_2 = -\bar{X}_{1e}^3 - 3\bar{X}_{1e}^2 x_1 + \bar{U}_e^3 + 3\bar{U}_e^2 u. \quad (4.14)$$

Note that the \dot{X}_{1e} and \dot{X}_{2e} terms are nonzero and therefore cannot be eliminated from 4.13 and 4.14. However, the terms on the right-hand sides of these equations involving only the equilibrium terms still cancel each other out. This shows that relaxing the static equilibrium assumption induces no additional dynamics in this particular plant, and (4.8) holds true for all τ .

Note also that the left-hand side expressions in 4.13 and 4.14 are equal to X_1 and X_2 respectively. This implies that, as long as the small perturbation condition holds, any compensator based on the time varying plant will also ensure adequate performance for the nonlinear plant. This explains the success of the time-varying compensator at controlling the LTV plant.

For large perturbations away from the equilibrium condition, the small perturbation assumption breaks down and dynamics due to the nonlinear terms in (4.12) become significant. This is the cause of the ultimate failure of the time-varying compensator to control the nonlinear plant. However, the fact that the optimal state space trajectories for the states and the perturbations in the states are equivalent assuming small departures from the nominal, that is $x_{1nom}(t) = X_{1nom}(t)$, $x_{2nom}(t) = X_{2nom}(t)$, and $u_{nom}(t) = U_{nom}(t)$, suggests an important relationship. Namely, that the state trajectory of the time-varying linear model will be the same as the state trajectory for the nonlinear model in general. The inputs required to produce these trajectories in the nonlinear case, though, will vary according the effect of the nonlinear terms in 4.14. For small departures from

equilibrium, $U \approx u$. As the tracking signal moves further from the quiescent point of the system, however, $u(t)$ and $U(t)$ diverge in a nonlinear fashion.

Fortunately, the divergence of $u(t)$ and $U(t)$ can be determined in real-time and corrected for. This is accomplished in a two-step process. First, the desired dynamics must be determined based on the output of the TVC and the known linearized model of the nonlinear plant. Second, the correct input U to the nonlinear plant must be determined based on the nonlinear plant model. These two steps equate to a model following procedure and can be accomplished on-line for the class of nonlinear systems including the plant currently under consideration [2].

An illustration of this nonlinear control scheme is shown in Figure 4.5. In this case, the nonlinear plant is described by (2.1) and (2.2), and the TVC is given by (3.2). The desired dynamics \dot{x}_2 can be determined by analyzing the second equation of the linearized plant (2.22). The first equation need not be considered as it is not directly impacted by the control input, only by x_2 . The desired \dot{x}_2 at any time t can then be determined by measuring Y to determine τ and x_1 . These quantities, along with the u produced by the TVC can be used to solve for the desired \dot{x}_2 using 2.22. The SIMULINK block performing this function is shown in Figure 4.6.

It is tempting to argue that the actual form of the desired dynamics is simply $\dot{x}_2 = \tau u$ because the time-varying nature of the compensator ensures that $x_1 = 0$ for all time. However, simulation shows that the system cannot be considered to have actually shifted equilibrium points until the dynamics go to zero. Therefore, though the determination of the ideal state trajectory is based on a TVC which assumes a changing equilibrium point, the $-\tau x_1$ term in 2.22 is still required to provide adequate retarding of the x_2 state model as the desired final state is reached.

The final step is to solve for the required U , and this is accomplished through (2.2). Rearranging this equation to solve for U , yields:

$$U = \sqrt[3]{(\dot{X}_2 + X_1^3)}. \quad (4.15)$$

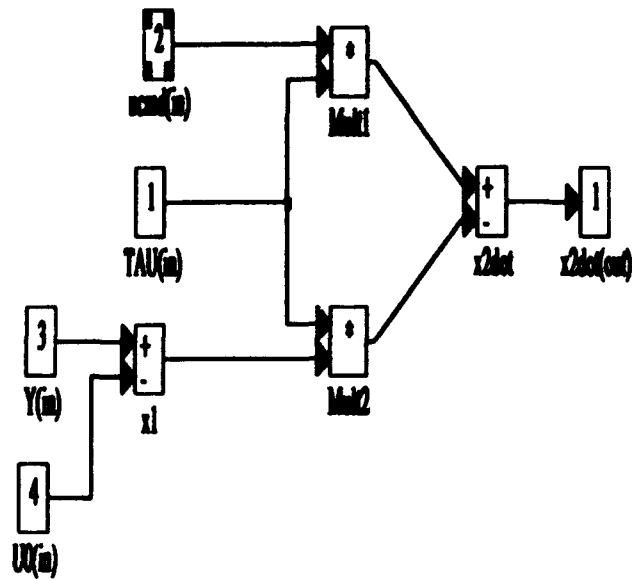


Figure 4.6 Determination of the desired x_2 based on compensator outputs

performance based on SIMULINK simulation. This plot also shows the disturbance rejection capabilities of the nonlinear system when a time-varying robust linear compensator is substituted for the non-robust compensator. The robust compensator performs as well as the nonrobust compensator for both tracking and regulation in this control configuration.

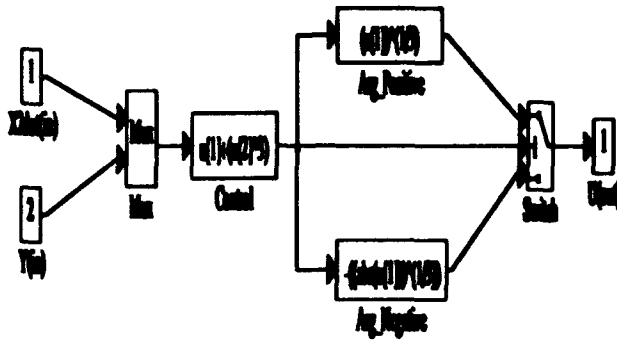


Figure 4.7 determination of U based on desired \dot{x}_2

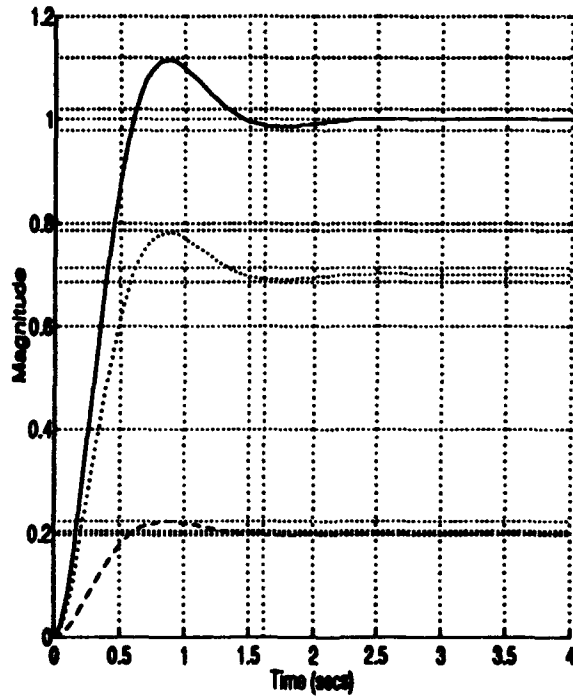


Figure 4.8 Closed-Loop simulations of nonlinear controller using time-varying linear compensation, starting from $Y = 0$

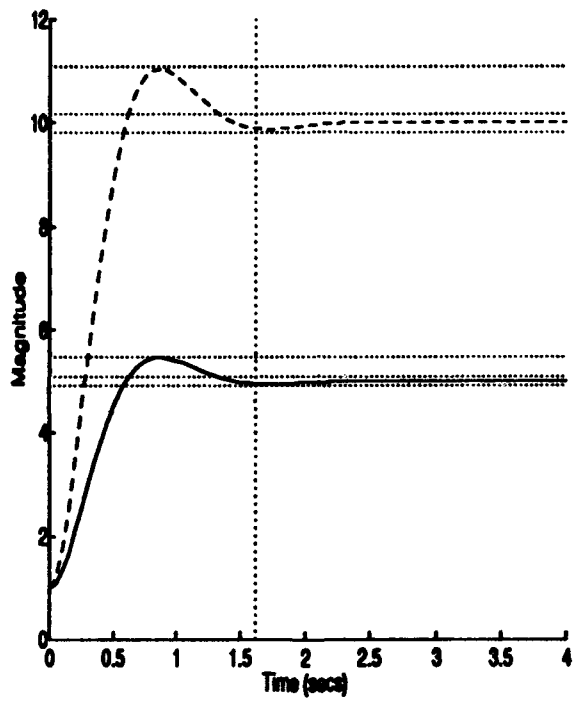


Figure 4.9 Closed-Loop simulations of nonlinear controller using time-varying linear compensation, starting from $Y = 1$

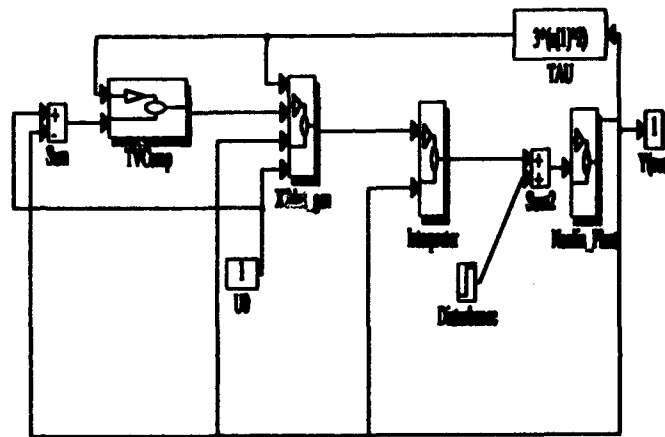


Figure 4.10 SIMULINK simulation to test the disturbance rejection capabilities of nonlinear control scheme

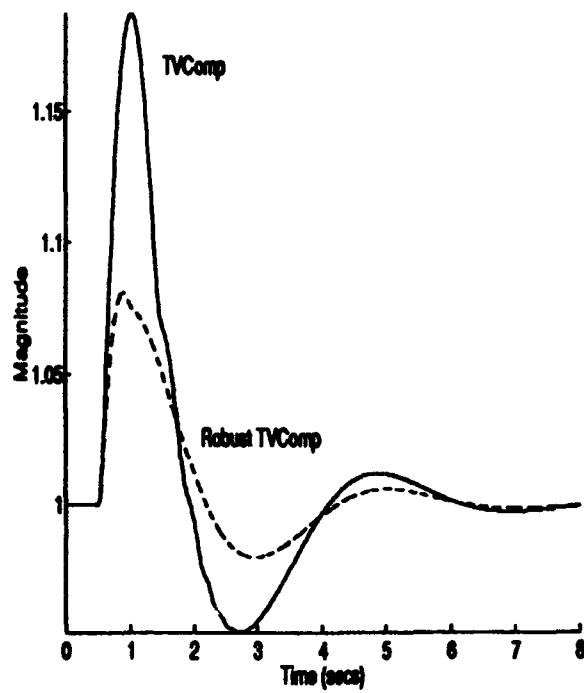


Figure 4.11 Disturbance rejection capabilities of nonlinear controller for unit step injected at plant input

4.5 Banked Compensator Approximation of Time-Varying Compensation

The above controller does meet desired performance expectations, but at the cost of all established design limitations. The stated objective of this research is to create a controller using only linear compensators and Fuzzy Logic. The challenge, then, is to approximate the above system using only these elements.

The first step in accomplishing this will be to eliminate the need for the time-varying compensator. This will be accomplished by using a bank of linear compensators weighted by Fuzzy Logic. Figure 4.12 shows a simple compensator bank for a Model-Based Fuzzy Logic Controller. In this case, five linear compensators are being used, corresponding to the equilibrium points $Y = 3, Y = 3.35, Y = 3.5, Y = 3.75$ and $Y = 4$. The optimal number of compensators required for a given application depends on the nonlinearities exhibited by the plant between the starting output and the objective output. This will be explored in more detail in the next chapter.

When the system is at $Y = 3$ or $Y = 4$, there is no doubt as to which compensator should be applied to the plant. The situation is not so clear when the system is, for example, at $Y = 3.887$. In this case, the best output would be a mix of both compensators. This is the function of the *Fuzzy Supervisor* shown in the Figure.

The internal structure of the Fuzzy Supervisor block is shown in Figure 4.13. It is referred to as a supervisor rather than a controller because it serves only a very specific function: To emphasize the compensator which most nearly reflects the true state of the system. It has the additional feature that, when the system is between regions of attraction, it will output a weighted average of the control actions advocated by each relevant compensator.

The weighting of the compensators can occur, as discussed last chapter, either before or after the compensators themselves. Both approaches have advantages, but post-weighting proves superior for hybrid Fuzzy/nonlinear applications. The reason is simple: there is very little uncertainty in this system. Preweighting makes for a more volatile bank of compensators and allows the Fuzzy Supervisor more control authority. In this application, however, the objective is simply to reproduce the time-varying compensator as faithfully as possible.

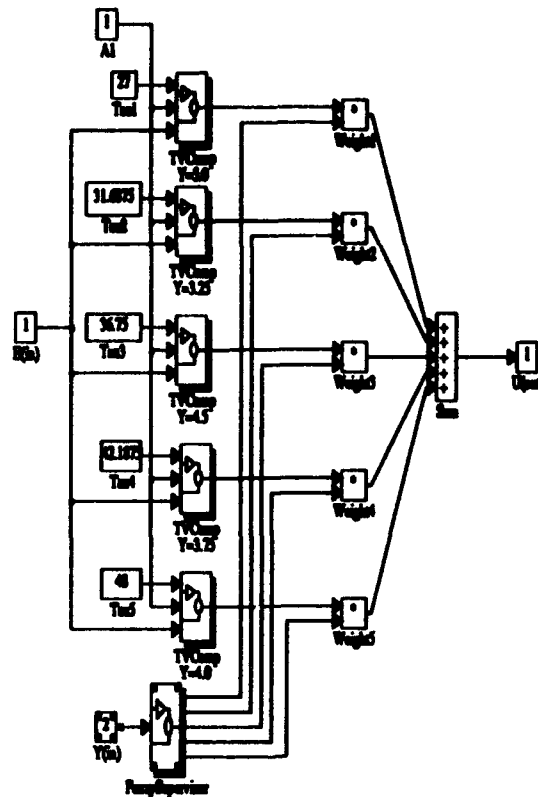


Figure 4.12 Simple compensator bank for MBFLC

The precise operation of the Fuzzy Supervisor is as follows:

1. The current value of Y is fed into the Fuzzy Supervisor.
2. Y is evaluated for membership into the Fuzzy Sets $Y = 3, Y = 3.35, Y = 3.5, Y = 3.75$ and $Y = 4$. The form of the memberships functions for these sets, given in (2.38) and repeated here, is:

$$\mu(x) = e^{-\frac{(x-y)^2}{\sigma^2}}, \quad (4.17)$$

These functions are evaluated over the universe of discourse, given the means and variances shown in Figure 4.13, are shown in Figure 4.14.

3. In the block *Normx* the activation value of each Fuzzy Set is divided by the total activation of all Fuzzy Sets in the the Fuzzy Supervisor. This scales all weighting outputs so that their sum is one.
4. The normalized weights are output to the compensator bank. The activation of the Fuzzy Set $Y = 3$ is used to weight the compensator for $\tau = 27$. The activation of $Y = 4$ is used to weight the input to the compensator for $\tau = 48$, etc.

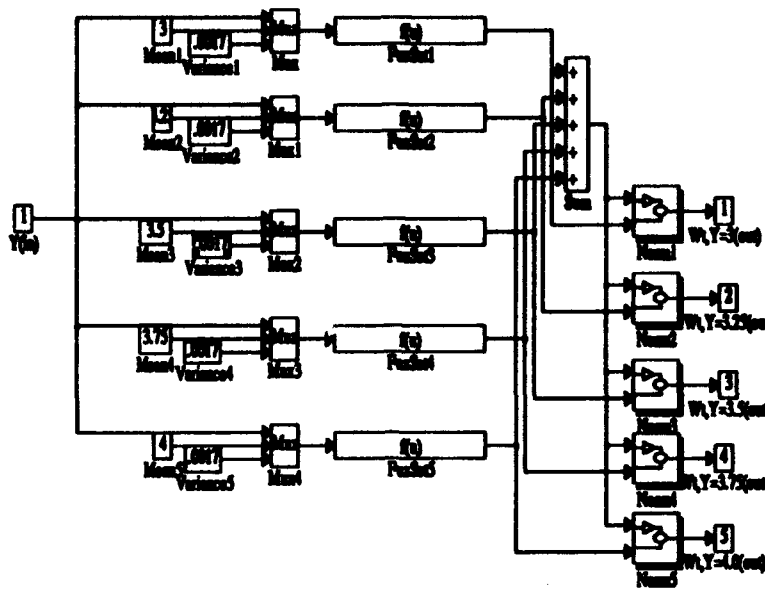


Figure 4.13 Internal Structure of Fuzzy Supervisor

This procedure is the same, regardless of the number of compensators the Fuzzy Supervisor is weighting. The Fuzzy supervisor could be replaced by a look-up table in final implementation, provided no on-line retuning is desired.

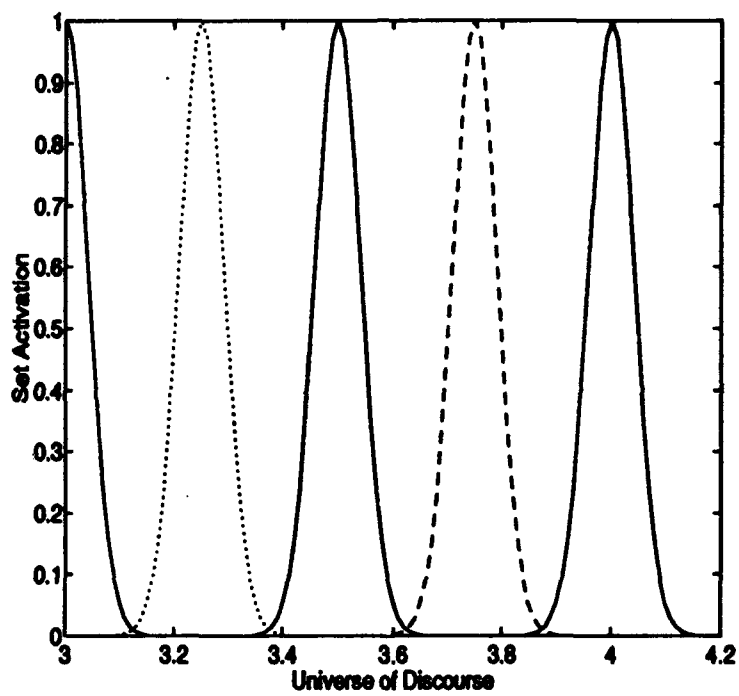


Figure 4.14 Activation of Fuzzy Membership functions for Fuzzy Supervisor

A comparison of the Fuzzy Weighted Bank and the time-varying compensator is shown in Figure 4.15. This plot shows the closed-loop compensator output histories (u) for the time-varying compensator, the Fuzzy Weighted Compensator Bank and a single linear compensator for $\tau = 27$. The time-varying compensator and Fuzzy Weighted Bank generate almost identical u time histories, and therefore are virtually indistinguishable in closed-loop simulation. The response of the nonlinear plant in closed-loop simulation with the Fuzzy Weighted Compensator Bank is shown in Figure 4.16. The response of the original time-varying, nonlinear system over the same interval is also shown in the Figure, though they are almost identical.

Figure 4.17 shows the state space trajectory of the hybrid nonlinear/Fuzzy Bank controller. This plot is very similar to the trajectory generated by the dynamic inversion-based compensator in Chapter 2. Notice that, after an initial jump in the value of U , the system departs from the locus of equilibrium points (shown as a dotted line), and does not return until the system is approaching the desired final equilibrium. This form of the response is reasonable, as the dynamics of the plant go to zero as the state approaches the equilibrium locus. However, Figure 4.17 predicts that linear compensators intermediate to the initial and final conditions of the simulation will not provide information relevant to control of the plant. The optimal state trajectory will be outside the regions of attraction for these compensators. This is, indeed, the case, as the final form of the MBFLC (given in Chapter 1) utilizes the equivalent of only two compensators.

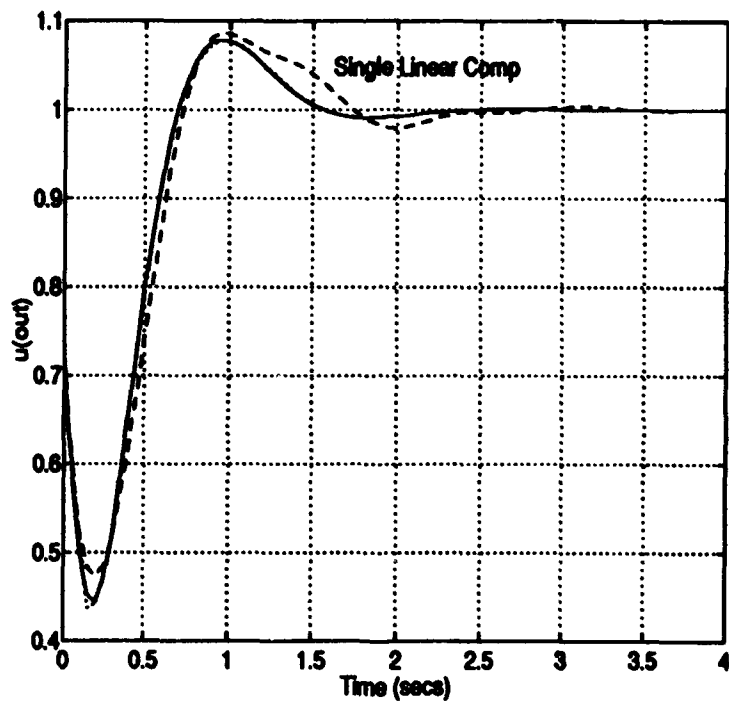


Figure 4.15 Time history of u outputs for time-varying compensator (TVC), Fuzzy Compensated Bank, and single linear compensator. The TVC and single linear compensator plots and nearly identical.

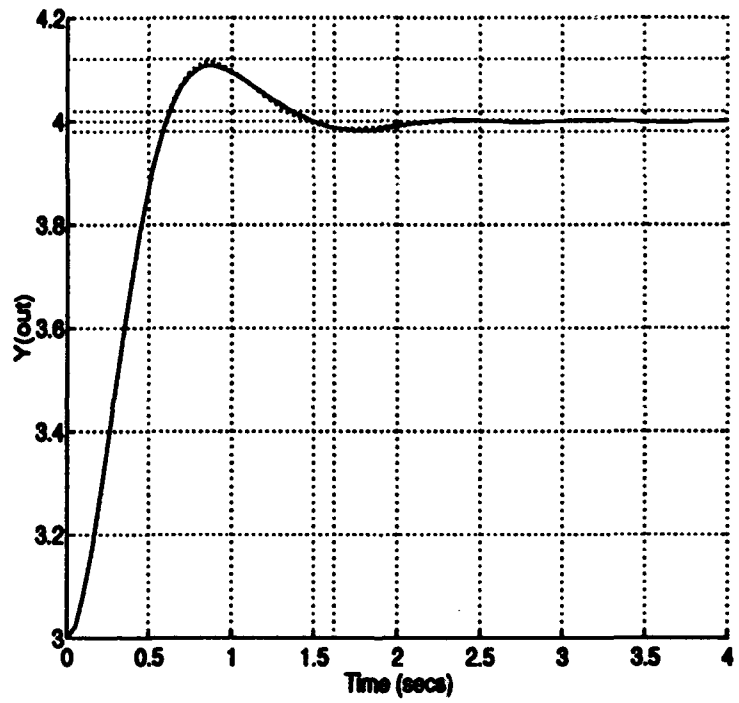


Figure 4.16 Responses of closed-loop system to a step input from $Y = 3$ to $Y = 4$ for both time-varying and Fuzzy Weight compensators.

State Space Representation of System Dynamics, Nonlinear/Fuzzy Compensator, $A=1$

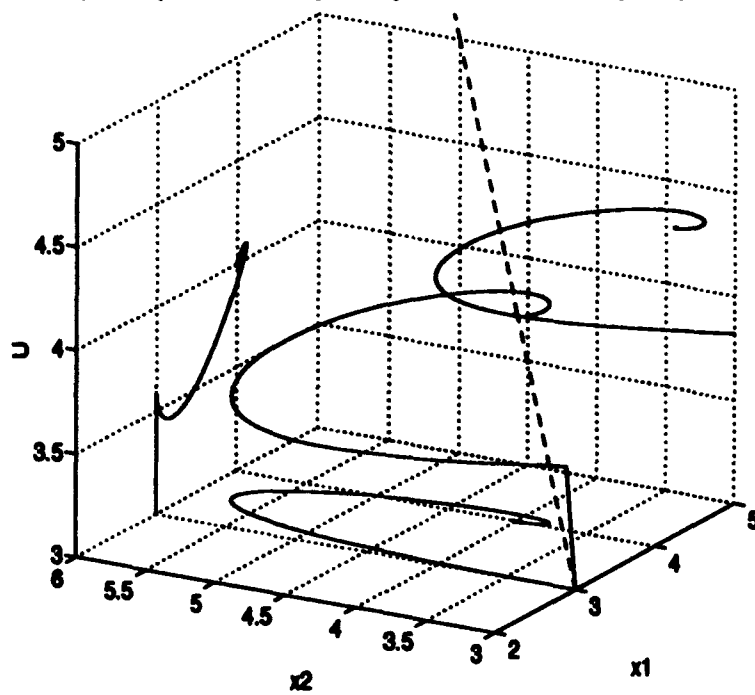


Figure 4.17 State space trajectory of Nonlinear Plant driven by hybrid nonlinear/Fuzzy Controller

4.6 Summary

In this chapter, the effectiveness of linear controllers applied to nonlinear plants was quantified. Regions of attraction were established to estimate the number of compensators that might be required in a compensator bank.

A time-varying linear control strategy was developed to adequately compensate the LTV plant. The successful design was then applied to the nonlinear plant. It was found that the time-varying linear approach was effective for the nonlinear plant for step inputs with small amplitudes. Additional nonlinear processing was developed to create a full-envelope nonlinear controller for the nonlinear plant.

The time-varying linear compensator in the nonlinear controller was then replaced with a bank of linear compensators pre-weighted with Fuzzy Logic. The performance of this hybrid compensator was found to be indistinguishable from the original time-varying linear case.

The state trajectory generated by the nonlinear/Fuzzy Bank controller is similar to the trajectory based on other nonlinear techniques. This suggests that the optimal trajectory path will lead outside the regions of effectiveness of intermediate linear compensators, and favors a two-compensator bank.

V. Development of Model-Based Fuzzy Logic Controller

5.1 Introduction

A controller was developed last chapter which utilizes both linear system models and Fuzzy Logic to control a nonlinear plant. Unfortunately, the controller also ultimately relied on a nonlinear model of the plant to convert the \dot{x}_2 trajectory produced by the Fuzzy Weighted Bank/ \dot{x}_2 traj blocks to a U plant input. The linear/Fuzzy elements of the controller serve only to provide a "model" for the plant to follow. The actual control signal was determined using nonlinear mathematics and an assumed equivalence between the dynamics of the linearized plant and the nonlinear plant starting from equilibrium. It should further be noted that the \dot{x}_2 history can be produced using other approaches as well. In fact, any mechanism which produces a valid state trajectory could be inserted in the controller in place of the linear/Fuzzy elements.

The objective of this chapter, then, is to remove all nonlinear processing elements from the controller other than Fuzzy Sets or equivalent look-up tables based on Fuzzy representations. This objective can be accomplished in two ways:

- Approximate the functionality of the *Interpreter* block using Fuzzy Logic. This could be accomplished using the technique of Wang [23] and would result in a controller very similar to Figure 4.5, with the nonlinear processing block replaced by a Fuzzy Logic approximation.
- Approximate the entire controller as Fuzzy with implicates of the Fuzzy IF...THEN rules supplied by the Fuzzy Weighted bank. In this approach, the structure of the controller is essentially that of a Fuzzy Logic Controller. The recommended control actions, however, are supplied by linear compensators, rather than a look-up table.

Examples of Fuzzy Logic Approximations of nonlinear functions can be found in the literature [23]. Therefore, this thesis will follow the second route to obtain an MBFLC.

This chapter contains the following sections:

1. Structure of Banked Model-Based Fuzzy Logic Controller
2. Full Envelope Banked Model-Based Fuzzy Logic Control
3. Contribution of Linear Compensators to MBFLC Design
4. Model-Following Hybrid Compensators
5. Summary

5.2 Structure of Banked Model-Based Fuzzy Logic Controller

The objective of the MBFLC is to apply linear compensators to the control of a nonlinear plant, using Fuzzy Logic to account for the errors committed by applying linear control theory to a nonlinear problem. By identifying specific linear/nonlinear disjunctions in the last two chapters, the development of the necessary Fuzzy Logic elements is straightforward. The operation of the controller is easily summarized: When agreement between linear and nonlinear theory is good, then apply the control recommended by the linear compensators. When agreement is poor, modify the control signal to ensure that the system responds with caution.

There are three sources of error that need to be addressed in the MBFLC design:

1. The state trajectory which produces the desired closed-loop response exists outside of the regions of attraction for compensators intermediate to the initial and final conditions.
2. The error signal is larger than the compensator regions of attraction.
3. The system will not be at equilibrium when the output reaches the desired final output due to linear/nonlinear mismatches.

One approach to overcome these errors would be to use a dedicated Fuzzy Logic element for each compensator. In this way, the bank would consist of a number of Linear Compensator/Fuzzy Compensator pairs, where each pair would operate independently, in the spirit of Figure 3.12. However, the analysis of banked compensation in Chapter 3 does not support this approach. Simulations show that reasonable performance of individual compensators over small regions does not necessarily imply good performance over larger regions using Banked Compensation. For the linear design presented in Chapter 3, the Banked Compensator actually did a poorer job than would have any individual compensator acting alone.

This motivates the designer to consider the MBFLC as a *single* compensator, rather than as a confederation of individual compensators. A top-level perspective is shown in Figure 5.1. The Banked MBFLC requires the inputs of both a Fuzzy Logic Controller (E and \dot{E}) and a linear banked controller (E and Y). The controller will be of the same basic structure as the FLC in Chapter 2, but with one important difference: The required control actions are obtained from a bank of linear compensators, rather than from a look-up table.

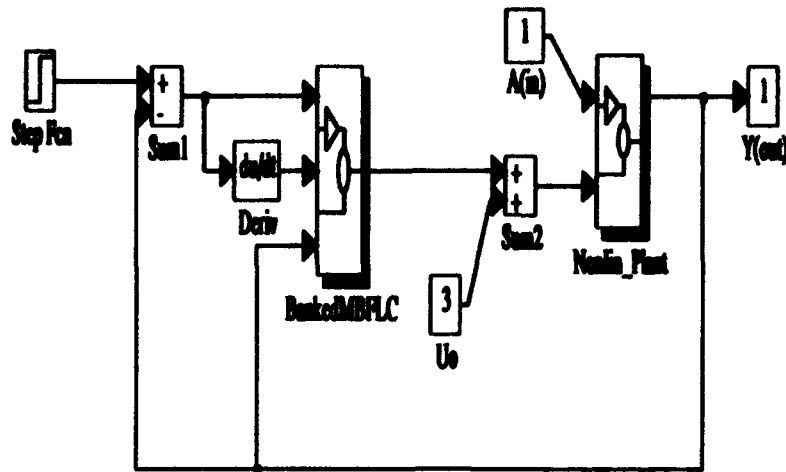


Figure 5.1 Banked Model-Based Fuzzy Logic Control paradigm

By considering the Banked MBFLC as a single unit, each error source can be addressed independently, rather than on a compensator-by-compensator basis. This is the approach adopted in this research. Each of the error sources above is discussed below to determine an appropriate control strategy by application of Fuzzy Logic principles. The universe of discourse for MBFLC development was chosen to be from $Y = 0.6$ to $Y = 0.7$, so that nonlinear effects would be evident.

5.2.1 Limited Effectiveness of Intermediate Linear Compensators. It was hoped that the system could be driven in a linear-like manner using only information available from linearized models of the nonlinear plant. Nonlinear analysis last chapter, however, demonstrated that the desired state trajectory for the nonlinear plant under consideration exists outside the regions of attraction for intermediate compensators. Further, the fact that the system is away from equilibrium throughout the transition creates an energy mismatch between compensators and the plant, as discussed in Chapter 3.

The success of the MBFLC, then, for any given transition, will hinge on three elements: An initiating compensator, a terminating compensator and a Fuzzy Logic Controlled transition between

the two. At this point it is assumed that the required initiating and terminating controllers are the linear compensators based about the appropriate equilibrium values. This assumption will be tested in this chapter, and will ultimately prove false.

Because the MBFLC is envisioned as a *full-envelope* controller, many linear compensators will be required to adequately represent all possible combinations of initial and final conditions. In theory, any number of compensators could be developed for a desired envelope. For this thesis, the number of linear compensators used is determined by the desire to have at least one valid compensator at any point between the starting condition and the final condition. From Table 4.1, the regions of effectiveness between $Y = 0.6$ and $Y = 0.7$ are about 0.009. Therefore, to cover a universe of discourse of 0.1, approximately 11 compensators are required. This number was rounded to ten for ease of implementation.

To determine the appropriate control action for regions of operation between compensator equilibrium values, a Fuzzy Supervisor will be utilized. The Fuzzy Supervisor was developed last chapter to approximate the time-varying linear compensator. Though linear analysis demonstrated that pre-weighting the compensators provided more tolerance for modeling errors, nonlinear analysis showed that post-weighting better emulated the time-varying compensator. Therefore, post-weighting will be used for this iteration of the MBFLC.

Figure 5.2 shows a compensator bank for a Model-Based Fuzzy Logic Controller between $Y = 0.6$ and $Y = 0.7$. The internal structure of the Fuzzy Supervisor for this application is the same as that shown in Figure 4.13, but with 10 Fuzzy Sets being evaluated simultaneously. The tuning values for the Fuzzy Sets are given in Table 5.1.

If the Fuzzy Weighted Compensator Bank is simulated in closed-loop with the nonlinear plant, the result is shown in Figure 5.3. Notice that overshoot is too large and the compensator does not cause the plant to settle out within the required settling time of 1.62 seconds. These errors are due to all three of the sources mentioned above. To determine the effect of intermediate compensators on the response, this simulation was repeated with all but the initiating and terminating compensators

Fuzzy Set	Mean	Variance
Y is 0.6	0.6	0.000027
Y is 0.614	0.614	0.000027
Y is 0.628	0.628	0.000027
Y is 0.642	0.642	0.000027
Y is 0.656	0.656	0.000027
Y is 0.67	0.67	0.000027
Y is 0.684	0.684	0.000027
Y is 0.698	0.698	0.000027
Y is 0.712	0.712	0.000027
Y is 0.726	0.726	0.000027

Table 5.1 Tuning Parameters for Fuzzy Supervisor Membership Function

disconnected. This had only a slight settling effect on the system, so the other errors must dominate.

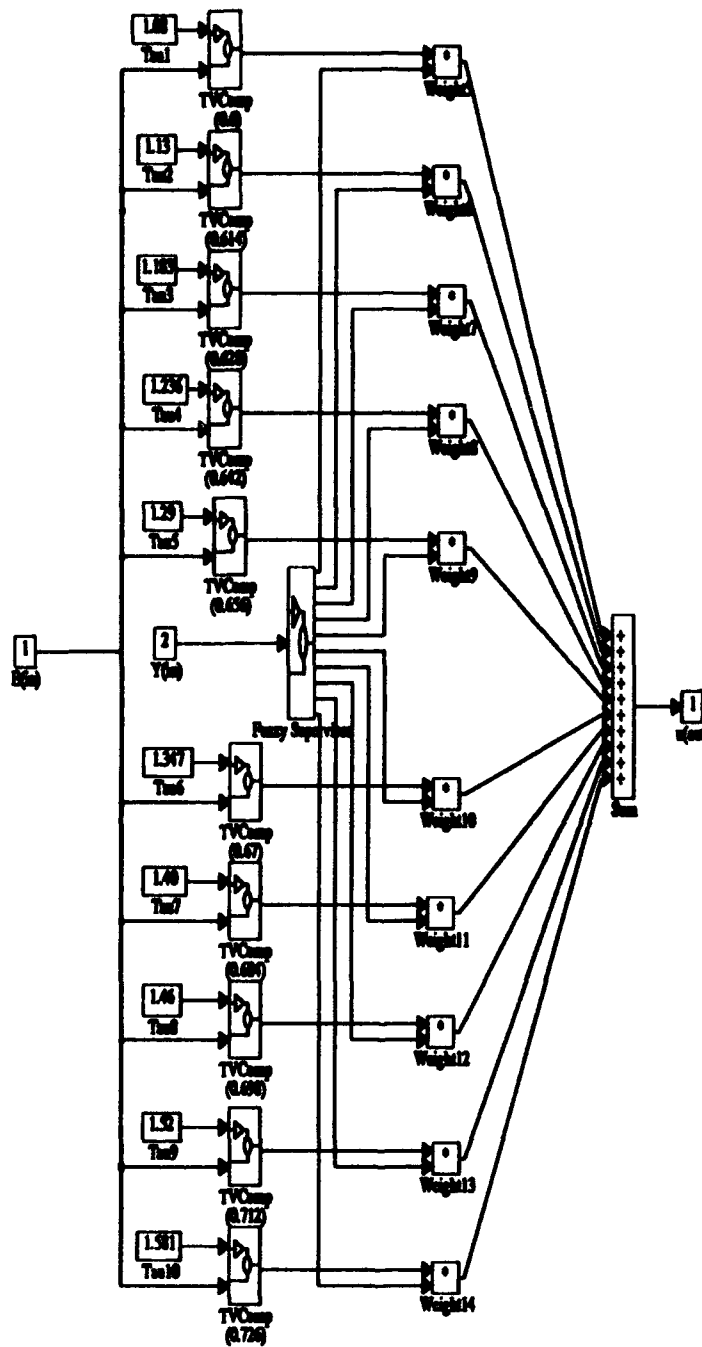


Figure 5.2 Compensator bank for MBFLC with universe of discourse from $Y = 0.6$ to $Y = 0.7$

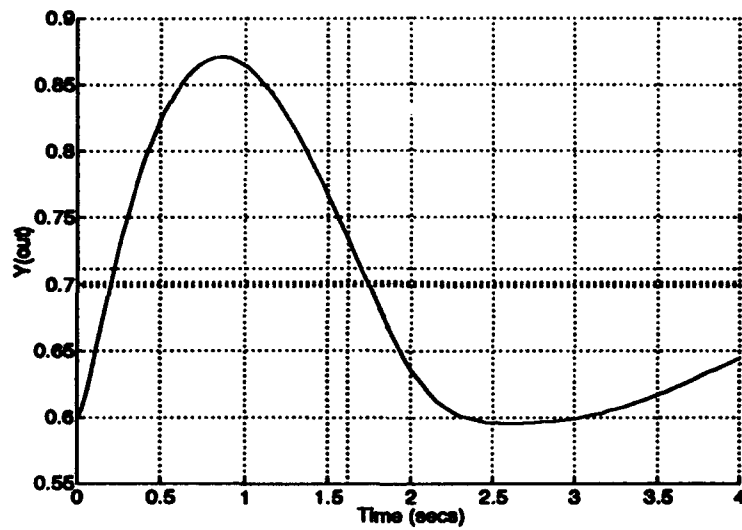


Figure 5.3 closed-loop response of nonlinear plant when driven by Fuzzy Weighted Compensator Bank from $Y = 0.6$ to $Y = 0.7$

Fuzzy Set	Mean	Variance	Implicate(Penalty)
E is 0.0	0.0	0.000021	1.0
E is 0.014	0.014	0.000021	0.6
E is 0.028	0.028	0.000021	0.56
E is 0.042	0.042	0.000021	0.48
E is 0.056	0.056	0.000021	0.44
E is 0.07	0.07	0.000021	0.41
E is 0.084	0.084	0.000021	0.38
E is 0.098	0.098	0.000021	0.37
E is 0.112	0.112	0.000021	0.35
E is 0.126	0.126	0.000021	0.34

Table 5.2 Tuning Parameters for Fuzzy Limiter Membership Functions

5.2.2 Full Error Signal Input to Linearized Plants. The error signal E is based on error between current and desired position. By feeding E directly into a compensator the tacit assumption is made that the compensator being driven is *valid* between the initial state and the final state. In the case of Banked Compensation, this assumption is not true, and feeding the entire E signal into any single compensator contributes significantly to the errors evident in Figure 5.3. To overcome this, E must be scaled to account for the limited validity of the compensators in the bank. This is the purpose of the *Fuzzy Limiter*.

The location of the Fuzzy Limiter is shown in Figure 5.4. It would be natural to place a Limiter immediately before each linear compensator in the bank. In this case, though, given a fixed starting point ($Y = 0.6$), each error magnitude will be associated with a specific compensator. Therefore, a single limiter can be constructed, eliminating some complexity. This consideration sets a non-rigorous lower limit on the number of Fuzzy Sets required within the Limiter: There should be at least one Fuzzy Set for each linear compensator in the Bank.

The internal Structure of the Fuzzy Limiter block is shown in Figure 5.5. The tuning parameters for the Fuzzy Sets are given in Table 5.2 Notice that this block is not strictly Fuzzy; the final output is a direct function of the input. In this case, the Fuzzy Logic is only used to determine a "penalty factor" for large error signals.

The rules for determining the appropriate weighting factor have single premises. The rules represented in the Figure are:

- IF —Error— is 0 THEN Weighting Factor is 1.0
- IF —Error— is 0.014 THEN Weighting Factor is 0.6
- IF —Error— is 0.028 THEN Weighting Factor is 0.56
- IF —Error— is 0.042 THEN Weighting Factor is 0.48
- IF —Error— is 0.056 THEN Weighting Factor is 0.44
- IF —Error— is 0.07 THEN Weighting Factor is 0.41
- IF —Error— is 0.084 THEN Weighting Factor is 0.38
- IF —Error— is 0.098 THEN Weighting Factor is 0.37
- IF —Error— is 0.112 THEN Weighting Factor is 0.35
- IF —Error— is 0.126 THEN Weighting Factor is 0.34

The operation of the Fuzzy Limiter is summarized as follows:

- The error signal E is input to the controller.
- The absolute value of the error signal is used to define the universe of discourse. The Fuzzy Limiter is only concerned with the magnitude of the error signal and how it compares with the regions of attraction of the linearized compensators.
- The magnitude of the error is evaluated for membership in ten Fuzzy Sets. The membership functions for these sets are shown in Figure 5.6
- The crisp weighting factor is determined by the method of Mamandi, which is given in (2.40). Simply stated, the membership value for each set is multiplied by the weighting factor implied by that Set. These terms are added together and divided by the sum of the membership values for all defined sets.
- The original error function, sign and magnitude, is multiplied by the weighting function.

It should be mentioned that the objective of the Fuzzy Limiter is *not* to place hard limits on the magnitude of the error function. This restriction would result in a closed-loop system with a very slow response time. The Fuzzy Limiter simply approximates a "squashing function" which scales the error to acknowledge the fact that the linearized model predicts a linear response to the input whereas the actual effect of the input will be cubic. The Fuzzy Limiter could well be a "Fuzzy Booster" in situations where the linear model leads to under-control of the actual nonlinear plant.

The values for the penalties implied by each Fuzzy Set are shown in Table 5.2. These values are based on an estimate of the error being introduced by a given magnitude Error signal and are

refined through closed-loop simulations. Notice that the penalty associated with the *EisZero* Fuzzy Set is 1, implying no penalty for small error signals. This will always be the case for a correctly modeled system.

The tuning simulations start with the smallest reference step away from the initial equilibrium corresponding to a Fuzzy Set within the Limiter. For this step, the penalty factor is tuned so that the peak overshoot exactly touches the M_p line. The process is repeated for each step size corresponding to a Fuzzy Set, until all penalties are adjusted. Step inputs are then simulated which correspond to regions between the fuzzy sets (such as from an equilibrium of .6043 to a final value of .67). If these steps do not exhibit the correct overshoot, then two actions can be taken to correct the problem. More Fuzzy Sets can be defined within the compensator, or the variance term σ^2 of the existing Sets can be altered to obtain adequate performance.

The character of the penalties depends on both the location and extent of the universe of discourse. A universe of discourse far from the origin will require smaller penalties because the regions of attraction for these compensators are large. If the universe of discourse itself is very large, however, commensurately large E signals are possible. This could require large penalties on the E signal, even far from the origin.

Figure 5.7 shows the closed-loop response of the nonlinear plant to a step input $R_{r,i}(t) = 0.6 + u_{-1}(t)$ with the Fuzzy Limiter in place. It is clear from the Figure that the tendency of the response to overshoot M_p has been eliminated. All that remains now are the lightly damped oscillations arising from modeling errors and compensator transfers occurring away from equilibrium points. This will be addressed in the next section.

Notice that the effect of the Fuzzy Limiter is a time-invariant function of the Error and the universe of discourse. The Fuzzy Limiter could be replaced with a look-up table in final implementation, unless Fuzzy Logic-based optimization was desired. A concept for a robust Fuzzy Limiter is presented at the end of this chapter.

The Banked Compensator, modified by the Fuzzy Supervisor and Fuzzy Limiter, will be referred to henceforth as the *Fuzzy Bank*.

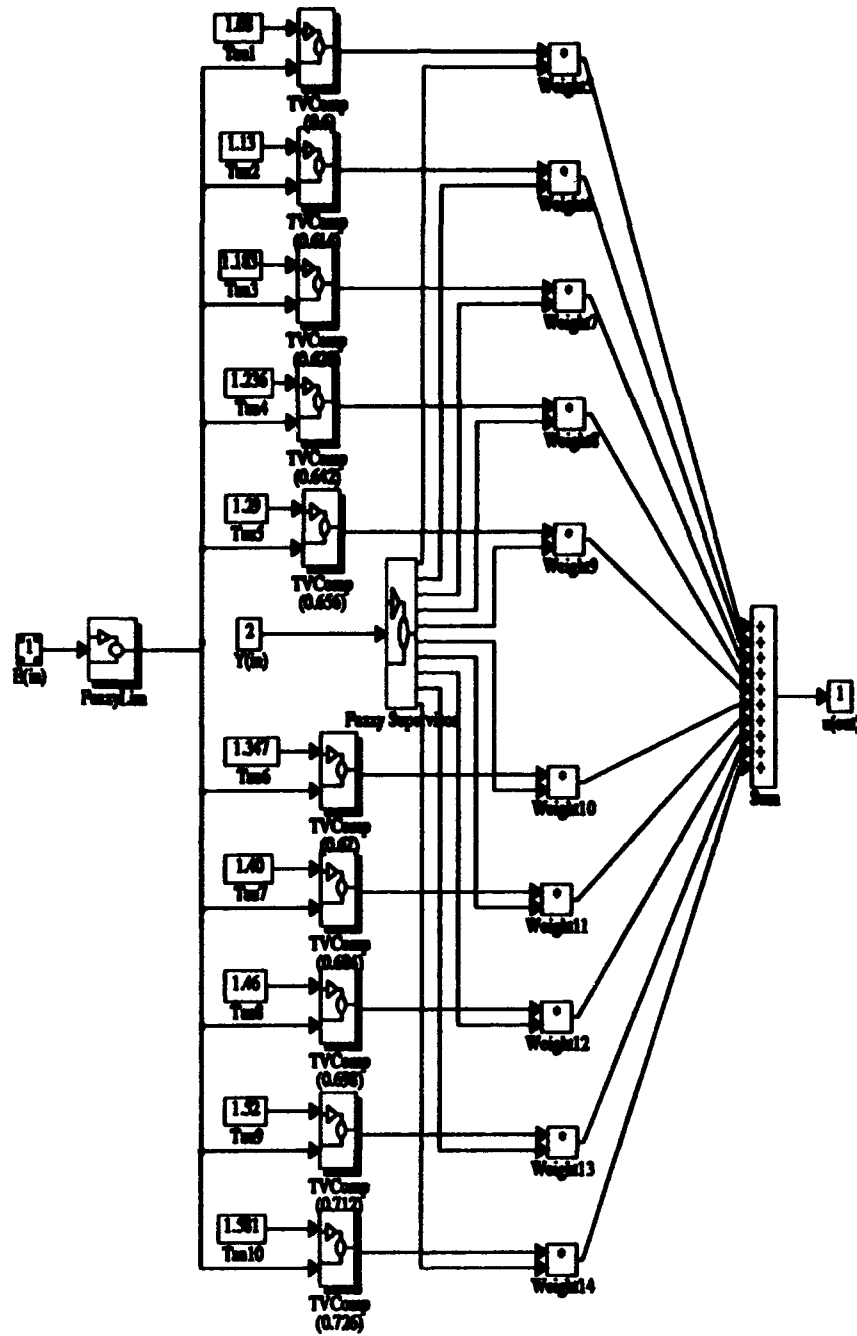


Figure 5.4 Fuzzy Weighted Compensator Bank with associated Fuzzy Limiter. This configuration is referred to henceforth as a Fuzzy Bank

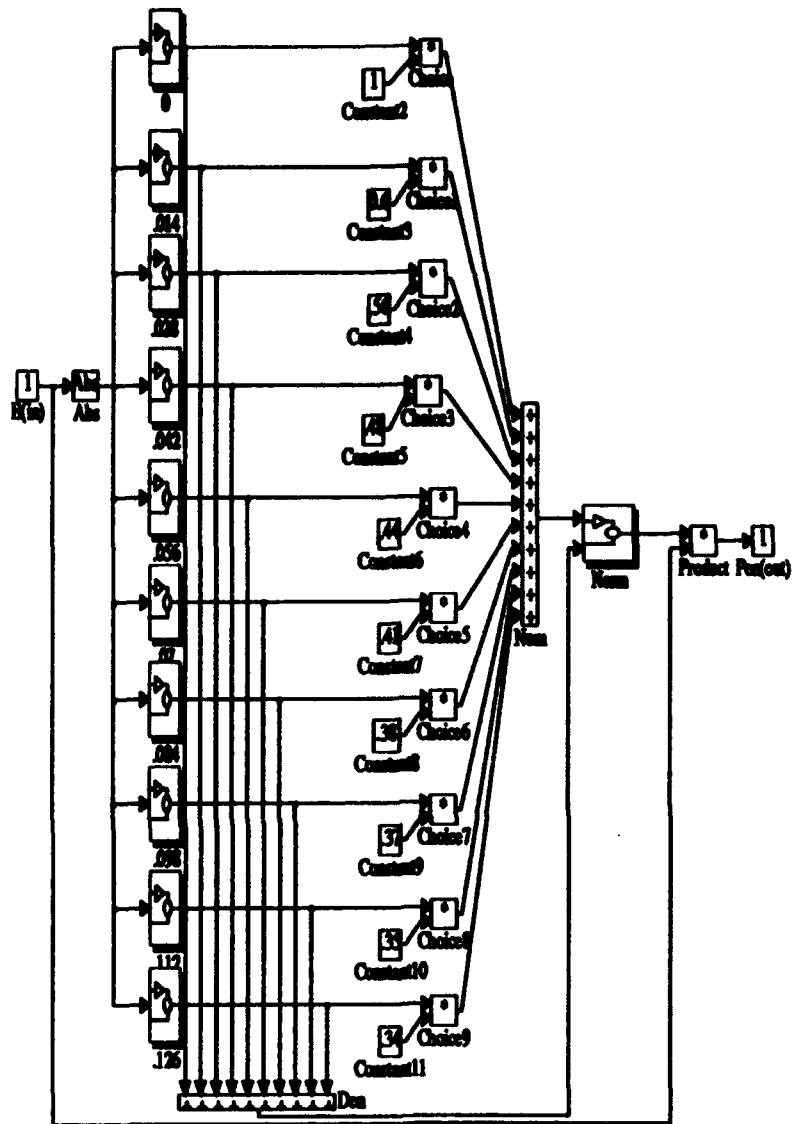


Figure 5.5 Structure of SIMULINK block Fuzzy Limiter

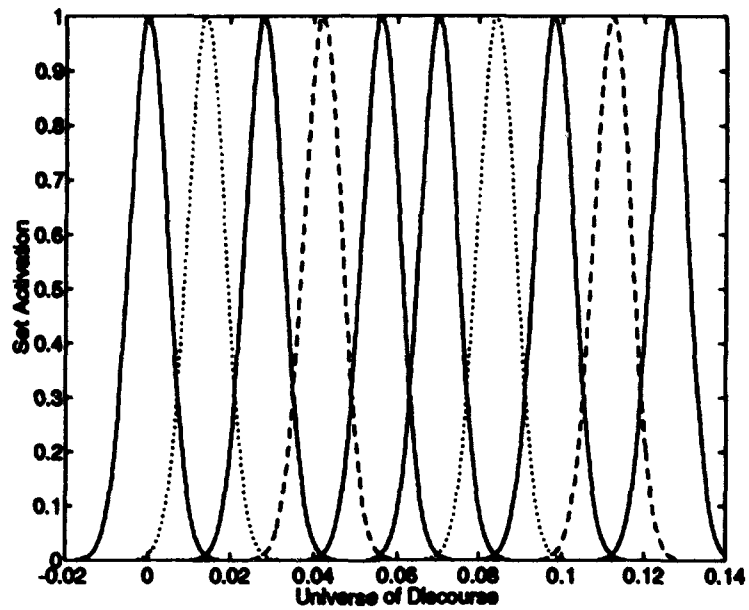


Figure 5.6 Membership functions for Fuzzy Sets in Fuzzy Limiter

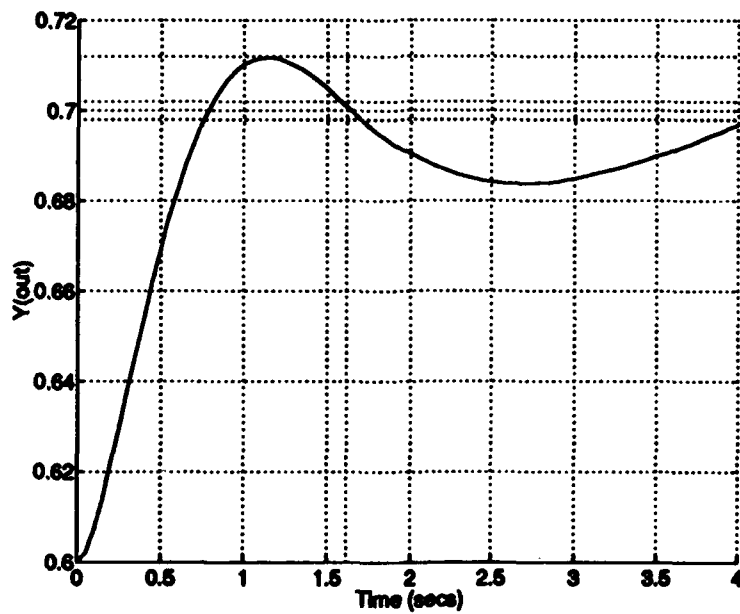


Figure 5.7 Closed-loop response of nonlinear system compensated by Fuzzy Bank

5.2.3 System is Not at Equilibrium when Output Reaches Final State. The Fuzzy Bank is capable of producing the correct initial transient response in the closed-loop system, given an adequate number of Sets within the Fuzzy Limiter. It is unable, however, to settle out the system upon reaching the desired output, as shown in Figure 5.7. Dynamics have been generated in the system which are not accounted for by the controller, the culmination of the mismodeling between the linear controller and the nonlinear plant. Further, the error signal is very small close to the input reference value. The Fuzzy Limiter, then, which only weights the error signal, has very little control authority. Therefore, an auxiliary control input is required to drive the system to steady-state.

The undesired oscillations can be eliminated by introducing an overall Fuzzy Logic architecture to the controller. Two rules are required to ensure proper system response.

1. IF Error is Not Zero AND \dot{Error} is not Positive THEN $U = U_{lin}$
2. IF Error is Zero AND \dot{Error} is Positive THEN $U = U_{lin} + C(t)$

As stated above, the structure is essentially a Fuzzy Logic Controller with two possible control actions: 1) Output the exact value of U produced by the Fuzzy Bank, or 2) Output the exact value of U produced by the Fuzzy Bank *plus* an auxiliary $C(t)$. The auxiliary provides an additional settling term when the system is dropping towards the reference value after the initial overshoot.

The form of $C(t)$ is based on the response of a bank of *pre-weighted* linear compensators, shown in Figure 3.14. Recall that, for pre-weighted compensators, once a compensator in the bank is activated it will produce an output for all time forward. The output of $G_1(t)$ in the Figure 3.14 proved fully capable of accounting for the fact that compensator $G_2(t)$ inherited a plant out of equilibrium. No oscillations were induced as long as there were no modeling inconsistencies. With inconsistencies present, the $G_2(t)$ predicted by linear analysis was incorrect. In our case, modeling errors are also inherent to the problem, so it is reasonable that the plant controls advocated by the linear-based Fuzzy Bank would ultimately induce undesirable oscillations. The question, then, is will *any* equivalent $G_2(t)$ be able quell the oscillations induced the Fuzzy Bank.

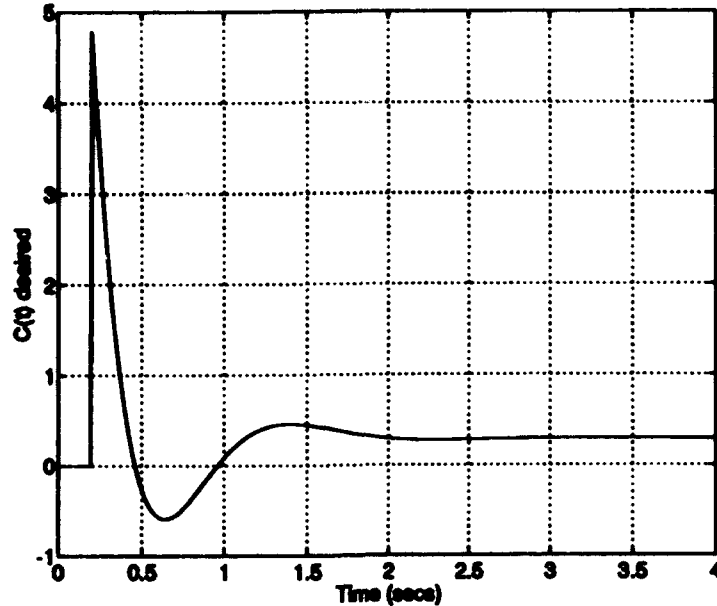


Figure 5.8 Desired form for $C(t)$ based on linear analysis of pre-weighted compensator bank

To answer this question a Fuzzy Logic element was created which would emulate the output of $G_2(t)$ in Figure 3.14, but with arbitrary transient response and steady-state output. The response of $G_2(t)$ in Figure 3.14 is repeated in Figure 5.8. The initial spike in the function will not be as important in this application, because the switches used in Chapter 3 have all been replaced with Fuzzy Sets for the MBFLC. Transitions between compensators, therefore, occur more gradually. However, an initial surge will be required to halt the state derivatives reducing to a steady-state offset value based on the requirement that the control input to the plant at t_∞ be:

$$U(t_\infty) = R_{ref}(t_\infty) - Y(t_0). \quad (5.1)$$

For an input $R_{ref}(t) = 0.6 + .1u_{-1}(t)$, starting from $Y(t_0) = 0.6$ then $U(t_\infty) = 0.1$.

The function shown in Figure 5.8 can be approximated using the Fuzzy Sets *Eis0* and *EisPositive*. The membership functions for these two sets are shown in Figure 5.9 based on the objective underdamped response. Notice that *Eis0* is activated initially when the closed-loop re-

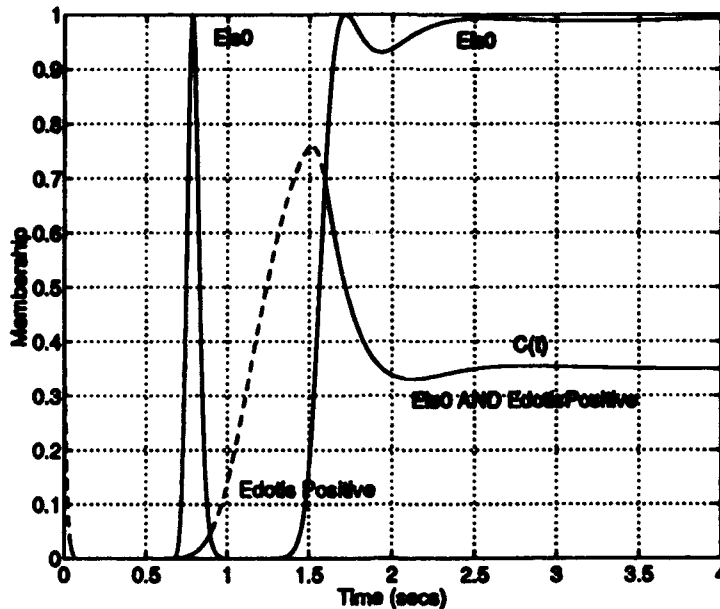


Figure 5.9 $C(t)$ function formed by ANDing of Fuzzy Sets $E=0$ and $E=0 \text{ Positive}$

sponse passes through zero. $E=0$ goes to zero as the system reaches its peak overshoot then, is driven to 1 again as the system settles out at the desired reference value.

The Fuzzy Set $E=0 \text{ Positive}$ indicates when the system is approaching the reference value from a negative value of Error. This can be seen from the fact that $\dot{E} = (ref - Y) = -\dot{Y}$. When Y initially begins climbing \dot{Y} is positive so \dot{E} is negative. \dot{E} will only become positive when the Y has reached its peak overshoot and started back down towards the reference value. As the system settles out at $Y = Ref$, the Set $E=0 \text{ Positive}$ reaches a steady-state value of membership, in this case $\mu_{E=0 \text{ Positive}} = 0.35$.

The desired function shape is obtained using the Fuzzy AND, discussed in Chapter 2. The result of the ANDing procedure is also shown in Figure 5.9. The resulting function reasonably approximates the function given in Figure 5.8 for an arbitrary starting time.

The exact form of the Fuzzy-derived $C(t)$ can be altered by the tuning parameters of the Fuzzy Sets and a constant weighting term χ , called the Fuzzy Offset. The procedure for determining initial

estimates of these parameters is given here. Of course, simulation is required to maximize the $C(t)$ damping effect.

The first step is to determine values for $\sigma^2_{\dot{E}isPositive}$, $\bar{X}_{\dot{E}isPositive}$, $\bar{X}_{EisZero}$, and $\sigma^2_{EisZero}$. These quantities completely define the Fuzzy Sets. The procedure for *EisZero* is straightforward. $C(t)$ must activate as the system output nears the desired state, or as E goes to 0. Therefore, $\bar{X}_{EisZero}=0$. $\sigma^2_{EisZero}$ determines how far away from zero $C(t)$ will begin to activate. For this design, it was iteratively decided that *EisZero* should be activated to a value of $\mu = 0.2$ when the response was within 5

The purpose of the *EisPositive* Fuzzy Set is two-fold: To prevent $C(t)$ from activating when the system response initially crosses $E = 0$, and to provide steady-state constant into the plant. It is decided, then, that $\mu_{\dot{E}isPositive}(\dot{E}) = 0.1$ for the value of \dot{E} induced by the $U_{lin}(t)$ when E first goes to zero and $\mu_{\dot{E}isPositive}(0) = 0.35$. The values for $\sigma^2_{\dot{E}isPositive}$ and $\bar{X}_{\dot{E}isPositive}$ can then be solved for by solving the system of two equations a two unknowns using:

$$\mu(x) = e^{-\frac{(x-\bar{x})^2}{\sigma^2}}. \quad (5.2)$$

The value of \dot{E} induced by the $U_{lin}(t)$ when E first goes to zero is determined by simulation.

χ can, in theory, be determined by the constraint given in (5.1). For for the case shown in Figure 5.9, for an input $R_{ref}(t) = 0.6 + .1u_{-1}(t)$:

$$\chi = \frac{U(t_{\infty}) - 0.1}{0.35}. \quad (5.3)$$

Unfortunately, this equation must be solved through simulation, because $U(t_{\infty})$ cannot be determined analytically.

The form of the Banked Model Based Fuzzy Logic Controller incorporating this emulated $G_2(t)$ is shown in Figure 5.10. In this Figure, the Fuzzy Bank is shown as a single block. The structure internal to the block *FuzzyBank* is identical to the compensator shown in Figure 5.5. It was determined that, through proper tuning, the oscillations in $Y(t)$ could, indeed, be eliminated

Fuzzy Set	Mean	Variance
<i>Eis0</i>	0.0	0.0000074
<i>EisPositive</i>	0.064	0.00021

Table 5.3 Tuning Parameters for Fuzzy Sets *E is Zero* and *E is Positive*

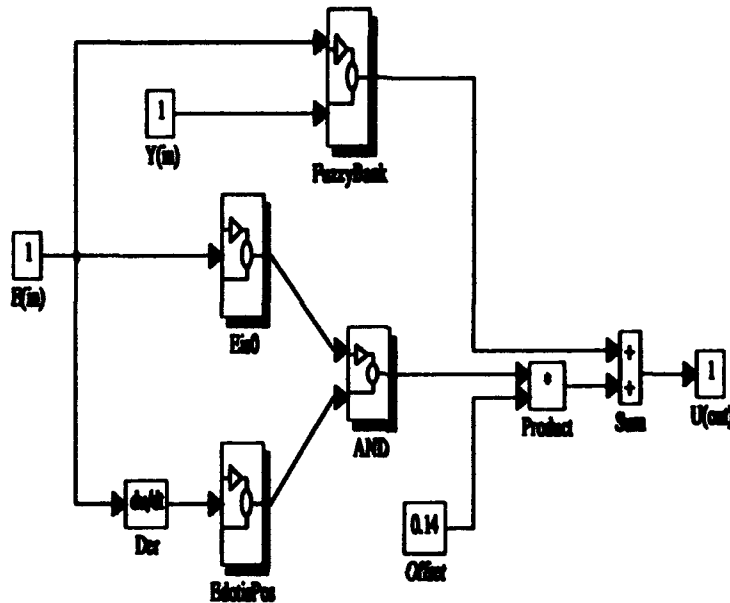


Figure 5.10 SIMULINK implementation of Banked MBFLC

for a given initial condition and step magnitude. This, therefore, is a successful form of the Model-Based Fuzzy Logic Controller.

The membership functions for the Fuzzy Sets *Eis0* and *EisPositive* are determined through simulation and are plotted versus their universes of discourse in Figure 5.11. The tuning data for these two Fuzzy Sets is given in Table 5.3. The Fuzzy tuning parameters were chosen so as to produce the correct shape of the $C(t)$ function. The magnitude of the $C(t)$ is determined by the Offset Value χ . χ is also determined through simulation, and in this case, $\chi = 0.13$.

The response of the final Banked MBFLC is shown in Figure 5.12. Both the initial transient and settling characteristics of this system are similar to a linear response. This demonstrates the applicability of a hybrid linear/Fuzzy approach to nonlinear control.

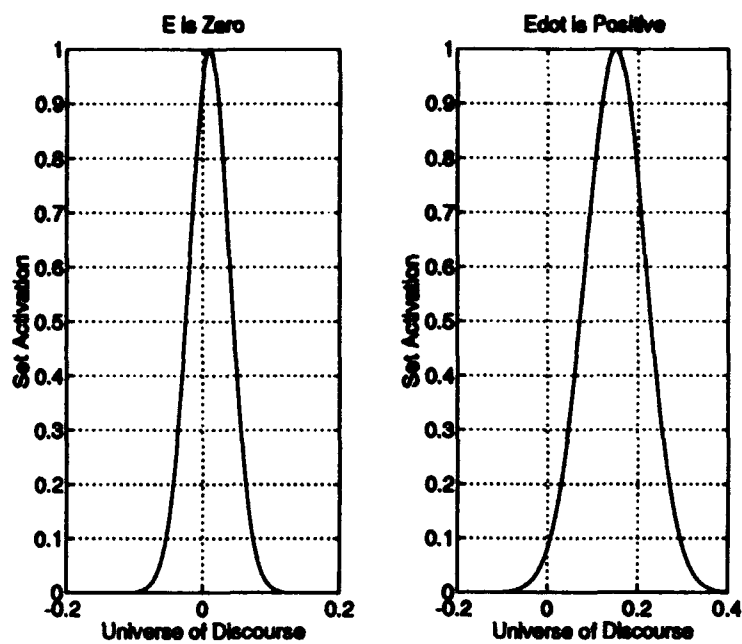


Figure 5.11 LEFT: Membership function for *E is Zero*. RIGHT: Membership function for *Edot is Positive*

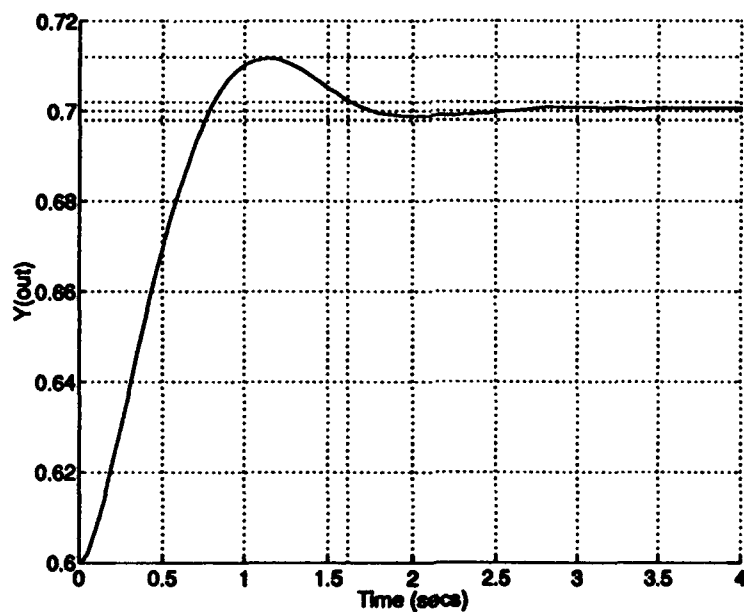


Figure 5.12 Response of nonlinear plant in closed-loop simulation with Banked MBFLC

5.3 Full-Envelope Banked MBFLC

The sources of error identified in the previous Section have now been accounted for in the MBFLC design. Errors caused by intermediate compensators were found to be minimal. Errors caused by input error signals larger than the regions of attraction for linear compensators are minimized by use of the Fuzzy Limiter. Other plant/compensator mismatch errors, which result in lightly damped oscillations near the desired state, are addressed with an additive signal derived using Gaussian Fuzzy Sets.

Consideration of these error sources results in a controller capable of driving a nonlinear plant from a given initial condition ($Y = 0.6$) to a given reference value ($Y = 0.7$) in a linear-like manner. The next step is to modify the compensator so that the linear-like behavior is exhibited regardless of the starting point and ending point. A compensator which yields linear-like performance throughout a specified operating range will be referred to as a *full-envelope* controller. This is a term from flight control, which implies a flight controller applicable throughout the flight envelope of an aircraft.

Consider the case where the objective is to develop a full-envelope controller for the envelope between $Y = 0.6$ and $Y = 0.7$, using equilibrium models at $Y = 0.6, 0.614, 0.628, 0.642, 0.656, 0.67, 0.684, 0.698, 0.712$ and 0.726 . The form of the Fuzzy Bank (Compensator Bank, Fuzzy Supervisor and Fuzzy Limiter) will be the same as the previous section (Figures 5.2, 5.4, and 5.5). The Fuzzy Supervisor will select as the initiating compensator that which most closely corresponds to the true starting equilibrium of the nonlinear plant. It has been shown, however, that the compensator based on the final desired equilibrium point is incapable of driving the system to steady-state within the desired settling time. An auxiliary signal $C(t)$ had to be defined to quickly drive the closed loop system to steady-state.

The system is very sensitive to the form of the $C(t)$ signal. Small errors in the shape of the Fuzzy Sets *EisZero* and *EisPositive* or in the offset term χ lead to degraded system response. Therefore, like the Fuzzy Limiter, the required $C(t)$ function for various step magnitudes within the envelope of operation must be developed in order to achieve full-envelope performance. The proper $C(t)$ for intermediate step inputs could then be determined through interpolation. The form of the

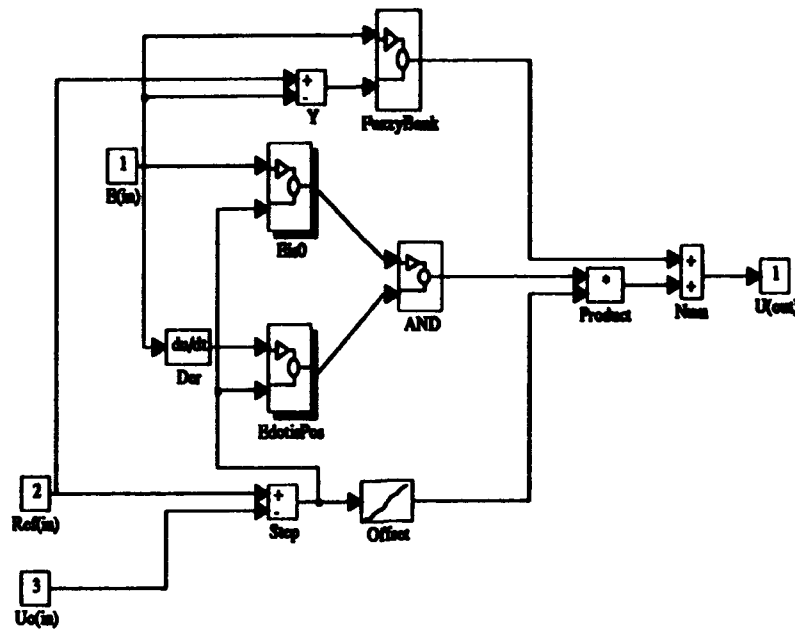


Figure 5.13 SIMULINK simulation of Full Envelope Banked MBFLC

controller, then, could be expressed as a bank of linear compensators and a bank of $C(t)$ -producing Fuzzy AND elements, with a second Fuzzy Supervisor providing the interpolation.

An alternate way to simulate the full-envelope compensator is through the use of look-up tables. Figure 5.13 shows the form of the Fuzzy Controller with a Fuzzy Offset look-up table included. The correct value for χ is obtained based on the magnitude of the reference step ($Ref(in) - U_o(in)$). Because the Fuzzy Sets X is 0 and $Xdot$ is Positive must also change based on the input, step magnitude is also fed into these blocks. Look-up tables supply the values of \bar{x} and σ^2 corresponding to the appropriate $C(t)$. Two other changes are made to minimize the number of inputs to the compensator:

- The derivative block is brought inside the compensator
- Y is now determined by $Y = Ref - E$

A new top-level view is shown in Figure 5.14.

Look-up tables are needed for χ (offset), $\sigma^2_{EisPositive}$, $\bar{X}_{EisPositive}$, and $\sigma^2_{EisPositive}$. Again, this information also could have been expressed by Fuzzy Sets, using a bank of $C(t)$ generators

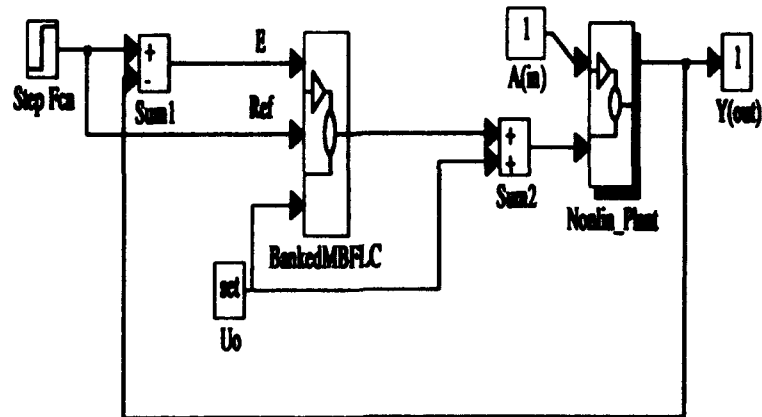


Figure 5.14 Top-level SIMULINK simulation of nonlinear plant in Full-Envelope Banked MBFLC and a Fuzzy Supervisor. The look-up tables serve to simplify the simulation. Look-up tables are limited in that they can only perform linear interpolation, while Fuzzy Supervisor can be tuned to enhance performance. In this case, linear interpolation is not a significant drawback. The data contained in the look-up tables is given in Table 5.4.

The response of this system to step inputs of various magnitudes is shown in Figure 5.15. The principle difference between the response of this closed-loop system and that of the model $M(s)$ 2.26 is that the system peaks slightly later in time. $M(s)$ is fully settled out by $t = 1.62\text{seconds}$ while the Full Envelope MBFLC is just reaching the reference value at this time. Some of this error is attributed to the integration routine used by SIMULINK to solve nonlinear equations. It is possible, however, that certain plant characteristics cause the Fuzzy Bank to exhibit trajectory errors.

Figure 5.16 shows the closed-loop response of the nonlinear plant for various values of the parameter a . The Figure shows that the MBFLC is more sensitive to modeling errors than either QFT or FLC. This is due to the tuning of the Fuzzy Limiter which assumes a given plant sensitivity.

Step Size	χ	$\sigma^2_{EisPositive}$	$\chi_{EisPositive}$	$\sigma^2_{EisZero}$
0.0	0.0	0.00001	0.009	0.000003
0.014	0.006	0.00006	0.009	0.000003
0.028	0.031	0.00013	0.018	0.000007
0.042	0.05	0.00032	0.027	0.000001
0.056	0.063	0.00064	0.036	0.000003
0.07	0.1	0.00096	0.045	0.000005
0.084	0.13	0.00124	0.0545	0.000006
0.098	0.14	0.0019	0.0634	0.000007
0.112	0.16	0.0026	0.072	0.000008
0.126	0.18	0.0032	0.08114	0.000009

Table 5.4 Look-up table data for full envelope MBFLC

The effect of modeling errors, however, is not catastrophic. The effect of retuning the Limiter on modeling errors is explored in the next section.

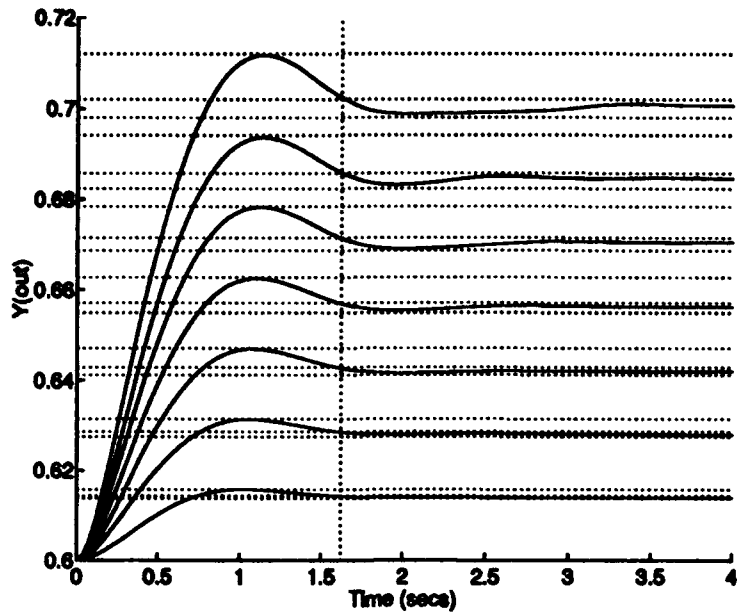


Figure 5.15 Closed-loop response of Full-Envelope MBFLC to step inputs of various magnitudes

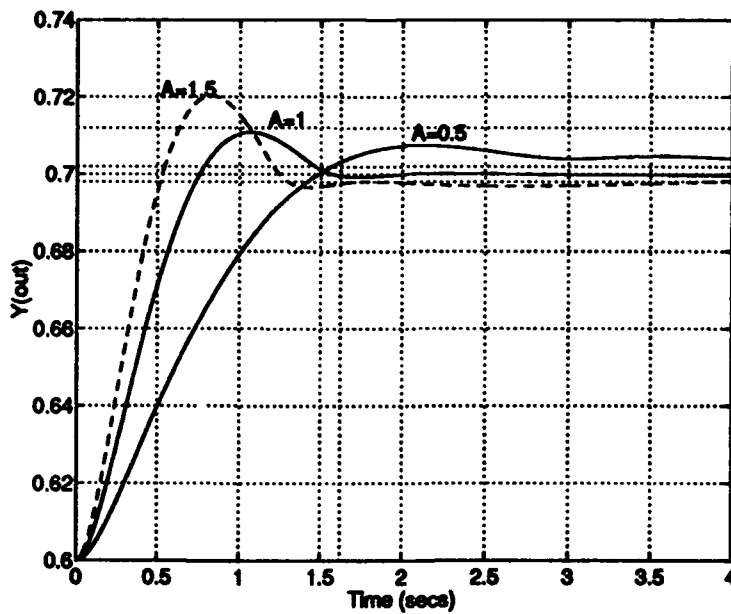


Figure 5.16 Closed-loop response of Full-Envelope MBFLC for $a = 0.5, 1.0, \text{ and } 1.5$

5.4 Contribution of Linear Compensators to Banked MBFLC Design

The previous section developed a Model-Based Fuzzy Logic Controller (MBFLC) that meets all established design specifications, with the exception of disturbance rejection. In essence, the MBFLC is a confederation of n controllers consisting of an initial linear compensator and a $C(t)$ generator. The Fuzzy Limiter is common to all the compensator/generator pairs. Fuzzy Logic, however, effects both the input to and the output from the bank of linear compensators. Therefore, it is reasonable to question just how critical a bank of correctly designed compensators is to the overall success of the design.

Several tests can be run on the MBFLC to determine the contribution made by the linear elements of this hybrid controller. One is to determine the performance of the Banked MBFLC as a function of the number of compensators in the bank. The bank currently uses enough compensators so that at least one is considered valid at any point in the state trajectory. If full coverage is, indeed, a requirement then reducing the number of linear compensators should be reflected by a degradation of system performance. A second test would be to substitute the nonrobust compensators in the current bank with the robust compensators developed in Chapter 3. If robustness in the linear sense translates directly into robustness in the nonlinear sense, this would suggest a significant contribution being made based on linear theory. A third test would be to alter the α parameter of the nonlinear plant to determine if mismodeling can be overcome through tuning. These questions are explored here.

5.4.1 Effect of Linearized Plants on MBFLC. Knowledge of the nonlinear system is resident in two components of the controller: the linearized plants and the Fuzzy Sets. These data sources, however, are interrelated. The Fuzzy Sets are tuned based on simulations, and the simulations are performed with a given number of linear compensators in place. It is reasonable, then, to assume that there is some redundancy in the compensator architecture, and that the structure can be ultimately simplified with little penalty in performance. Based on the analysis of the previous sections, It is assumed that only the initiating and terminating compensators contribute significantly to the success or failure of the compensator. In addition, it has been shown

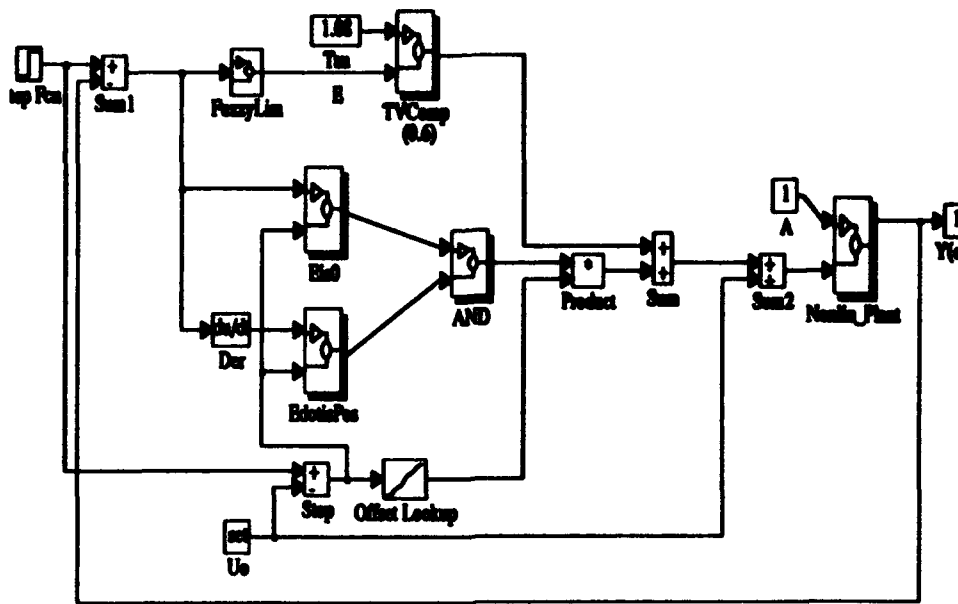


Figure 5.17 SIMULINK simulation of MBFLC using only a single linear controller

that the linear compensator based on the desired output of the system is unable to drive the system to the reference value with zero steady-state error. This indicates that only the initiating compensator could be considered a linear element of the MBFLC.

Consider the simulation shown in Figure 5.17. Here the bank has been replaced by a single compensator, with τ corresponding to $Y = 0.6$. This results greatly simplifies the simulation, allowing it to be displayed on a single screen. The Fuzzy Supervisor can be removed, as there are no alternate compensators to weight. The closed-loop response of this system to step inputs $Y = 0.6 + 0.025u_{-1}(t)$, $Y = 0.6 + 0.05u_{-1}(t)$, and $Y = 0.6 + 0.1u_{-1}(t)$ is shown in Figure 5.18. As anticipated, the response is not adversely affected by the deletion of the other compensators in the bank. In fact, the response has improved in some respects, such as settling time. What is surprising, however, is that this increase in performance is independent of the starting equilibrium condition. Figure 5.19 shows closed-loop responses for $Y = 0.65 + 0.025u_{-1}(t)$, $Y = 0.65 + 0.05u_{-1}(t)$, and $Y = 0.62 + 0.03u_{-1}(t)$. All of these exhibit acceptable closed-loop responses.

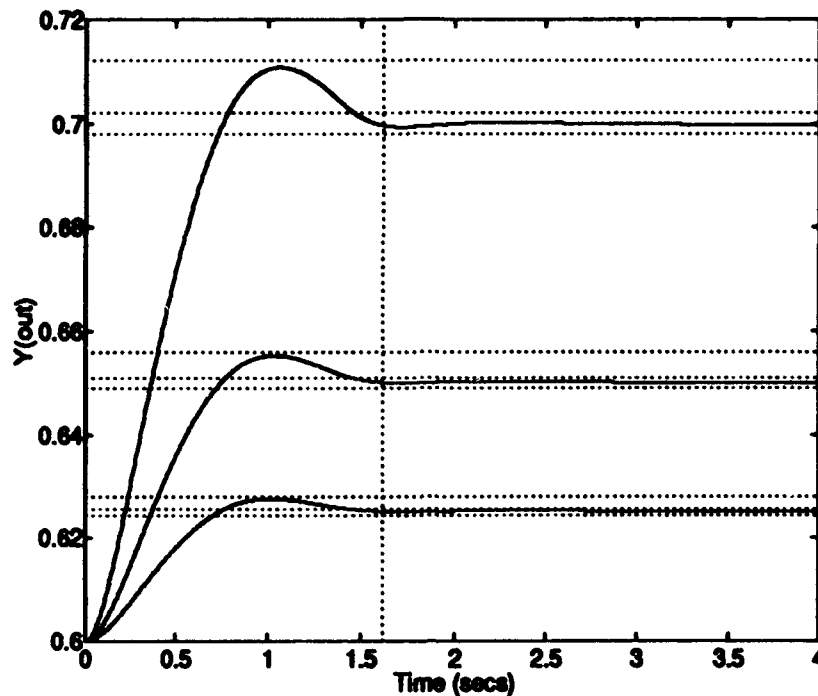


Figure 5.18 Closed-loop response of single-compensator MBFLC to step inputs of various magnitudes

This independence of the initial state is *not* independent of the choice of compensator. In fact, the larger the value of τ (that is, the smaller the gain in the single compensator) the more sluggishly the system responds. This holds for steps both above and below the equilibrium point of the compensator. This is illustrated in Figure 5.20. The single compensator in Figure 5.17 is altered to correspond to $Y = 0.65$ ($\tau = 1.2675$). Figure 5.20 shows the closed-loop response of the system, starting from equilibrium both above and below the equilibrium about which the compensator is designed. In both cases performance is sluggish.

The performance of the Single-Compensator MBFLC, then is a function of compensator selection. The Fuzzy-emulated $G_2(t)$ will correctly stabilize the system response provided the linear compensator drives the system to the correct overshoot. The Fuzzy Limiter, however, will overdamp all compensators but the one with the highest gain in the original Limiter design. The

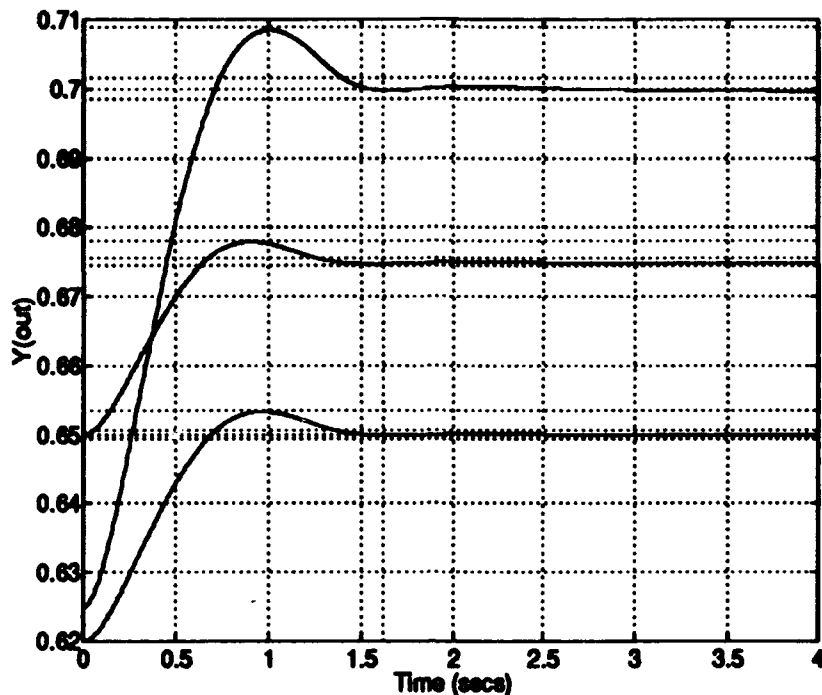


Figure 5.19 Closed-loop response of single-compensator MBFLC to step inputs starting from various initial equilibria

conclusion, therefore, is that the single compensator should be the one with the highest gain in the envelope of operation. For this design, the "correct" single compensator corresponds to $Y = 0.6$.

It has now been established that a single-compensator MBFLC can be developed given the tuned elements of the full 10-compensator MBFLC. It is reasonable to ask if the same tuning data could have been obtained using the single compensator design. The answer is yes. The tuning procedure can be accomplished even with only a single compensator providing trajectory information. An arbitrary number of Fuzzy Sets can be defined within the Fuzzy Limiter and the magnitude of the required E penalty can be determined using the progressive step procedure discussed in the last section. The last Fuzzy Set should correspond to the largest expected input to the system. The look-up tables for χ (offset), $\sigma^2_{EisPositive}$, $\bar{X}_{EisPositive}$, and $\sigma^2_{EisPositive}$ must then be tuned through simulation to minimize the oscillatory tendencies of the system.

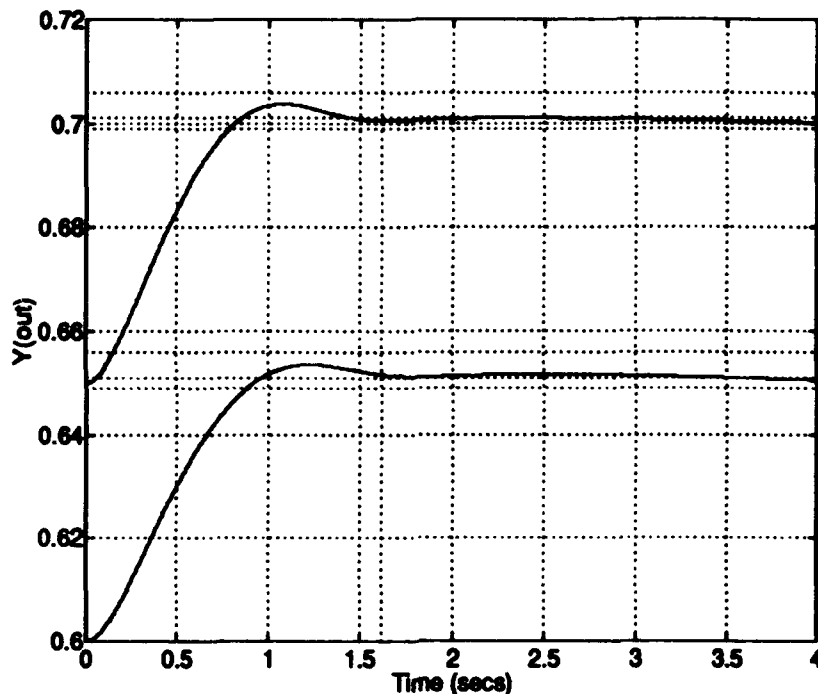


Figure 5.20 Closed-loop response of single-compensator MBFLC to step inputs starting from equilibria both above and below the equilibrium of the linear compensator

The final issue to resolve is the minimum number of Fuzzy Sets in the Limiter required to provide full-envelope control of the nonlinear plant. Figure 5.21 shows the MBFLC simulation with the Fuzzy Limiter reduced to two Sets. Because of the greatly reduced size of the Fuzzy Limiter, its special block was removed so the entire simulation could be viewed in a single diagram. The Fuzzy Limiter and Linear compensator could be adjusted to ensure the correct overshoot. However, to accomplish this, the requirement that the *Erroris0* Fuzzy Set in the Limiter carry a penalty of 1 by definition had to be eased. By setting the penalty associated with this Fuzzy Set to 0.8 and tuning the look-up tables to damp oscillations, the response in Figure 5.22 is obtained.

Figure 5.22 also shows the response of the compensator to steps of other magnitudes starting from the same equilibrium condition. This shows that the two-set Limiter is *not* adequate to control the full envelope of this system.

The conclusions of this analysis are as follows:

- Only one linear compensator is required in a MBFLC. This compensator should correspond to that portion of the plant envelope requiring the highest gain.
- In general, one Fuzzy Set will be required in the Fuzzy Limiter for each desired final state. However, a break-even point occurs where the entire operating envelope is "adequately covered" and a step input to any point the envelope can be made. The number of sets required to reach this point seems to vary according to the extent of the nonlinearity.
- Increasing the number of linear compensators does not overcome a deficiency in the granularity of the Fuzzy Limiter.
- Removing all linear compensators or replacing the single compensator with a simple gain results in poor performance.
- The Fuzzy elements play a significant role forcing the nonlinear system to exhibit linear behavior.

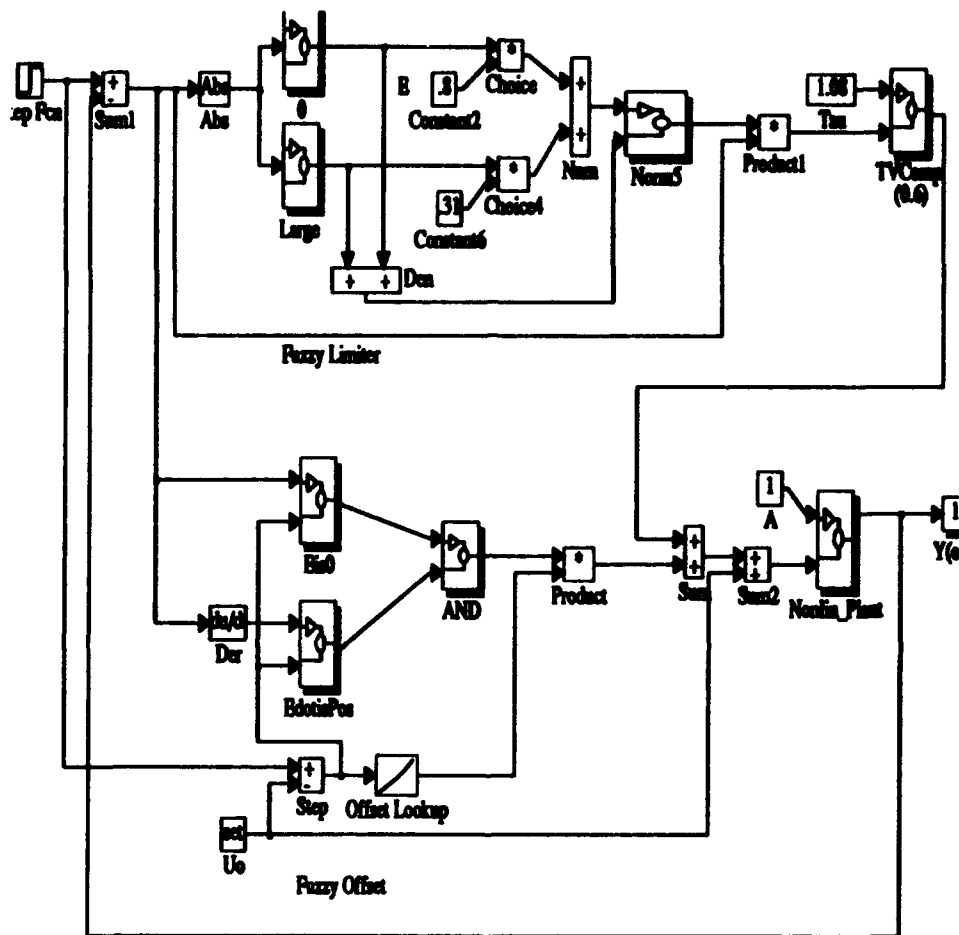


Figure 5.21 Single-compensator MBFLC with a simplified 2-set Fuzzy Limiter

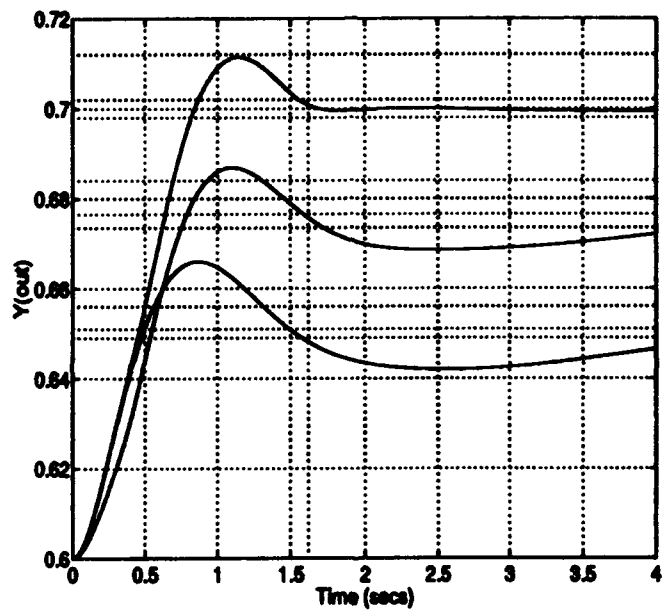


Figure 5.22 SIMULINK simulation of MBFLC with a two-set Fuzzy Limiter and a single linear compensator

Fuzzy Set	Mean	Variance	Penalty
$E_{is0.0}$	0.0	0.00002	0.70
$E_{is0.025}$	0.025	0.00002	0.055
$E_{is0.05}$	0.05	0.00002	0.0414
$E_{is0.075}$	0.075	0.00002	0.031
$E_{is0.1}$	0.1	0.00002	0.0279

Table 5.5 Tuning parameters for Fuzzy Limiter driving robust linear compensator

Step Size	χ	$\sigma^2_{\dot{E}_{isPositive}}$	$\bar{X}_{\dot{E}_{isPositive}}$	$\sigma^2_{E_{isZero}}$
0.0	0.0	0.00001	0.000000001	0.0000004
0.025	0.064	0.00013	0.018	0.0000007
0.05	0.132	0.00064	0.036	0.000003
0.075	0.23	0.00096	0.045	0.000005
0.1	0.3	0.00019	0.0634	0.000007

Table 5.6 Look-up table data for MBFLC incorporating the robust linear compensator

5.4.2 Effect of Robust Linear Compensators on MBFLC. A second test of the contribution being made by linear control theory is to replace the linear compensator used in the last section with the robust compensator developed in Chapter 3. If robustness in the linear sense translates via the MBFLC architecture into nonlinear robustness, this indicates a direct application of linear synthesis to nonlinear control through Fuzzy Logic.

Figure 5.23 shows the single compensator MBFLC with the robust controller inserted. Five equilibrium conditions were chosen for tuning: $Y_{oi} = 0.6, 0.625, 0.65, 0.675,$ and 0.7 . Fuzzy Sets were defined within the Fuzzy Limiter corresponding to each of these equilibrium conditions and the MBFLC was tuned as discussed in the last section. The Fuzzy Limiter tuning data is given in Table 5.5. The tuning data for the look-up tables χ , E_{is0} variance, $\dot{E}_{isPositive}$ variance, and $\dot{E}_{isPositive}$ mean are given in Table 5.6.

Notice the data in the look-up tables are much different from the case of the nonrobust controller. Though the values for the E and \dot{E} Fuzzy Sets are still nearly the same, the offset value χ is significantly larger. The penalties associated with the Error signal in the Fuzzy Limiter are

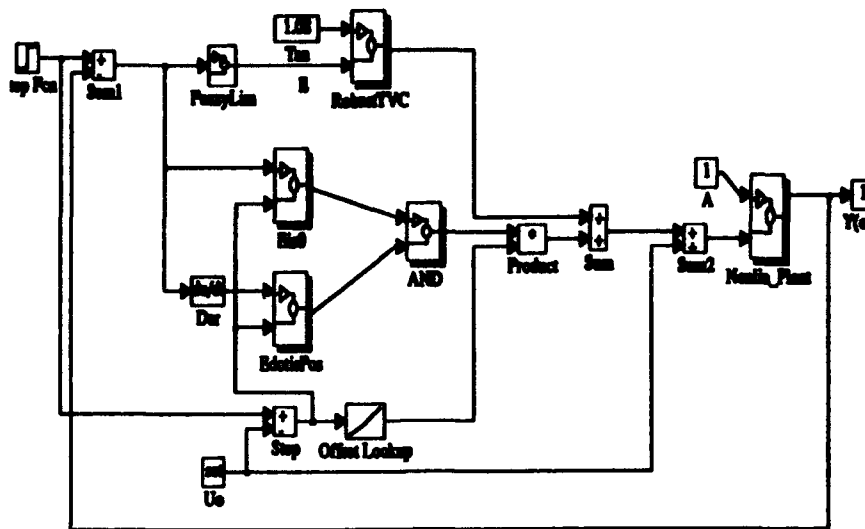


Figure 5.23 SIMULINK simulation of single compensator MBFLC using robust compensator

also an order of magnitude higher in the nonrobust case. These differences are necessary to account for the much higher gain of the robust compensator.

The response of this system to step inputs of various amplitudes is shown in Figure 5.24. Performance is equivalent to the nonrobust case of the previous section. Figure 5.25, however, shows the responses of both the robust and nonrobust single compensator MBFLCs to a step disturbance of magnitude 0.1 at the input of the plant. This Figure shows that the nonrobust compensator actually exhibits *better* signal rejection characteristics than does the robust compensator.

The disparity in performance is due to the Fuzzy Limiter. With the Fuzzy Limiter removed, the single robust compensator MBFLC meets the $|Y_{DISTURBANCE}(t)| \leq |0.1U_{DISTURBANCE}(t)|$ specification, but cannot track a signal. With the Fuzzy Limiter inserted, the system can track a step input, by the penalties associated with a large E signal inhibit signal rejection. The other branch of the MBFLC activated by $E \leq 0$ and \dot{E} is Positive does not contribute to the regulation problem.

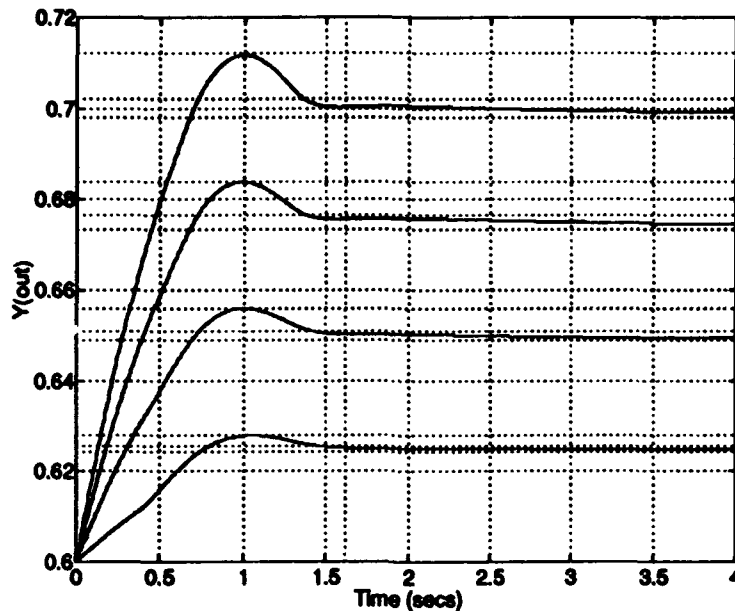


Figure 5.24 Closed-loop tracking response of robust Single Compensator MBFLC to step inputs of various magnitudes

For the case of the nonrobust compensator, a balance is struck. The error signal is not attenuated nearly as fast as in the robust case. Therefore, as the E gets larger, the compensator is still able to drive the plant back to the reference value in a timely manner. Even in this case, the Fuzzy Limiter serves to inhibit adequate tracking. The effect of the Limiter, though, is not nearly as severe. Notice that, for regulation with the Limiter removed, disturbance response is approximately that which was determined through linear analysis in Chapter 3. This equivalence of linear and nonlinear controllers for regulation could be an area for future exploration.

An additional simulation was done to determine if reintegration of the full compensator bank would have a significant effect on signal rejection. The conclusion was that it did not. Therefore, this analysis suggests that linear robustness does *not* contribute directly to robustness in the MBFLC. The robustness provided by the controller in the linear case will be observed in the nonlinear case in inverse proportion to the weights which determine the squashing effect of the Fuzzy Limiter. The smaller the slope of this line, the greater the region of attraction of the linearized compensator, and the more robustness will be observed in the nonlinear system.

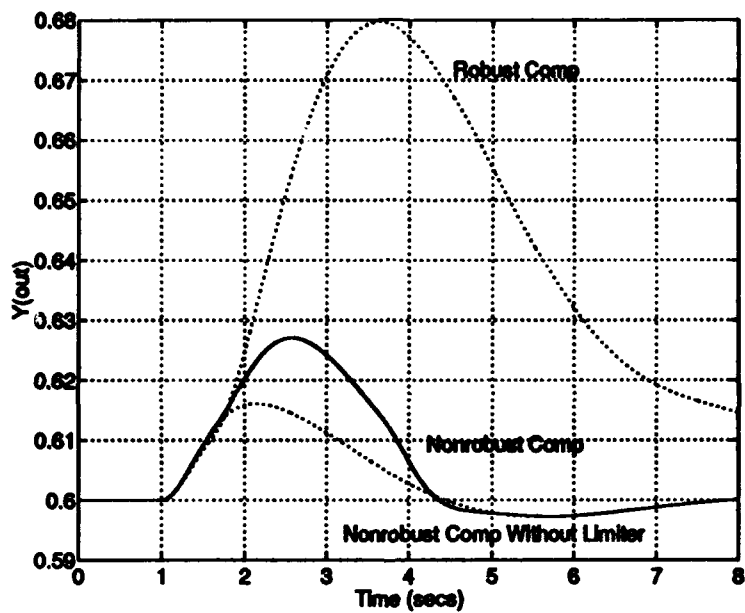


Figure 5.25 Disturbance rejection response of both robust and nonrobust MBFLC to a step disturbance of magnitude 0.1 injected at the plant input. Also shown is the response of the nonrobust compensator with the Fuzzy Limiter removed.

5.4.3 Effect of Mismatching on Compensator Tuning. For this experiment, the value of the a parameter within the nonlinear plant was altered to $a = 1.5$. With the MBFLC tuned as in the other two experiments, the response is extremely underdamped. The tuning procedure was repeated, both for the Fuzzy Limiter and the $C(t)$ functions. Upon retuning, the closed-loop system could be driven within the normal design specifications.

Changing the value of a alters the equilibrium condition of the nonlinear plant. The starting conditions on X_1 and X_2 were altered to account for this. For $a = 1.5$, $X_1(t_0) = 1.5X_2(t_0)$. The tuning parameters for the case of a mismatched plant/compensator are given in Tables 5.7 and 5.8. Note that the effect of the mismatching was to force the reduction of the penalty in the Limiter associated with $E_{is0.0}$ from 1 to 0.8. If this penalty had not been reduced the values of the penalties would not have gotten steadily smaller as the error grew.

This experiment suggests that the design of the linear compensator is not critical to proper performance. There is some design latitude as long as the compensator/Fuzzy Limiter pair induce a smooth transition from the initial state.

This experiment also shows that the MBFLC architecture is potentially very robust, given a mechanism to adjust the weights in the Fuzzy Limiter, based on perceived performance. Table 5.8 shows that the values determining $C(t)$ changes very little, as long as the Fuzzy Limiter and linear compensator induce the correct overshoot.

Fuzzy Set	Mean	Variance	Penalty
<i>Eis</i> 0.0	0.0	0.00002	0.8
<i>Eis</i> 0.025	0.025	0.00002	0.47
<i>Eis</i> 0.05	0.05	0.00002	0.42
<i>Eis</i> 0.075	0.075	0.00002	0.36
<i>Eis</i> 0.1	0.1	0.00002	0.325

Table 5.7 Tuning parameters for Fuzzy Limiter driving the mismodeled nonlinear plant ($a=1.5$)

Step Size	χ	$\sigma^2_{EisPositive}$	$\bar{X}_{EisPositive}$	$\sigma^2_{EisZero}$
0.0	0.0	0.00001	0.000000001	0.0000004
0.025	0.033	0.00013	0.018	0.0000007
0.05	0.072	0.00064	0.036	0.0000003
0.075	0.12	0.00096	0.045	0.0000005
0.1	0.17	0.00019	0.0634	0.0000007

Table 5.8 Look-up table data for MBFLC incorporating the robust linear compensator

5.5 Model-Following Hybrid Compensators

The previous section showed that there was very little contribution to the success of the MBFLC made by its linear elements. Though the MBFLC architecture is based largely on linear design considerations, the controller ultimately relies on Fuzzy Sets, tuned through simulation, to achieve successful full-envelope performance. Linear compensators, it seems, have significant limitations, even when employed in conjunction with Fuzzy Logic.

Linearized plant models are not the only way in which linear theory can contribute to the control of a nonlinear plant. An alternate approach is to consider an actual model-following design, similar to the nonlinear/Fuzzy hybrid controller from Chapter 4. In this design, the linear system model developed in Chapter 2 is integrated directly into the controller structure. Fuzzy Logic is then used to drive the error between the plant states and model states to zero at all times.

Linear/Fuzzy model following is illustrated in Figure 5.26. For this controller, two signals are fed back: $Y(X_1)$ and \dot{X}_1 . Y is used to drive the linear system model contained in the SIMULINK block *Model* and described by (2.26). The internal structure for the *Model* block is shown in Figure 5.27. This block is essentially a closed-loop simulation of the model poles with the reference signal and the feedback term supplied externally.

Based on the model response, a desired \dot{X}_1 trajectory is generated. The actual \dot{X}_1 is subtracted from the desired value and the difference (trajectory error) is input to the block called *FuzzyDriver*. The purpose of the Fuzzy Driver is to produce an error signal which will drive the error between \dot{X}_1 -desired and \dot{X}_1 -actual to zero. The error signal is fed into a linear compensator, and the compensator ultimately drives the plant.

The internal structure of the Fuzzy Driver is shown in Figure 5.28. Within the Fuzzy Driver, the \dot{X}_1 Error signal is evaluated for membership in three different Fuzzy Sets: Negative, Zero, and Positive. The membership functions for these sets are shown in Figure 5.29. The membership functions for *Negative* and *Positive* are open-ended. That is, they approach 1 as the \dot{X}_1 Error signal approaches either positive or negative ∞ .

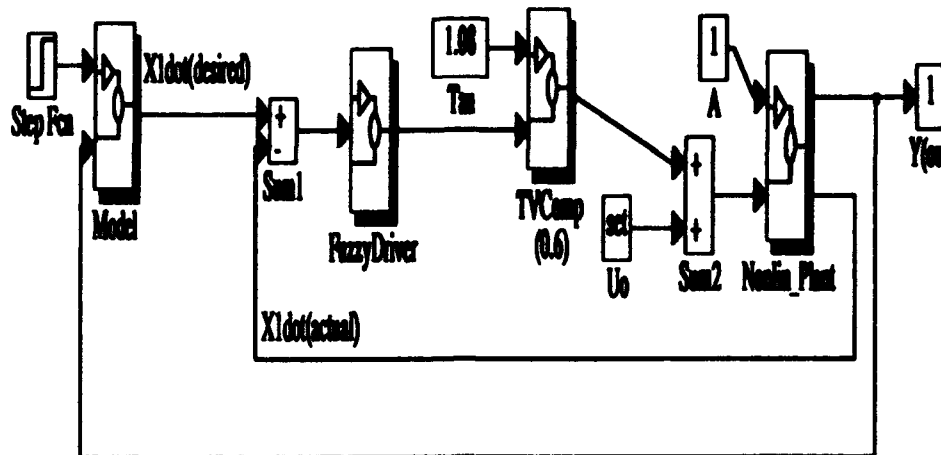


Figure 5.26 Hybrid linear/Fuzzy Controller using linear model-following and Linear/Fuzzy control input generation

Each Fuzzy Set has associated with it an error signal, very large relative to the control inputs typically required to drive the plant. Small deviations in \dot{X}_1 , then, result in a large correcting error signal to the linear compensator, shown in Figure 5.26. The linear compensator drives the nonlinear plant. Error signals of ± 10 were chosen arbitrarily to provide excellent model-following and signal rejection regardless of the value of the parameter α . Large error signals associated with small error signals is typical of a bang/bang type controller [21].

The linear compensator is required to hold the system at steady-state once all dynamics have subsided. Because there is no error signal associated with an \dot{X}_1 Error of Zero within the Fuzzy Driver, no control will be generated when the actual and desired trajectories coincide. The integrators within the linear compensator are needed to obtain a constant input to the plant after all dynamics have subsided.

The response of this system to step inputs of various magnitudes is shown in Figure 5.30. All restrictions on the region of operation can be removed, resulting in a true full-envelope controller.

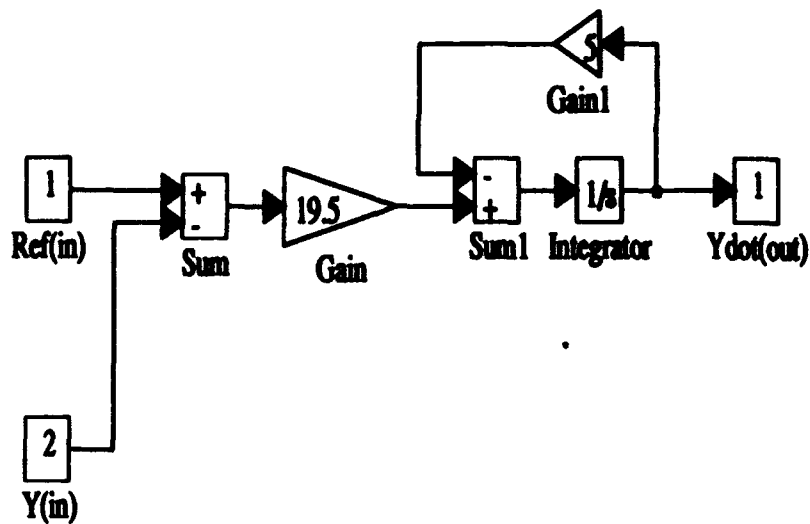


Figure 5.27 Internal structure of SIMULINK block *Model*

This strategy only breaks down for extremely large step inputs which require larger control inputs than are provided for by the Implicates of the Fuzzy Sets. Variations in the α parameter produces no change in the system response. Similarly, this controller demonstrates almost complete rejection of unwanted signals at the input to the nonlinear plant.

The price paid for this performance is in extreme swings at the plant input. Figure 5.31 shows the input to the nonlinear plant after the Fuzzy Driver and the linear compensator. The Figure shows a great number of input spikes which would cause havoc in any physical system. Of course, the input spikes are exaggerated by the choice ± 10 for the implicate Error signals within the Fuzzy Driver. For the original region of operation, between $Y=0.6$ and $Y=0.7$, implicate error signals of ± 0.8 are adequate to drive the plant to within a reasonable approximation of the model. Input spikes are still present in the plant input, but are not nearly as severe as those shown in the Figure.

The control spike problem can be mitigated by reinserting the Fuzzy Limiter and inputting the sum of the Driver output and the Limiter output to the linear compensator. In this configuration,

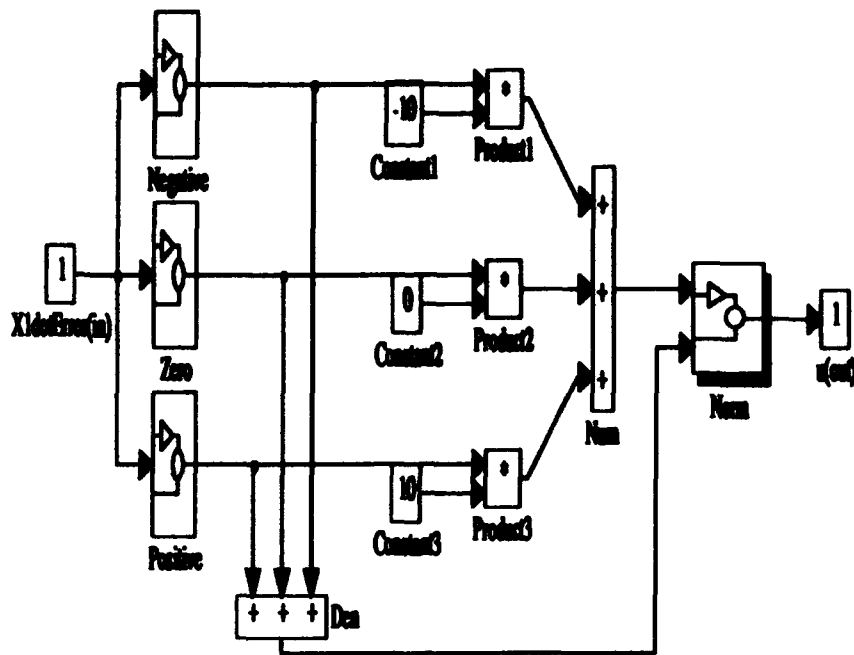


Figure 5.28 Internal structure of SIMULINK block *FuzzyDriver*

the Fuzzy Driver will only need to generate a driving signal when the plant model deviates from the model trajectory. The errors seen by the Driver will generally be much smaller, and the generated driving signal commensurately smoother.

This controller design, unfortunately, invokes the state directionality argument that the Model-Based Fuzzy Logic Control approach was seeking to avoid. It is assumed that the correct sign (positive or negative) of the input can be inferred by the sign of the error signal. This may not always be the case for nonlinear plants [16].

5.6 Summary

A successful MBFLC can be developed by accounting for the three error sources identified in Chapters 3 and 4 separately. The resulting design is capable of achieving linear-like behavior from the nonlinear plant, given fixed initial conditions and final states. With the insertion of look-up tables or an additional Fuzzy Bank of $C(t)$ generators, full-envelope controller performance can be obtained.

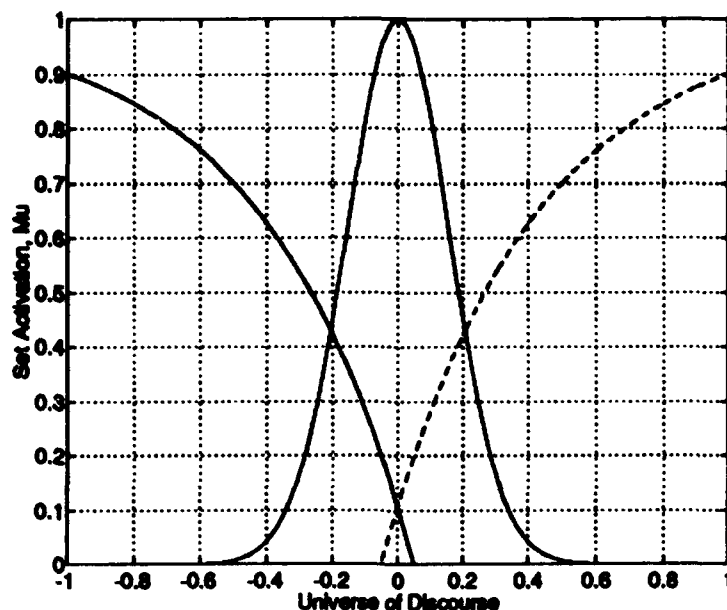


Figure 5.29 Membership functions for Fuzzy Sets within the Fuzzy Driver

Initial analysis indicates that Fuzzy Logic plays the significant role in the adequate compensation of the nonlinear plant. Only one linearized compensator was found to be necessary, and its correct design was not critical. The addition of more compensators was actually detrimental to the closed-loop response of the nonlinear plant. Further, mismodeling between the single compensator and the plant can be easily compensated for in the Fuzzy Limiter.

Because the full bank of compensators is not necessary, this design clearly does not emulate the fuzzy/nonlinear controller developed at the end of the last chapter. In the Fuzzy/Nonlinear design of Chapter 4, the contribution of the linear compensators was understood in the context of the Time-Varying Linear Plant. The time-varying linear compensator and its time invariance approximation, the Fuzzy Bank, were able to successfully control the LTV plant, which exhibits a subset of the nonlinear dynamics of the full nonlinear plant under consideration. The Fuzzy Weighted Bank was shown to closely approximate the time-varying linear compensator. The current Fuzzy/Linear design was shown to approximate two pre-weighted linear compensators, with the output of the second linear compensator being emulated via Fuzzy Logic.

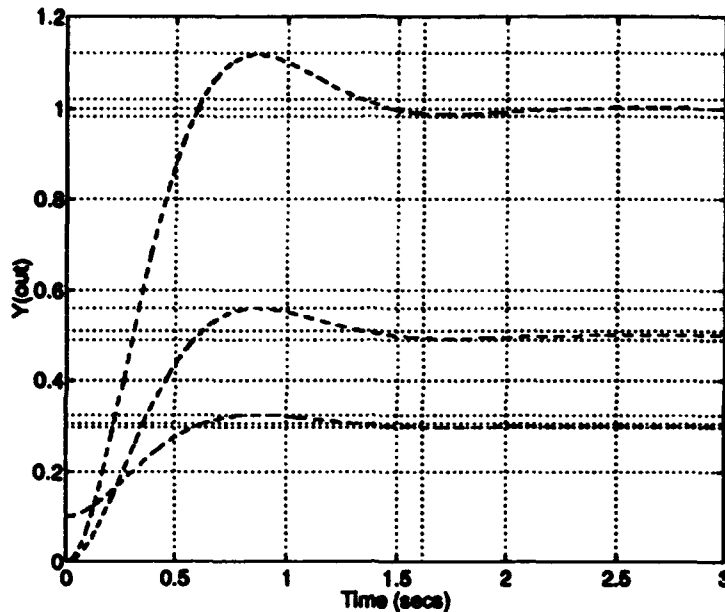


Figure 5.30 Closed-loop responses of Model-Following hybrid controller for step inputs of various magnitudes and initial conditions.

The single-compensator MBFLC was found to possess some disturbance rejection capabilities. The Fuzzy Limiter, however, actually inhibits robustness in inverse proportion to the magnitude of the penalties on E . This effect becomes significant when tuning the compensator for the robust linear compensator. Any advantages to using the robust compensator are completely lost due to the weights required in the Fuzzy Limiter to ensure tracking performance.

An actual model-following hybrid linear/Fuzzy controller was shown to meet all performance and signal rejection requirements, though at the expense of signal spikes at the plant input. A balance between desired performance and maximum allowable input variation could result in a successful hybrid controller design for real-world applications.

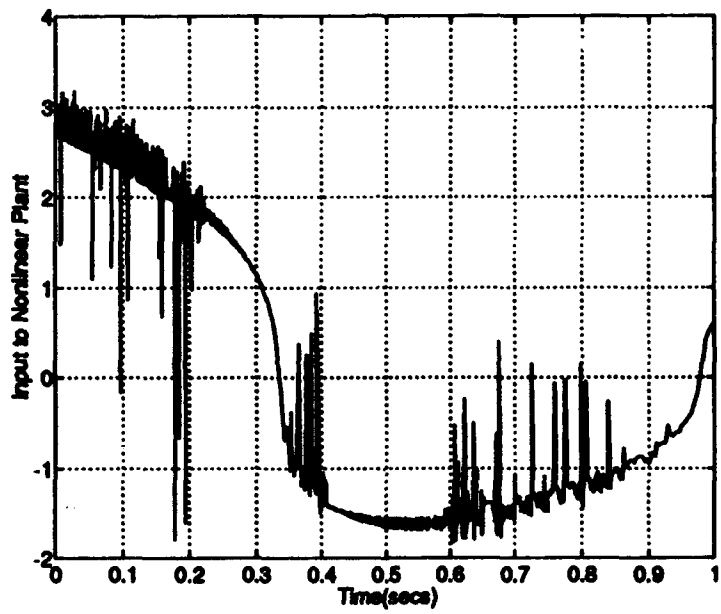


Figure 5.31 Input signal to nonlinear plant generated by Fuzzy Driver and linear compensator

VI. Conclusions and Recommendations

6.1 Introduction

Most systems of interest in engineering are nonlinear, at least at the extremes of their envelopes of operation. Controllers for these systems are often based on a linearized model of the plant, or on multiple linearizations when the plant exhibits significant nonlinearities. This practice leads to significant modeling error between the physical plant and the plant model.

The objective of this research effort was to develop a hybrid control approach to account for the plant/linear model ambiguity in a meaningful but non-statistical way. The non-statistical nature of the approach was important due to the difficulty in accurately gauging the extent of the modeling error. Other error sources such as time-varying parameters can also manifest themselves in a manner similar to modeling error and further motivates a non-statistical approach. Fuzzy Logic concepts were chosen as a natural framework within which to address these errors.

The developed control approach, dubbed Model-Based Fuzzy Logic Control (MBFLC), is a logical extension of both linear and Fuzzy Logic Control ideas. In essence, the controller is Fuzzy but with a resident system "expert," represented by a linear compensator. The MBFLC approach is designed to take advantage of the strengths of both linear systems theory and Fuzzy Set theory. Linear elements are to contribute a degree of a priori synthesis and analysis capability and the ability to utilize available but inaccurate/incomplete system models. Fuzzy Logic elements are to contribute robustness in the face of modeling (and linearization) errors, enabling the application of the resulting compensator to uncertain linear and/or nonlinear problems. The final form of the controller was developed in the last chapter, and tests were performed to assess the relative contributions of the Fuzzy and linear elements.

The degree to which the desired performance characteristics were obtained in simulation is the subject of this concluding chapter. The success of MBFLC is assessed in light of the established research objectives.

The chapter is divided into three sections:

1. Controller Summary

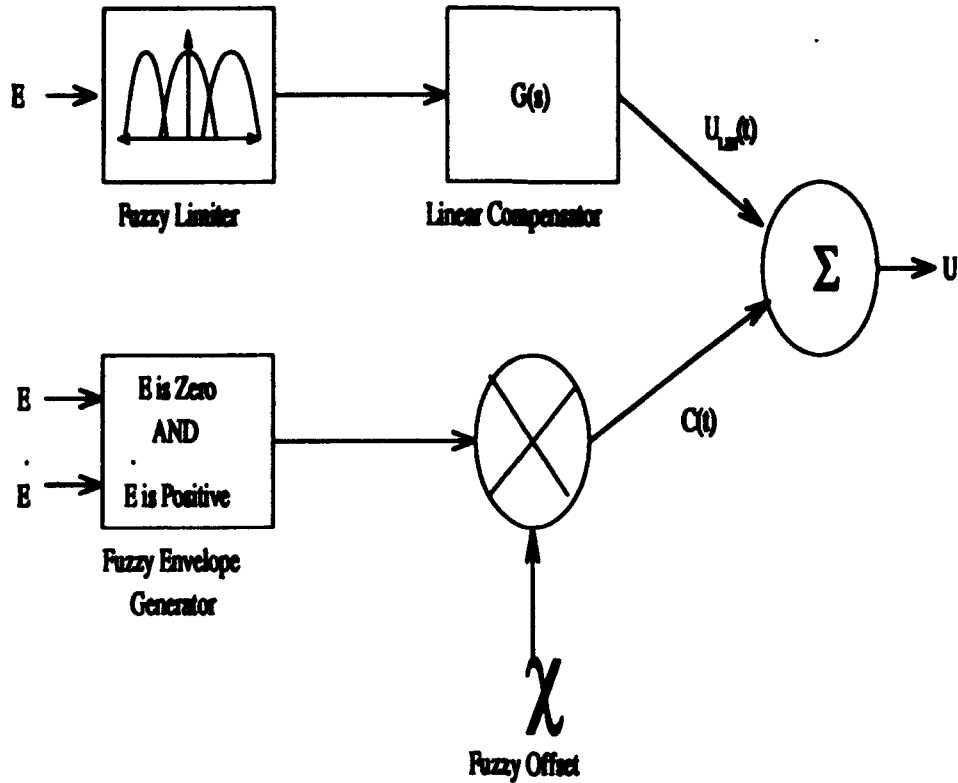


Figure 6.1 MBFLC Block Diagram

2. Thesis Conclusions
3. Recommendations for Future Research
4. Summary

6.2 Controller Summary

The objective of this thesis was to develop a full-envelope controller for a nonlinear plant using both linear control systems theory and Fuzzy Logic. Based on the linear and nonlinear design considerations discussed in previous chapters, the MBFLC of Figure 6.1 was obtained.

The MBFLC is essentially a Fuzzy Controller with only two rules:

1. If Error is not Zero AND \dot{Error} is not Positive THEN $U = U_{lin}(t)$
2. If Error is Zero AND \dot{Error} is Positive THEN $U = U_{lin}(t) + C(t)$

That is to say, as long as the system is far from the reference value and still climbing (\dot{Error} is negative), then the control input to the plant is $U_{lin}(t)$. When close to the reference value and

dropping back towards the reference value after the overshoot, the input to the plant is $U_{lin}(t) + C(t)$. Neither U_{lin} nor $C(t)$ are directly derived from linear control theory, though both are based on linear concepts. These signals are discussed in more detail below.

6.2.1 Formation of $U_{lin}(t)$. As shown in the Figure, U_{lin} is formed in two stages. First, the Error signal is fed through a "squashing function" implemented in Fuzzy Logic. This Fuzzy Limiter allows small error signals to pass through unaffected, but rapidly attenuates larger errors. The Limiter is necessary to acknowledge the fact that the linear compensator is not valid over the entire range from Y_o to Y_{ref} . The exact form of the Fuzzy Limiter is determined through simulation.

The modified Error signal is then input to a linear compensator. The compensator is based on a linearized model of the nonlinear plant and is designed to the performance specifications desired for the overall simulation. Because the Limiter is designed to only *constrict* the Error signal and not to amplify it, the compensator used should correspond to the most "sluggish" part of the nonlinear plant envelope. In other words, the compensator with the highest DC gain should be selected for the MBFLC.

It was shown through simulation that, by adjusting the Error Magnitude penalties associated with the Fuzzy Limiter, a closed-loop response with the correct overshoot and initial Y_{ref} settling time can be obtained from the U_{lin} signal alone. With no other compensation, however, large, lightly-damped oscillations will be induced in the nonlinear plant. It is the purpose of the added signal $C(t)$ to damp out these oscillations.

6.2.2 Formation of $C(t)$. The correct form for the damping signal $C(t)$ is also drawn, in a non-rigorous way, from linear analysis. Simulations were performed to test the feasibility of driving a *linear* plant using a bank of two identical linear compensators in closed-loop simulation. It was found that control of the linear plant could be transferred from compensator $G_1(s)$ to $G_2(s)$ at any point along the state trajectory provided that the *input* of $G_1(s)$ be driven to zero at the time of the transfer and that the *output* of $G_1(s)$ be allowed to continue to influence the plant for all

time forward. The residual signal produced by $G_1(s)$ successfully accounted for the non-equilibrium condition of the plant at the time of the compensator transfer.

This effect of two compensators perfectly complementing each other was only observed for identical linear compensators driving a LTI plant. When there was a mismatch between the two compensators or the compensators and the plant, lightly damped oscillations resulted. Linear analysis, then, infers that there may exist a combination of the signals, similar to the linear/no-mismatch outputs of $G_1(s)$ and $G_2(s)$, even for the case when modeling errors and compensator mismatches exist (as would be the case in a nonlinear simulation). The transfer functions for these functions, however, cannot be predicted by linear analysis.

In applying this two-signal paradigm to the control of the nonlinear plant, $U_{lin}(t)$ drives the signal from t_0 and so should resemble the output of the $G_1(s)$ compensator for the linear case. Simulations show that this is indeed the case, and that the Limiter/Linear Compensator pair induce a linear-like error history from the nonlinear plant. $C(t)$ then, by analogy, should also resemble the linear output time history of $G_2(s)$.

The exact form and magnitude of $G_2(s)$ is unclear when errors are introduced due to nonlinearities, so the contribution of the second linear compensator is emulated using Fuzzy Logic. The exact form of $C(t)$ can then be determined through simulation. $C(t)$ is given by:

$$C(t) = \chi * \min(\mu_{EisZero}(E), \mu_{EisPositive}(\dot{E})) \quad (6.1)$$

where χ is a weighting function and $\min(\mu_{EisZero}(E), \mu_{EisPositive}(\dot{E}))$ is the smaller of two time-varying Fuzzy Membership Functions. This function $\min(\bullet, \bullet)$ is one realization of the Fuzzy AND operation, hence the two Fuzzy rules stated above.

By specifying the weight χ and the (\bar{x}, σ^2) parameters which define the Fuzzy Sets *EisZero* and *EisPositive*, $C(t)$ can be modified to damp out the induced oscillations. The precise values necessary must be determined by simulation, and are functions of the input step magnitude. That is, the farther the reference signal is from the quiescent condition, the larger the dynamics that will be induced in the plant. The universe of discourse for *EisPositive* must be rescaled to accommodate

larger state derivatives and the overall force of $C(t)$, established by χ , must be larger. The extent to which the oscillations are damped out is highly sensitive to changes in any of these parameters.

The MBFLC, then, is analogous to a bank of two linear compensators, weighted at their Error inputs, as was shown in Figure 3.12. Notice, however, that in the Figure 6.1 there is no mechanism to drive the Error signal into the Fuzzy Limiter to zero when $C(t)$ activates, as was the case for the linear bank. No mechanism is necessary in this case because $C(t)$ only becomes active when the system output approaches Y_{ref} ($E \rightarrow 0$). Therefore, $C(t)$ activates as the signal into the linear compensator goes to zero naturally. A properly tuned $C(t)$ will keep the error at zero and allow the linear compensator to approach steady-state.

Full-envelope performance is exhibited over a prespecified range of operation, as shown in Figure 6.2. The MBFLC clearly forces the nonlinear plant to exhibit linear-like behavior and to perform within the specifications established by the linear compensator. Only the disturbance rejection specification is violated slightly by the final design. This eliminates the need for gain scheduling within the envelope of operation established by the Fuzzy Logic.

6.3 Thesis Conclusions

The expected benefits of MBFLC are restated here from Chapter 1:

1. Force a nonlinear plant to exhibit linear-like performance and conform to linear design specifications.
2. Incorporate available models into controller structure.
3. Enhance robustness of controller in the face of unmodeled uncertainties (system damage, noise).
4. Obtain full envelope operation without the need for gain scheduling.
5. Introduce some a priori synthesis and analysis capability into Fuzzy Controller Design.

The success of the MBFLC controller at meeting these objectives is examined below.

6.3.1 Force a nonlinear plant to exhibit linear-like performance and obey linear design specifications. The simulation responses shown in Figure 6.2 demonstrate that the MBFLC is capable of inducing a linear-like response from the nonlinear plant such that it falls within estab-

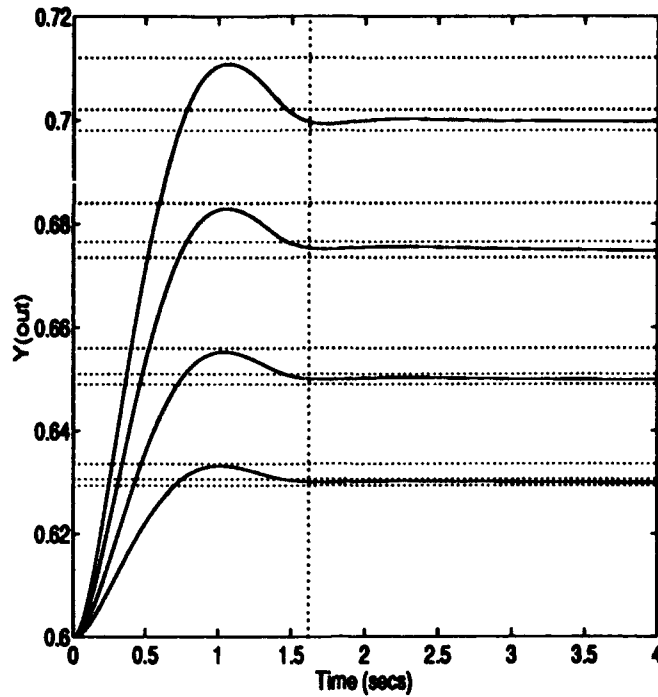


Figure 6.2 Closed-loop response of Nonlinear plant for step inputs of $Y_{ref} = 0.6 + 0.035u_{-1}(t)$, $0.6 + 0.05u_{-1}(t)$, $0.6 + 0.075u_{-1}(t)$, and $0.6 + 0.1u_{-1}(t)$

lished design parameters. Only the disturbance rejection specification is violated by the MBFLC. In this respect, the MBFLC is a success.

When compared to the other approaches developed in Chapter 2, the MBFLC controller also shows promise. Figures 6.3 and 6.4 compare the responses derived from applying QFT and dynamic inversion with that from the MBFLC. These Figures show that the MBFLC delivers performance approximately equivalent to the DI compensator for the nonlinear plant given a specified region of operation. The Fuzzy Logic Compensator developed in Chapter 2 could not be compared with the MBFLC because its tuning is only valid for one input, $Y_{ref} = u_{-1}(t)$. Any other input or operating point would required redesign of the FLC.

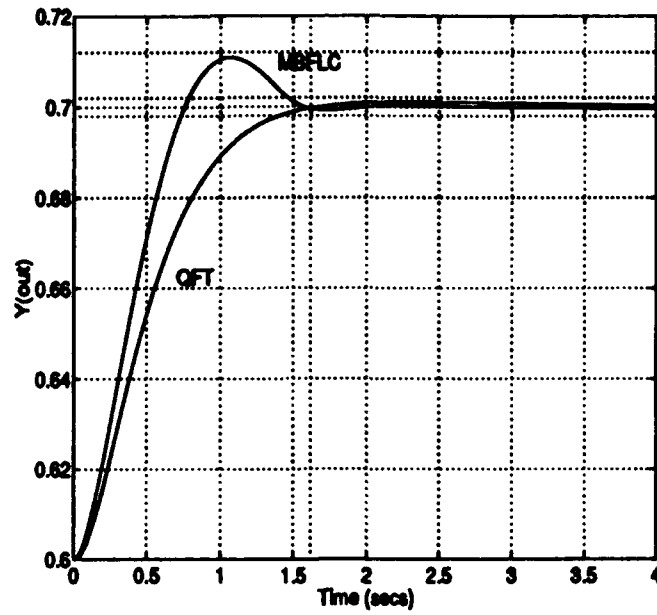


Figure 6.3 Closed-loop responses for QFT-based design and MBFLC design

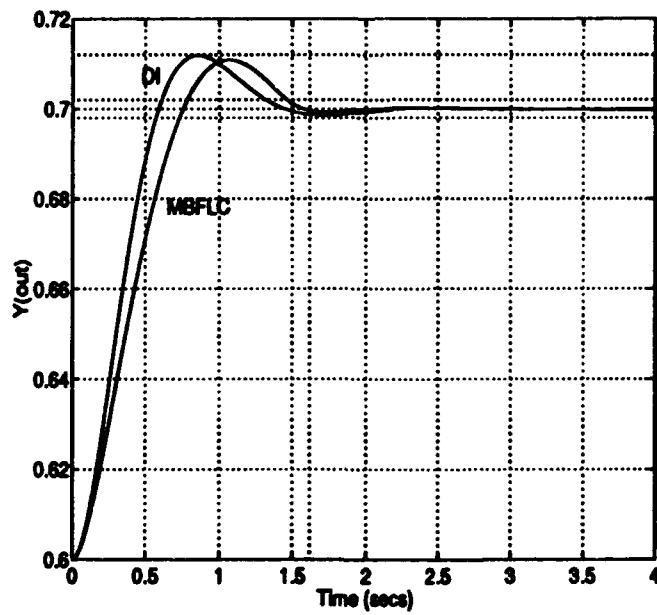


Figure 6.4 Closed-loop responses for Dynamic Inversion-based design and MBFLC design

6.3.2 Incorporate available models into controller structure. The MBFLC clearly utilizes driving data derived from a linear compensator rather than from a look-up table, as for the FLC of Chapter 2. The settling term $C(t)$ is also based on linear simulations, though its exact value must be determined through simulation. The contribution ultimately made by the linear compensators, however, is small. The response generated by the Fuzzy Limiter/Linear Compensator does reflect the figures of merit for which the linear compensator is designed, but this is largely due to the tuning of the Fuzzy Sets.

Several experiments from Chapter 5 support this conclusion. First, it was demonstrated that a MBFLC based on a single linear compensator was actually *superior* in some ways to one based on a bank of linear compensators. This suggests that the additional linearizations do not contribute to the control of the nonlinear plant, even in the neighborhoods about which the linearizations are based. Second, it was shown that linear robustness does not translate directly into nonlinear robustness. Finally, it was shown that large errors in the assumed model of the nonlinear plant could be compensated for within the Fuzzy Logic with very little degradation in performance. These results indicate that the contribution of the linear compensators in the MBFLC is minimal.

It should be pointed out, however, that removal of all linear compensators results in a very undesirable response. The the Fuzzy Logic elements can produce a stable response without the linear compensator, but the plant output is highly irregular and violates the established performance boundaries.

6.3.3 Enhance robustness of controller in the face of uncertainties. The MBFLC architecture is very tolerant of modeling error, given the opportunity to retune the Fuzzy Sets. Once retuned, the effect of mismodeling is exhibited in the initial overshoot and time to reach steady-state operations. All information on the intended design characteristics is contained in the linear compensator. If the compensator begins to significantly differ from any of the linearizations of the plant, the correct characteristics are distorted.

If no retuning is allowed, the MBFLC is slightly more sensitive to plant mismodeling than QFT or FLC. However, the system response is stable throughout the range of variation for the parameter α .

6.3.4 Eliminate the need for gain scheduling. Once tuned, the MBFLC induces linear-like behavior throughout the specified operating envelope. This eliminates the need for gain scheduling in the conventional sense. The extent to which the envelope can be expanded given a single-compensator MBFLC is unclear. For very large envelopes of operation, the bank of compensators may prove superior to the single compensator. Further research will be required to resolve this issue.

6.3.5 Introduce some a priori synthesis and analysis capability. The linear element of the MBFLC can be designed outside of the simulation environment. In this respect, some degree of a priori synthesis capability is derived through the MBFLC approach. The final design, however, relies heavily on tuning of the Fuzzy Sets to establish proper weighting and granularity.

Though the MBFLC has only a limited a priori synthesis characteristic, it still has a well-defined internal structure which separates it from other Fuzzy Logic based approaches. The FLC from Chapter 2 and elsewhere [10, 11, 12, 19] is based only on empirical tuning data. Even when some data is available, as from the DI design, the look-up table based on this data may well be inadequate. The MBFLC has a systematically derived internal structure, assuming the existence of some form of plant model. This greatly simplifies controller development over the traditional FLC approach. Further, the MBFLC approach can be applied to systems which exhibit high-order system dynamics.

6.4 Recommendations for Future Research

The topics touched on in this thesis are rich for future research. Recommended areas of focus are given below:

6.4.1 Analysis of MBFLC error sources. Further research into the actual workings of the MBFLC are warranted. The claim made in this thesis is that the Fuzzy Limiter/Linear Compensator induces essentially a "linear" response in the nonlinear plant. This argument is then invoked to justify the form of the damping signal $C(t)$ and to explain why the figures of merit about which the linear compensator is designed are ultimately exhibited by the nonlinear plant. The validity of these claims are borne out in simulation, but difficult to justify theoretically.

6.4.2 Self-Tuning of Fuzzy Sets. As used in this thesis, Fuzzy Logic is simply an alternate way to express a nonlinear look-up table. However, the true utility of the Fuzzy Set Theory is reasoning under uncertainty, and learning by example [33, 34]. A Fuzzy learning algorithm integrated into this controller could greatly reduce tuning requirements and enhance robustness in the face of modeling error.

The greatest tuning burden is to determine the required $C(t)$ to damp out oscillations. The forms of the $C(t)$ responses for each magnitude step input are currently encapsulated in look-up tables. These tables show consistent general trends but are difficult to estimate precisely prior to simulation. A fuzzy learning algorithm could be developed to perform the tuning on-line based on the perceived performance of the system. Of course, this would require some sort of optimal state trajectory or an integrated model to compare against the actual system.

If learning were successful, very little tuning would be required ad hoc. The system would tune itself, thereby "getting to know" its host system through actual operations. A form of parameter identification could be performed by optimizing the desired performance of the plant over time through Fuzzy or neuro-fuzzy unsupervised learning. Self tuning controllers is an area of current active research [24, 23, 35].

6.4.3 Development of equivalent $G_2(s)$. A great deal of the complexity of the MBFLC comes from the emulation of the second controller in Fuzzy Logic. The output signal $C(t)$, however, is very similar to that produced by a linear controller. Therefore, $C(t)$ could possibly be produced by

an equivalent linear network developed through input/output parameter identification techniques [21].

This would reduce the role of Fuzzy Logic in this compensator to that originally envisioned – providing appropriate weighting to a bank of linear filters. The bank itself would consist of the Fuzzy Limiter/Linear Compensator Pair to initiate the trajectory, and then a bank of linear compensators each corresponding to the damping signal required for a different reference input. This design may not perform as well as the current MBFLC, due to the sensitivity of the closed-loop response to small changes in $C(t)$.

6.4.4 Compensation of plants at non-zero initial conditions. Banked compensator analysis demonstrated the difficulties associated with developing compensators for plants which are away from equilibrium at t_0 . A technique should be explored, perhaps based on the linear banked analysis of Chapter 3, to develop linear compensators for the control of non-quiescent plants. For the linear case, this could be pursued by examining both the homogeneous and the particular solutions for the plants in question. This is a very basic problem in linear control and should be explored.

For the nonlinear case, the results 6.4.3 could be utilized. The equivalent linear controllers developed through simulation would, in effect, be designed to dissipate state energy to establish a quiescent condition. This type of "damping" controller could have applications in other branches of control as well.

6.4.5 Polynomial approximations to look-up table data. If adequate equivalent linear approximations of the $G_i(s)$ signals cannot be developed, the look-up tables upon which the MBFLC currently relies could be approximated using linear or piecewise linear equations. This could lead to a more linear controller which provides equivalent control as the MBFLC, as well as provide insights into on-line retuning opportunities.

6.4.6 Model-Following Fuzzy Logic Controllers. Model-following hybrid controllers were shown to have advantages in performance over any of the designs explored in this research. Unfortunately, this performance is achieved at the cost of unrealistic input "spikes" into the nonlinear

plant. There are many design trade-offs that could be made to adapt a model-following approach for actual systems.

The hybrid linear/Fuzzy model follower, for example, could be used in conjunction with other controllers. Given an existing controller, the hybrid controller could provide inputs only when the system response deviates from the established model. In this fashion, the FLC would only be active when absolutely needed, perhaps even through auxiliary control surfaces.

6.4.7 Nonlinear Mathematical Analysis. By approximating all of the Fuzzy Logic sets within the MBFLC as nonlinear nth-order functions, nonlinear stability analysis techniques could be applied to examine the stability of the MBFLC. This technique is discussed in [36]. This technique could lead mathematically rigorous insights into how the MBFLC can be improved.

6.4.8 Test controller in realistic environment. This thesis largely addresses non-statistical uncertainty due to nonlinearity. The problem was framed in Chapter 1, however, for an environment which includes parameter uncertainty and noise. These elements should be added to a MBFLC simulation.

The current MBFLC design does not demonstrate an exceptional ability to cope with unknown parameters without retuning. System noise essentially adds an uncertainty into the firing of the $C(t)$ signal, which has varying effects depending on the desired reference value of the controller. A desensitized MBFLC (by self-tuning, linear approximation, application to linear plants, or through bang/bang compensation) should be considered for these more "real world" simulations.

6.4.9 Implement Fuzzy Supervisor Between $U_{fn}(t)$ and $C(t)$. One of the factors contributing to tuning difficulty is that the relative contributions of $U_{fn}(t)$ and $C(t)$ must sum to the reference value as steady state. An additional level of control should be investigated to eliminate the need for this precarious balance.

This could be accomplished by reinserting preweighting terms, implemented through either switches or a Fuzzy Supervisor. In this case the linear compensator could be forced to reach

a steady-state value and all remaining control responsibility would be left to the Fuzzy Logic emulation.

6.4.10 Apply MBFLC Approach to Uncertain Linear Systems. Though the MBFLC demonstrated limited robustness in the face of modeling error for nonlinear plants, robustness may be exhibited when considering uncertain linear plants. In the linear case, the information contained in the linear compensators is much more complete than in the nonlinear scenario, with fewer "modes" of failure.

As long as the Fuzzy Logic is actually producing a signal to emulate a linear element, the overall design will exhibit some sensitivity to modeling errors. The conventional FLC (from Chapter 2) gets its robustness by, in effect, over-controlling the plant. An approach similar to the Fuzzy bang/bang controller would probably be more effective at minimizing the sensitivity of the overall system to undesired dynamics. There are, however, other practical considerations which discourage the implementation of bang/bang controllers on physical systems [14].

6.5 Summary

The initial hybrid linear/Fuzzy controller concept for this thesis was based on the use of multiple linearizations of a nonlinear plant. Linear compensators based on the linearized plants were to produce plant control data, assuming the plant was, in fact, in the region where the compensator was valid. These multiple control signals would then be blended together using Fuzzy Logic to produce a composite control signal which would be used to drive the nonlinear plant. The questions addressed in this thesis were tailored to show conclusively why this approach would or would not work.

Unfortunately, analysis showed that a Linear/Fuzzy compensator based only on a bank of linear compensators was not feasible. This is due largely to the small regions of validity for the linearized models and energy considerations within the plant/controller system. This analysis itself, however, suggested an alternate form for a hybrid Linear/Fuzzy approach, which was developed in to the MBFLC controller.

The Model-Based Fuzzy Logic controller adds a new dimension in capability over conventional Fuzzy Logic designs. Current FLCs rely on heuristic input/output relationships to derive appropriate control commands. The MBFLC, in contrast, utilizes linear models and linear waveforms which are then tuned through simulation to induce the desired closed-loop behavior. The controller design presented in this thesis is capable of driving a nonlinear plant to any point within a predefined envelope of operation utilizing only Fuzzy Logic and linearized plant models. Its performance is comparable to a controller derived using deterministic nonlinear techniques. The MBFLC also proved to be approximately as robust to modeling errors as the other control approaches considered.

It was shown that limitations in the current MBFLC can be overcome by model-following type designs, or by introducing a self-tuning capability. In addition, many elements of the MBFLC could be implemented as linear networks, simplifying the existing architecture. All of these areas should be explored in follow-on efforts.

The development of "intelligent controllers" is contingent on the successful integration of artificial intelligence into conventional control methodologies. This thesis demonstrates that the introduction of Fuzzy sets into a linear controller yields new capabilities not exhibited by linear or Fuzzy Logic-based control alone. The fusion of Fuzzy Logic techniques and conventional control ideas offers many possibilities for productive future research.

Bibliography

1. Maybeck, Peter S. *Stochastic Models, Estimation, and Control, Vol 3*. New York: Academic Press, 1982.
2. Maybeck, Peter S. *Stochastic Models, Estimation, and Control, Vol 1*. New York: Academic Press, 1982.
3. Blakelock, John H. *Automatic Control of Aircraft and Missiles*. New York: John Wiley and Sons, 1991.
4. D'Azzo, John J. and Constantine H. Houpis. *Linear Control System Analysis and Design*. New York: McGraw-Hill Book Company, 1989.
5. Schwartz, Daniel G. and George J. Klir. "Fuzzy Logic Flowers in Japan," *IEEE Spectrum* 29(7):32-35 (July 1992).
6. Kauffmann, A. "Progress in Modeling of Human Reasoning by Fuzzy Logic," in *Fuzzy Automata and Decision Processes*. Ed. Madan Gupta and Others. Amsterdam, The Netherlands: North-Holland Publishing, 1977.
7. Cox, Earl. "Fuzzy Fundamentals," *IEEE Spectrum* 29(10):58-61 (October 92).
8. Sugeno, M. and S. Murakami. "An Experimental Study of Fuzzy Parking Control Using a Model Car," *Industrial Applications of Fuzzy Control*. Ed. Michio Sugeno. Amsterdam, The Netherlands: North-Holland Publishing, 1985.
9. Murakami, S. and M. Maeda. "Application of Fuzzy Controller to Automobile Speed Control," in *Industrial Applications of Fuzzy Control*. Ed. Michio Sugeno. Amsterdam, The Netherlands: North-Holland Publishing, 1985.
10. King, Peter J. and Ehmat H. Mamdani. "The Applications of Fuzzy Control Systems to Industrial Processes," *Automatica* 13(3):235-242 (Fall 1977).
11. Yasanobu, S. and M. Su. "Automatic Train Operation by Predictive Fuzzy Control," in *Industrial Applications of Fuzzy Control*. Ed. Michio Sugeno. Amsterdam, The Netherlands: North-Holland Publishing, 1985.
12. Larkin, Lawrence I. "Fuzzy Logic Control for Aircraft Flight Control," *Proceedings of the 23rd Conference on Decision and Control*. 884-885. New York: IEEE Press, 1984.
13. Berenji, Hamid R. "Fuzzy Logic Controllers" in *An Introduction to Fuzzy Logic Applications in Intelligent Systems*. Ed. R Yager and L. Zadeh. Cambridge, MA: Kluwer Academic Publishers, 1991.
14. Pachter, Meir, Stewart Sheldon, and Mark Mears. "Intelligent Flight Control," Technical Paper, US Air Force Flight Dynamics Laboratory, 1991 (distribution pending).
15. Zimmermann, Hans J. *Fuzzy Set Theory and its Applications*. Boston: Kluwer Academic Press, 1991

16. Pachter, Meir and D.H. Jacobson, "The Stability of Planar Dynamical Systems Linear-in-Cones," *IEEE Transactions on Automatic Control* 26(2): 587-590 (April 1981).
17. Reid, Gary J., *Linear System Fundamentals*. New York: McGraw-Hill Publishing Company, 1983.
18. Young, Christina M., "Fuzzy Controller for Pitot-Static Test Set," *Proceedings of the 1993 National Aerospace Electronics Conference*. New York: IEEE Press, 1993.
19. Chiu, Stephen and Sujeet Chand, "Fuzzy Controller Design and Stability Analysis for an Aircraft Model," *Control Systems Magazine*: 92-98 (June 91)
20. Nelson, Robert C. *Flight Stability and Automatic Control*. New York: McGraw-Hill Book Company, 1989.
21. Pachter, Meir, Unpublished Lecture Notes, Air Force Institute of Technology, Wright-Patterson Air Force Base, OH, June 1993.
22. Pachter, Meir. Class Handout, EENG 641, Automatic Flight Control I. School of Electrical and Computer Engineering, Air Force Institute of Technology, Wright-Patterson AFB, OH, January 1993.
23. Wang, Li-Xin and J. M. Mendel. "Generating Fuzzy Rules by Learning From Examples," *Proceedings of the IEEE International Symposium on Intelligent Control*: 263-268. New York: IEEE Press, 1991.
24. Graham, B. P. and Newell R.B. "Fuzzy Adaptive Control of a First Order Process." *Fuzzy Sets and Systems* 31:47-65 (1989)
25. Nassirharand, Amir, and J. H. Taylor, "Synthesis of Linear PID Controllers for Nonlinear Multivariable Systems," *Proceedings of the 1990 Control Conference*: 2223-2228. New York: IEEE Press, 1990.
26. Chen, Yung-Yaw and J-S Jang, "Imitation of State Feedback Controller by Fuzzy Linguistic Control Rules," *Proceeding of the 29th Conference on Decision and Control*. 1545-1546. New York: IEEE Press, 1990
27. Cook, Peter A. *Nonlinear Dynamical Systems*. Englewood Cliffs, NJ: Prentice/Hall Inc., 1986.
28. Kandel, Abraham. *Fuzzy Mathematical Techniques with Applications*. Reading, Ma: Addison-Wesley Publishing Company, 1986.
29. Houpis, C.H., *Quantitative Feedback Theory, Technique for Designing Multivariable Control Systems*, AFWAL-TR-86-3107, Wright Aeronautical Laboratories, Wright-Patterson AFB, OH, January 1987.
30. Kailath, Thomas. *Linear Systems*. Englewood Cliffs, NJ: Prentice/Hall Inc., 1980.
31. Holtzman, Jack M. *Nonlinear System Theory*. Englewood Cliffs, NJ: Prentice-Hall Inc., 1970.
32. Lu, Zhuxin and B. R. Holt, "Nonlinear Robust Control: Table Look-Up Controller Design," *Proceedings of the 1990 American Control Conference*. 2758-2763. New York: IEEE Press, 1990.

33. Swinarski, Roman W., "Neuromorphic Fuzzy Variable Structure Controller," *Proceedings of the 29th Conference on Decision and Control*. 1221-1226. New York: IEEE Press, 1990.
34. Takayuki, Yamada and T. Yabuta, "Nonlinear Neural Network Controller for Dynamic System," *Proceedings of the 1990 American Control Conference*. 1244-1249. New York: IEEE Press, 1990
35. Swinarski, Roman W. "Neural Network Based Self-Tuning Controller with Fourier Transformation of Temporal Patterns," *Proceedings of the 29th Conference on Decision and Control*: 1227-1232. New York: IEEE Press, 1990.
36. Braae, M. and D. A. Rutherford, "Theoretical and Linguistic Aspects of the Fuzzy Logic Controller." *Proceedings of the International Federation of Automatic Control*. 553-577. London: Pergamon Press Ltd, 1979.

Vita

Captain Michael W. Logan was born January 25, 1967 in St Louis, Missouri, to Bill and Pat Logan. He graduated from high school in Olathe, Kansas in 1985. He went on to graduate with a BS in Electrical Engineering from Northwestern University in June of 1989, where he graduated with departmental honors. After receiving his commission through the Reserve Officer Training Corps, he was assigned to the Plans and Advanced Programs Directorate of Electronic Systems Division at Hanscom AFB in Massachusetts. He served as project engineer and later project manager of the ESD Unmanned Air Vehicle Office, which supported the Joint DoD Unmanned Air vehicle Program. He was assigned to the Air Force Institute of Technology in May 92. He has a wife, Jana.

Permanent address: 8723 Mardi Gras
Huber Heights, OH 45424